

# CHAPTER 4

## THE GENERALIZED NEWTONIAN FLUID

This chapter is devoted to the generalized Newtonian fluid, which results from a minor modification of the Newtonian fluid constitutive equation given in Eq. 1.2-2. This equation incorporates the idea of a shear-rate-dependent viscosity, and hence can describe the non-Newtonian viscosity curves shown in Figs. 3.3-1 to 4. It cannot, however, describe normal stress effects or time-dependent elastic effects. There are many industrial flow problems in which the non-Newtonian viscosity effects are of paramount importance, and hence the generalized Newtonian fluid is useful; in addition it is a relatively simple constitutive equation, and many problems have been solved using it.

In §4.1 we introduce the model and give several useful empiricisms for the non-Newtonian viscosity, in particular, the “power-law model.” Then in §4.2 we show how to use the power-law model by going through a series of illustrative examples; the problems in these examples are sufficiently simple that analytical solutions may be obtained. For more complicated problems a variational principle is available, and it is discussed in §4.3. Up to this point it is presumed that the flow system is isothermal. Many industrial non-Newtonian problems are nonisothermal, and §4.4 provides a brief introduction to this rather large subject; particular attention is paid to viscous heating, because this effect is generally present in plastics processing operations and in lubrication problems. In §§4.2 to 4.4 all the illustrative examples are worked out for the power-law model; in §4.5 we discuss several other models and illustrate their use. Finally, in §4.6 we summarize the limitations on the generalized Newtonian fluid model and discuss the extent to which its use can be legitimized.

### **§4.1 THE GENERALIZED NEWTONIAN FLUID AND USEFUL EMPIRICISMS FOR THE NON-NEWTONIAN VISCOSITY**

For the industrial chemical engineer, the most important property of macromolecular fluids discussed in Chapter 3 is the non-Newtonian viscosity—that is, the fact that the viscosity of the fluid changes with the shear rate. Since for some fluids the viscosity can change by a factor of 10, 100, or even 1000, it is evident that such an enormous change cannot be ignored in pipe flow calculations, lubrication problems, design of on-line viscometers, extruder operation, and polymer processing calculations. Therefore it is not surprising that one of the earliest empiricisms to be introduced was a modification of

Newton's law of viscosity in which the viscosity is allowed to vary with the shear rate. That is, for the elementary flow  $v_x = v_x(y)$ ,  $v_y = 0$ ,  $v_z = 0$ , the early rheologists replaced

$$\text{Newtonian fluid:} \quad \tau_{yx} = -\mu \frac{dv_x}{dy}, \quad \mu = \text{a constant for a given temperature, pressure, and composition} \quad (4.1-1)$$

by the empiricism:<sup>1</sup>

$$\text{Generalized Newtonian fluid:} \quad \tau_{yx} = -\eta \frac{dv_x}{dy}, \quad \eta = \text{a function of } |dv_x/dy| \quad (4.1-2)$$

Absolute value signs have been used at the right of Eq. 4.1-2, since one would expect the change in viscosity to depend on the magnitude but not on the sign of the velocity gradient. Having written Eq. 4.1-2 one can then introduce various empiricisms to describe the experimental non-Newtonian viscosity curves.

We now wish to extend the ideas above to an arbitrary flow. First, for an incompressible Newtonian fluid, for any flow field  $\mathbf{v} = \mathbf{v}(x, y, z, t)$  we have:

$$\text{Incompressible Newtonian fluid:} \quad \tau = -\mu \dot{\gamma} \quad \mu = \text{a constant for a given temperature, pressure, and composition} \quad (4.1-3)$$

in which  $\dot{\gamma}$  is the rate-of-strain tensor  $\nabla \mathbf{v} + (\nabla \mathbf{v})^\dagger$  (cf. Eq. 1.2-2). To include the idea of a non-Newtonian viscosity, we write<sup>1</sup>

$$\text{Incompressible generalized Newtonian fluid:} \quad \tau = -\eta \dot{\gamma} \quad \eta = \text{a function of the scalar invariants of } \dot{\gamma} \quad (4.1-4)$$

If the non-Newtonian viscosity, a scalar, is to depend on the tensor  $\dot{\gamma}$ , then it must depend only on those particular combinations of components of the tensor that are not dependent on the coordinate system.<sup>2</sup> As described in §A.3 we may select as three independent combinations:

$$I = \sum_i \dot{\gamma}_{ii} \quad (4.1-5)$$

$$II = \sum_i \sum_j \dot{\gamma}_{ij} \dot{\gamma}_{ji} \quad (4.1-6)$$

$$III = \sum_i \sum_j \sum_k \dot{\gamma}_{ij} \dot{\gamma}_{jk} \dot{\gamma}_{ki} \quad (4.1-7)$$

For an incompressible fluid  $I = 2(\nabla \cdot \mathbf{v}) = 0$ . For shearing flows  $III$  turns out to be zero (see Problem 4B.8); since, as we will point out later, Eq. 4.1-4 should be used only for shearing

<sup>1</sup> M. Reiner, *Deformation, Strain, and Flow*, Interscience, New York (1960).

<sup>2</sup> K. Hohenemser and W. Prager, *J. Appl. Phys.*, **12**, 216-226 (1932); J. G. Oldroyd, *Proc. Camb. Phil. Soc.*, **45**, 595-611 (1949); **47**, 410-418 (1950).

flows, or at least flows that are very nearly shearing, omitting  $III$  from any further consideration is not a serious restriction. Hence  $\eta$  is taken to depend only on  $II$ . Actually we shall prefer to use  $\dot{\gamma}$ , the magnitude of the rate-of-strain tensor  $\dot{\gamma}$ , instead of  $II$

$$\dot{\gamma} = \sqrt{\frac{1}{2} \sum_i \sum_j \dot{\gamma}_{ij} \dot{\gamma}_{ji}} = \sqrt{\frac{1}{2} II} \tag{4.1-8}$$

In taking the square root one must affix the proper sign so that  $\dot{\gamma}$  will be positive. In shearing flows  $\dot{\gamma}$  is called the “shear rate.”

Equation 4.1-4 with  $\eta = \eta(\dot{\gamma})$  is then the starting point for all of the calculations in this chapter. Its principal usefulness is for calculating flow rates and shearing forces in steady-state shear flows, such as:

- a. Tube flow.
- b. Axial annular flow.
- c. Tangential annular flow.
- d. Helical annular flow.
- e. Flow between parallel planes.
- f. Flow between rotating disks.
- g. Cone-and-plate flow.

Although Eq. 4.1-4 gives correct results for flow rates and shearing forces in steady shear flows, we hasten to add that engineers have not hesitated to apply this equation to somewhat more complicated flows and systems slowly varying with time. A thorough assessment of the errors inherent in such calculations is not available, but one feels intuitively that such a practice probably represents good engineering empiricism. We give a few examples of this presently, and then in §4.6 we discuss the limits on the use of the model.

Let us now turn to the empiricisms for  $\eta(\dot{\gamma})$ . From Chapter 3 we know the appearance of the  $\eta$  vs.  $\dot{\gamma}$  curves. Although for some problems one can use the raw data for  $\eta(\dot{\gamma})$ , it is often useful to make calculations and derivations with simple empirical equations for  $\eta(\dot{\gamma})$  that are known to describe the experimental data with sufficient accuracy. Many such empiricisms are available, and we make no attempt at completeness. We cite only two here and mention some others in Table 4.5-1.

a. The Carreau–Yasuda Model (Parameters:  $\eta_0, \eta_\infty, \lambda, n, a$ )

This five-parameter model has sufficient flexibility to fit a wide variety of experimental  $\eta(\dot{\gamma})$  curves; it has proven to be useful for numerical calculations in which one needs an analytical expression for the non-Newtonian viscosity curve. The model is<sup>3,4</sup>

$$\frac{\eta - \eta_\infty}{\eta_0 - \eta_\infty} = [1 + (\lambda \dot{\gamma})^a]^{(n-1)/a} \tag{4.1-9}$$

Here  $\eta_0$  is the zero-shear-rate viscosity,  $\eta_\infty$  is the infinite-shear-rate viscosity,  $\lambda$  is a time constant,  $n$  is the “power-law exponent” (since it describes the slope of  $(\eta - \eta_\infty)/(\eta_0 - \eta_\infty)$  in the “power-law region”), and  $a$  is a dimensionless parameter that describes the transition region between the zero-shear-rate region and the power-law region. Some examples of

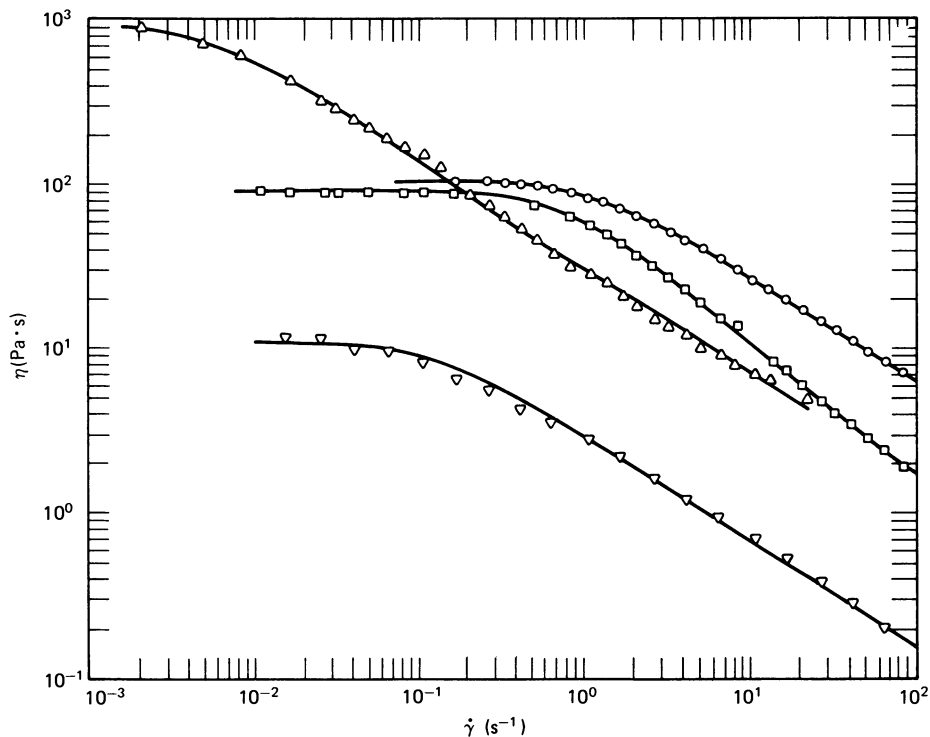


FIGURE 4.1-1. Non-Newtonian viscosity of three polymer solutions and a soap solution as fitted by the Carreau viscosity equation (Eq. 4.1-9, with  $a = 2$ ). [R. B. Bird, O. Hassager, and S. I. Abdel-Khalik, *AIChE J.*, **20**, 1041-1066 (1974).]  $\Delta$  2% polyisobutylene in Primol 355; data of J. D. Huppler, E. Ashare, and L. A. Holmes, *Trans. Soc. Rheol.*, **11**, 159-179 (1968):  $\eta_0 = 9.23 \times 10^2$  Pa·s,  $\eta_\infty = 1.50 \times 10^{-1}$  Pa·s,  $\lambda = 191$  s,  $n = 0.358$ .  $\circ$  5% polystyrene in Aroclor 1242; data of E. Ashare, Ph.D. Thesis, University of Wisconsin, Madison (1968):  $\eta_0 = 1.01 \times 10^2$  Pa·s,  $\eta_\infty = 5.9 \times 10^{-2}$  Pa·s,  $\lambda = 0.84$  s,  $n = 0.364$ .  $\nabla$  0.75% polyacrylamide (Separan-30) in a 95/5 mixture by weight of water and glycerin; data of B. D. Marsh (1967), as cited by P. J. Carreau, I. F. Macdonald, and R. B. Bird, *Chem. Eng. Sci.*, **23**, 901-911 (1968):  $\eta_0 = 10.6$  Pa·s,  $\eta_\infty = 10^{-2}$  Pa·s,  $\lambda = 8.04$  s,  $n = 0.364$ .  $\square$  7% aluminum soap in decalin and *m*-cresol; data of J. D. Huppler, E. Ashare, and L. A. Holmes, *loc. cit.*:  $\eta_0 = 89.6$  Pa·s,  $\eta_\infty = 10^{-2}$  Pa·s,  $\lambda = 1.41$  s,  $n = 0.200$ .

curve-fitting of experimental data are given in Figs. 4.1-1, 2, and 3, and sample values of the parameters in the Carreau-Yasuda model are given in Table 4.1-1 for polystyrene solutions. For many concentrated polymer solutions and melts, good fits can be obtained for  $a = 2$  and  $\eta_\infty = 0$ ; then only three parameters  $\eta_0$ ,  $\lambda$ , and  $n$  need to be determined. Equation 4.1-9, with  $a = 2$ , is usually referred to as the Carreau equation,<sup>3</sup> since the parameter  $a$  was added later by Yasuda.<sup>4</sup>

#### b. The "Power-Law" Model<sup>5</sup> of Ostwald and de Waele (Parameters: $m$ and $n$ )

In almost all industrial problems the descending linear region (the "power-law region") of the plot of  $\log \eta$  vs.  $\log \dot{\gamma}$ , seen in Figs. 4.1-1, 2, and 3, is the most important

<sup>3</sup> P. J. Carreau, Ph.D. Thesis, University of Wisconsin, Madison (1968).

<sup>4</sup> K. Yasuda, Ph.D. Thesis, Massachusetts Institute of Technology, Cambridge (1979); K. Yasuda, R. C. Armstrong, and R. E. Cohen, *Rheol. Acta*, **20**, 163-178 (1981).

<sup>5</sup> W. Ostwald, *Kolloid-Z.*, **36**, 99-117 (1925); A. de Waele, *Oil Color Chem. Assoc. J.* **6**, 33-88 (1923).

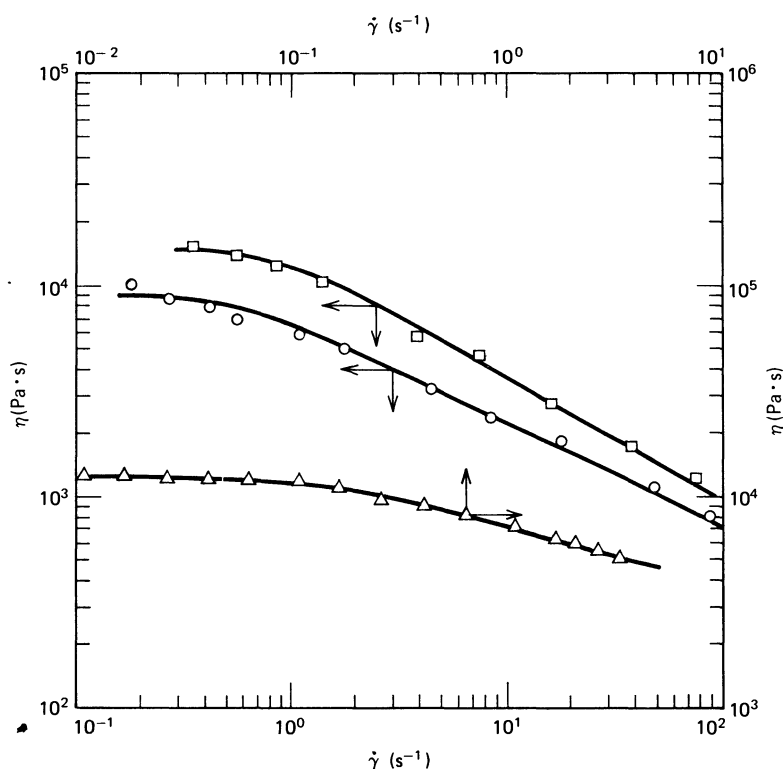


FIGURE 4.1-2. Non-Newtonian viscosity of three polymer melts as described by the Carreau viscosity equation (Eq. 4.1-9, with  $a = 2$ ). [S. I. Abdel-Khalik, O. Hassager, and R. B. Bird, *Polym. Eng. Sci.*, **14**, 859–867 (1974).]  $\square$  Polystyrene at 453 K; data of T. F. Ballenger, I.-J. Chen, J. W. Crowder, G. E. Hagler, D. C. Bogue, and J. L. White, *Trans. Soc. Rheol.*, **15**, 195–215 (1971):  $\eta_0 = 1.48 \times 10^4 \text{ Pa}\cdot\text{s}$ ,  $\eta_\infty = 0$ ,  $\lambda = 1.04 \text{ s}$ ,  $n = 0.938$ .  $\circ$  High-density polyethylene at 443 K; data of Ballenger, *et al.*, *loc. cit.*:  $\eta_0 = 8.92 \times 10^3 \text{ Pa}\cdot\text{s}$ ,  $\eta_\infty = 0$ ,  $\lambda = 1.58 \text{ s}$ ,  $n = 0.496$ .  $\triangle$  Phenoxy-A at 485 K; data of B. D. Marsh as cited by P. J. Carreau, I. F. Macdonald, and R. B. Bird, *Chem. Eng. Sci.*, **23**, 901–911 (1968):  $\eta_0 = 1.24 \times 10^4 \text{ Pa}\cdot\text{s}$ ,  $\eta_\infty = 0$ ,  $\lambda = 7.44 \text{ s}$ ,  $n = 0.728$ .

region. In fact, for many inexpensive viscometers and for many fluids, it is almost impossible to obtain data for the horizontal region of the  $\eta(\dot{\gamma})$  curve. The tilted straight line can be described by a simple “power-law” expression:

$$\eta = m\dot{\gamma}^{n-1} \quad (4.1-10)$$

which contains two parameters:  $m$  (with units of  $\text{Pa}\cdot\text{s}^n$ ), and  $n$  (dimensionless). Equation 4.1-10 may also be regarded as the limiting expression for high shear rates obtained from Eq. 4.1-9 (with  $\eta_\infty = 0$ ); it is then evident that the exponent  $n$  in the power-law model has the same meaning as the  $n$  in the Carreau–Yasuda equation, and that the  $m$  of the power law (sometimes referred to as the “consistency index”) is  $\eta_0 \lambda^{n-1}$ . When  $n = 1$  and  $m = \mu$  the Newtonian fluid is recovered. If  $n < 1$ , the fluid is said to be “pseudoplastic” or “shear thinning,” and if  $n > 1$ , the fluid is called “dilatant” or “shear thickening.”<sup>6</sup> Some sample

<sup>6</sup> M. Reiner, *op cit.*, pp. 306–308, and others use the term “dilatancy” to describe the change in volume of granular masses necessitated by a distortion. The standard example is the apparent drying of wet sand when stepped on.

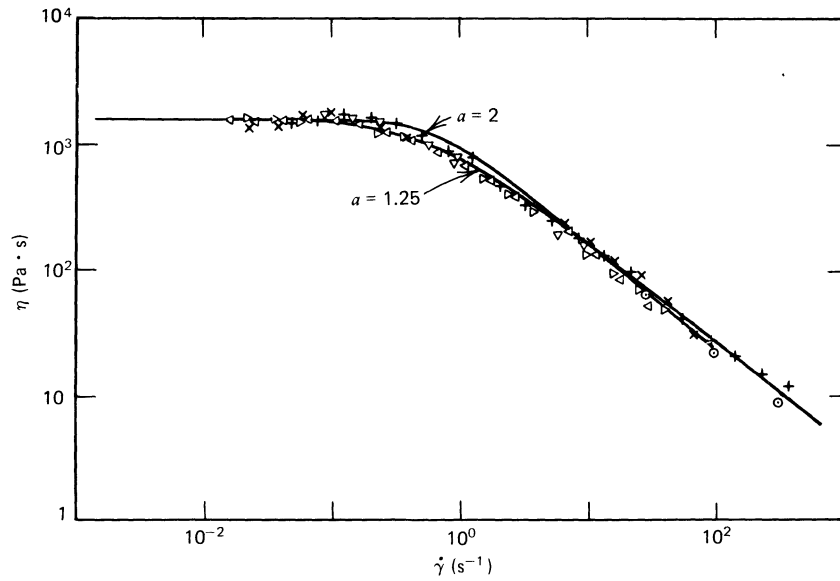


FIGURE 4.1-3. Non-Newtonian viscosity of a solution of linear, monodisperse polystyrene in 1-chloronaphthalene as fitted by the Carreau-Yasuda viscosity equation in Eq. 4.1-9. The concentration of polymer is 0.15 g/ml, and  $\bar{M}_w = 2 \times 10^6$ . Fits are shown for two different choices of the parameter  $a$ . For  $a = 1.25$ , the other model parameters are  $\eta_0 = 1400$  Pa·s,  $\lambda = 1.60$  s,  $n = 0.2$ , and  $\eta_\infty = 0$ . [K. Yasuda, Ph.D. Thesis, Massachusetts Institute of Technology, Cambridge (1979).]

TABLE 4.1-1

Parameters in Carreau-Yasuda Model for Some Solutions of Linear Polystyrene in 1-Chloronaphthalene<sup>a</sup>

Properties of Solution		Parameters in Eq. 4.1-9 ( $\eta_\infty$ is taken to be zero)			
$\bar{M}_w$ (g/mol)	$c$ (g/ml)	$\eta_0$ (Pa·s)	$\lambda$ (s)	$n$ (---)	$a$ (---)
$2 \times 10^6$	0.15	1400	1.60	0.200	1.25
$2 \times 10^6$	0.088	90	$3.79 \times 10^{-1}$	0.265	0.98
$3.9 \times 10^5$	0.45	8080	1.109	0.304	2
$3.9 \times 10^5$	0.30	135	$3.61 \times 10^{-2}$	0.305	2
$1.1 \times 10^5$	0.52	1180	$9.24 \times 10^{-2}$	0.441	2
$1.1 \times 10^5$	0.45	166	$1.73 \times 10^{-2}$	0.538	2
$3.7 \times 10^4$	0.62	3930	$1 \times 10^{-1}$	0.217	2

<sup>a</sup> Values of the parameters are taken from K. Yasuda, R. C. Armstrong, and R. E. Cohen, *Rheol. Acta*, **20**, 163-178 (1981).

**TABLE 4.1-2**  
**Power-Law Parameters for Aqueous Solutions<sup>a</sup>**

Solution	Temperature (K)	$m$ (Pa · s <sup><i>n</i></sup> )	$n$ (—)
0.5% Hydroxyethylcellulose	293	0.84	0.509
	313	0.30	0.595
	333	0.136	0.645
2.0% Hydroxyethylcellulose	293	93.5	0.189
	313	59.7	0.223
	333	38.5	0.254
1.0% Polyethylene oxide	293	0.994	0.532
	313	0.706	0.544
	333	0.486	0.599

<sup>a</sup> R. M. Turian, Ph.D. Thesis, University of Wisconsin, Madison (1964), pp. 142–148.

numerical values of  $m$  and  $n$  are given in Table 4.1-2; note that  $m$  and  $n$  are both temperature dependent, the parameter  $m$  decreasing rapidly with increasing temperature.

The power-law model for  $\eta(\dot{\gamma})$  is the most well-known and widely-used empiricism in engineering work, because a wide variety of flow problems have been solved analytically for it. One can often get a rough estimate of the effect of the non-Newtonian viscosity by making a calculation based on the power-law model. However its shortcomings must not be overlooked: (i) it cannot describe the viscosity for very small shear rates, and in some problems this can lead to large errors, (ii) a characteristic time and a characteristic viscosity cannot be constructed from the parameters  $m$  and  $n$  alone, and this can be awkward in pursuing dimensional-analysis arguments (see §2.8), and (iii) there is no way to relate the parameters  $m$  and  $n$  to molecular weight and concentration, since the standard correlations are in terms of  $\eta_0$  and  $\eta^*(\omega)$  (see §3.6). Keep in mind that Eqs. 4.1-9 and 10 are just empirical curve fits of the experimental  $\eta(\dot{\gamma})$  curves. Because of the widespread use of the power-law model we illustrate its application in the next section.

## §4.2 ISOTHERMAL FLOW PROBLEMS

The procedure for the solution of elementary flow problems for generalized Newtonian fluids is exactly the same as for Newtonian fluids, except that the mathematics is more awkward because of the additional complexity introduced by the non-Newtonian viscosity function. In this section we give a series of examples to illustrate the solution procedure for power-law fluids. A summary of power-law solutions is given in Table 4.2-1.

**EXAMPLE 4.2-1** Flow of a Power-Law Fluid in a Straight Circular Tube and in a Slightly Tapered Tube

Rework Examples 1.3-2 and 1.3-3 for the power-law model.

**SOLUTION** For a straight tube of uniform cross section we postulate a solution of the form  $v_z = v_z(r)$ ,  $v_\theta = 0$ ,  $v_r = 0$ , and  $\mathcal{P} = \mathcal{P}(z)$ . The  $z$ -component of the equation of motion, in terms of  $\tau$ , is

$$0 = -\frac{d\mathcal{P}}{dz} - \frac{1}{r} \frac{d}{dr} (r\tau_{rz}) \quad (4.2-1)$$

**TABLE 4.2-1**  
**Solutions to Flow Problems for Power-Law Model**

Problem	Solution
Axial flow through a slit of width $W$ , thickness $2B$ , and length $L$ under a pressure drop $\mathcal{P}_0 - \mathcal{P}_L$ (with $B \ll W \ll L$ )	$Q = \frac{2WB^2}{(1/n) + 2} \left( \frac{(\mathcal{P}_0 - \mathcal{P}_L)B}{mL} \right)^{1/n}$ (A)
Axial flow through a circular tube of radius $R$ and length $L$ under a pressure drop $\mathcal{P}_0 - \mathcal{P}_L$ (with $R \ll L$ )	$Q = \frac{\pi R^3}{(1/n) + 3} \left( \frac{(\mathcal{P}_0 - \mathcal{P}_L)R}{2mL} \right)^{1/n}$ (B)
Axial flow through an annulus with inner and outer radii $\kappa R$ and $R$ , and length $L$ , under a pressure drop $\mathcal{P}_0 - \mathcal{P}_L$ ( $r = \beta R$ is the location of the maximum in the velocity profile—see Table 4.2-2)	$Q = \frac{\pi R^3}{(1/n) + 3} \left( \frac{(\mathcal{P}_0 - \mathcal{P}_L)}{2mL} \right)^{1/n} \cdot [(1 - \beta^2)^{1+(1/n)} - \kappa^{1-(1/n)}(\beta^2 - \kappa^2)^{1+(1/n)}]$ (C)
Axial flow through an annulus with no axial pressure drop; inner cylinder moves with velocity $V$ ( $\kappa, R, L$ have same meanings as in Eq. C)	$Q = \pi R^2 V \frac{(3 - (1/n))(1 - \kappa^2) - 2(1 - \kappa^{3-(1/n)})}{(3 - (1/n))(1 - \kappa^{1-(1/n)})}$ (D)
Applied torque $\mathcal{T}$ in tangential annular flow between two coaxial cylinders the inner one of which is being made to rotate at an angular velocity $W$ ( $\kappa, R, L$ have the same meanings as in Eq. C)	$\mathcal{T} = 2\pi(\kappa R)^2 mL \left( \frac{2W/n}{1 - \kappa^{2/n}} \right)^n$ (E)
Radial flow between two parallel disks separated by $2B$ , with pressure drop $\mathcal{P}_1 - \mathcal{P}_2$ over the distance from $r = R_1$ to $r = R_2$	$Q = \frac{4\pi B^2}{(1/n) + 2} \left( \frac{(\mathcal{P}_1 - \mathcal{P}_2)B(1 - n)}{m(R_2^{1-n} - R_1^{1-n})} \right)^{1/n}$ (F) <sup>a</sup>
Squeezing flow between two circular disks of radius $R$ , with applied force $F(t)$ and instantaneous disk separation $2h$ (the instantaneous plate velocity is $\dot{h}$ )	$F(t) = \frac{(-\dot{h})^n}{h^{2n+1}} \left( \frac{2n+1}{2n} \right)^n \left( \frac{\pi m R^{n+3}}{n+3} \right)$ (G) <sup>b</sup>

<sup>a</sup> Lubrication-approximation expression obtained by applying Eq. A locally in the space between disks.

<sup>b</sup> Approximate expression obtained by applying Eq. A locally and using a quasi-steady-state assumption.

or using the arguments given in Example 1.3-2

$$\frac{1}{r} \frac{d}{dr} (r\tau_{rz}) = \frac{\mathcal{P}_0 - \mathcal{P}_L}{L} \quad (4.2-2)$$

This may be integrated to give:

$$\tau_{rz} = \frac{(\mathcal{P}_0 - \mathcal{P}_L)r}{2L} + \frac{C_1}{r} \quad (4.2-3)$$

The constant  $C_1$  has to be zero since one does not expect to have an infinite stress at the tube axis. Equation 4.2-3 then is the result of the application of the equation of motion (i.e., conservation of momentum). Equation 4.2-3 may be written in the alternative form

$$\tau_{rz} = \tau_R \cdot \frac{r}{R} \quad (4.2-4)$$

where  $\tau_R$  is the wall shear stress; that is  $\tau_{rz} = \tau_R$  at  $r = R$ .

Next we have to use the power-law equation for the stress, as given by Eqs. 4.1-4 and 4.1-10. In the latter equation  $\dot{\gamma}$ , which must be a positive quantity, is given by  $(-dv_z/dr)$ . Then

$$\tau_{rz} = -\eta \frac{dv_z}{dr} = -m\dot{\gamma}^{n-1} \frac{dv_z}{dr} = m \left( -\frac{dv_z}{dr} \right)^n \quad (4.2-5)$$

Combination of Eqs. 4.2-4 and 4.2-5 then gives the differential equation for  $v_z$ :

$$m \left( -\frac{dv_z}{dr} \right)^n = \tau_R \cdot \frac{r}{R} \quad (4.2-6)$$

Taking the  $n$ th root of both sides and integrating the first-order, separable equation gives

$$v_z = -\left( \frac{\tau_R}{mR} \right)^{1/n} \frac{r^{(1/n)+1}}{(1/n)+1} + C_2 \quad (4.2-7)$$

The constant  $C_2$  is evaluated by requiring that  $v_z$  be zero at  $r = R$ . One then gets finally

$$v_z = \left( \frac{\tau_R}{m} \right)^{1/n} \frac{R}{(1/n)+1} \left[ 1 - \left( \frac{r}{R} \right)^{(1/n)+1} \right] \quad (4.2-8)$$

For  $n < 1$  this gives a velocity profile that is flatter than the parabolic profile in Eq. 1.3-10 for Newtonian fluids (see Fig. 4.2-1).

It is then easy to get the volume rate of flow  $Q$ :

$$\begin{aligned} Q &= \int_0^{2\pi} \int_0^R v_z r \, dr \, d\theta \\ &= 2\pi R^2 \int_0^1 v_z \cdot \frac{r}{R} \, d\left(\frac{r}{R}\right) \\ &= \frac{\pi R^3}{(1/n)+3} \left( \frac{\tau_R}{m} \right)^{1/n} \\ &= \frac{\pi R^3}{(1/n)+3} \left[ \frac{(\mathcal{P}_0 - \mathcal{P}_L)R}{2mL} \right]^{1/n} \end{aligned} \quad (4.2-9)$$

For  $n = 1$  and  $m = \mu$  this reduces to the Hagen-Poiseuille equation for Newtonian fluids.<sup>1</sup>

<sup>1</sup> Laminar-turbulent transition has been studied by D. W. Dodge and A. B. Metzner, *AIChE J.*, **5**, 189-204 (1959); they found that the laminar-turbulent transition occurred in the modified Reynolds number range  $2100 < \text{Re}_n < 3100$ , where  $\text{Re}_n = (D^n \langle v_z \rangle^{2-n} \rho / m)(3 + (1/n))^{-n} 2^{3-n}$  for power-law fluids. For other studies see N. W. Ryan and M. M. Johnson, *AIChE J.*, **5**, 433-435 (1959); R. W. Hanks, *ibid.*, **9**, 306-309 (1963); D. M. Meter, *ibid.*, **10**, 881-884 (1964).

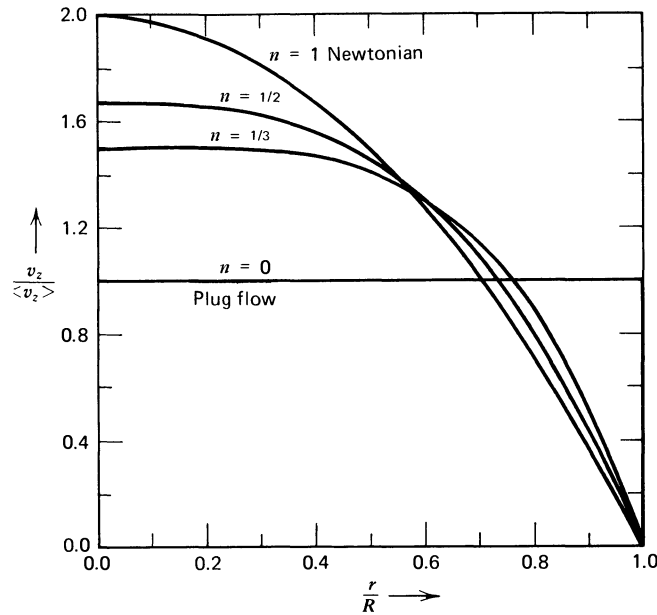


FIGURE 4.2-1. Tube flow velocity profiles for a power-law fluid from Eq. 4.2-8. Note that the profiles become increasingly flatter as  $n$  decreases;  $n = 0$  corresponds to plug flow. The Newtonian (parabolic) profile is shown as  $n = 1$ .

The shear rate at the tube wall,  $\dot{\gamma}_R = (-dv_z/dr)|_{r=R}$  is a quantity that is sometimes of interest in viscometry. An expression for this quantity can be obtained from Eqs. 4.2-6 and 9; it is found that  $\dot{\gamma}_R = [(3n + 1)/4n]\dot{\gamma}_a$ , where  $\dot{\gamma}_a = 4\langle v_z \rangle/R$  is the “apparent shear rate” (note that for a Newtonian fluid  $\dot{\gamma}_a$  is identical to  $\dot{\gamma}_R$ ).

As already pointed out, the power-law model gives an unreasonably high value for the viscosity  $\eta(\dot{\gamma})$  for small values of the shear rate. It is therefore appropriate to ask what limitations have to be placed on Eq. 4.2-9 because of this defect of the power law. It is shown in Problem 4B.13 that the power-law expression for  $Q$  can be expected to be reliable when  $\tau_R \gg \eta_0 \dot{\gamma}_0$ , where  $\eta_0$  is the zero-shear-rate viscosity and  $\dot{\gamma}_0$  is the value of the shear rate at which shear thinning begins (see §3.6).

For a tapered tube whose radius decreases linearly from  $R_0$  at  $z = 0$  to  $R_L$  at  $z = L$ , we get by applying Eq. 4.2-9 locally for a small segment  $dz$  of the tube

$$\mathcal{P}_0 - \mathcal{P}_L = \frac{2mL}{3n} \left[ \frac{Q}{\pi} \left( \frac{1}{n} + 3 \right) \right]^n \left( \frac{R_L^{-3n} - R_0^{-3n}}{R_0 - R_L} \right) \tag{4.2-10}$$

This gives the relation between pressure drop and volume rate of flow<sup>2</sup>.

Sutterby<sup>3</sup> found that the use of a generalized Newtonian fluid model described adequately the  $Q$  vs.  $\mathcal{P}_0 - \mathcal{P}_L$  relationship for the slow flow of polymer solutions in a converging tube. For very fast flow, on the other hand, the data were well described by the results of an ideal (inviscid) fluid calculation; this is perhaps not too surprising since the inviscid fluid corresponds to  $Re \rightarrow \infty$ .

The flow of non-Newtonian fluids in tapered tubes has also been studied by Oka and Murata.<sup>4</sup>

<sup>2</sup> J. M. McKelvey, V. Maire, and F. Haupt, *Chem. Eng.*, **83**, 94-102 (1976).

<sup>3</sup> J. L. Sutterby, *Trans. Soc. Rheol.*, **9**:2, 227-241 (1965).

<sup>4</sup> S. Oka, *Zairyō*, **14**, 241-244 (1965); S. Oka and T. Murata, *Jpn. J. Appl. Phys.*, **8**, 5-8 (1969); S. Oka, *Biorheology*, **10**, 207-212 (1973).

**EXAMPLE 4.2-2** Thickness of a Film of Polymer Solution Flowing Down an Inclined Plate

Obtain an expression for the thickness of a film of polymer solution as it flows down an inclined plate making an angle  $\alpha$  with the vertical. Use the power-law fluid model for the derivation. Take the origin of coordinates to be such that  $x = 0$  at the film surface and  $x = \delta$  at the plate; the film extends along the plate from  $z = 0$  to  $z = L$ .

**SOLUTION** From the equation of motion we get

$$0 = -\frac{d\tau_{xz}}{dx} + \rho g \cos \alpha \quad (4.2-11)$$

When this is integrated, using the boundary condition that  $\tau_{xz} = 0$  at the liquid-air interface at  $x = 0$ , we get

$$\tau_{xz} = \rho g x \cos \alpha \quad (4.2-12)$$

We know that  $v_z$  decreases with increasing  $x$ , so that  $\dot{\gamma}$  will be taken to be  $(-dv_z/dx)$  in order to ensure that  $\dot{\gamma}$  be a positive quantity. Then the power law gives the following expression for  $\tau_{xz}$ :

$$\begin{aligned} \tau_{xz} &= -\eta \frac{dv_z}{dx} = -m \left( -\frac{dv_z}{dx} \right)^{n-1} \frac{dv_z}{dx} \\ &= +m \left( -\frac{dv_z}{dx} \right)^n \end{aligned} \quad (4.2-13)$$

Combination of Eqs. 4.2-12 and 4.2-13 then gives

$$-\frac{dv_z}{dx} = \left( \frac{\rho g x \cos \alpha}{m} \right)^{1/n} \quad (4.2-14)$$

Integration with the boundary condition that  $v_z = 0$  at  $x = \delta$  gives

$$v_z = \left( \frac{\rho g \delta \cos \alpha}{m} \right)^{1/n} \frac{\delta}{(1/n) + 1} \left[ 1 - \left( \frac{x}{\delta} \right)^{(1/n) + 1} \right] \quad (4.2-15)$$

for the velocity distribution.

Integration over the cross section of flow (thickness  $\delta$  and width  $W$ ) gives for the volume rate of flow

$$Q = \frac{W\delta^2}{(1/n) + 2} \left( \frac{\rho g \delta \cos \alpha}{m} \right)^{1/n} \quad (4.2-16)$$

Solution for the film thickness then gives

$$\delta = \left( \frac{m}{\rho g \cos \alpha} \right)^{1/(2n+1)} \left( \frac{Q[(1/n) + 2]}{W} \right)^{n/(2n+1)} \quad (4.2-17)$$

This shows how the film thickness depends on the flow rate  $Q$ , the fluid properties  $m$  and  $n$ , and the angle of inclination  $\alpha$ .

**EXAMPLE 4.2-3** Plane Couette Flow<sup>5</sup>

A macromolecular fluid is confined to the space between two horizontal planes ( $x = 0$  and  $x = B$ ) the upper one of which is moving in the positive  $z$ -direction with a constant speed  $V$ . In addition there is a pressure gradient in the  $z$ -direction, the pressure at  $z = 0$  being  $p_0$  and that at  $z = L$  being  $p_L$ . Obtain an expression for the volume rate of flow in the  $z$ -direction in the slit that results from the combined effects of the motion of the upper plate and the pressure gradient. Ignore the effect of gravity.

Problems of this type arise in diverse processing operations, such as in certain types of extruders, and in various lubrication problems.

**SOLUTION** For this flow the equation of motion is

$$0 = -\frac{dp}{dz} - \frac{d\tau_{xz}}{dx} \quad (4.2-18)$$

which may be integrated to give

$$\tau_{xz} = -\left[\frac{(p_0 - p_L)B}{L}\right](\beta - \xi) \quad (4.2-19)$$

where  $\beta$  is a constant of integration, and  $\xi = x/B$ .

Equation 4.1-4 gives

$$\tau_{xz} = -\eta \frac{dv_z}{dx} \quad (4.2-20)$$

By way of illustration, we use the power law for  $\eta$ . Two cases have to be distinguished here:

*Case I:* There is no maximum in the velocity profile  $v_z(x)$

*Case II:* There is a maximum in the velocity profile  $v_z(x)$

We consider only Case I, although the final results for Case II will be given.

For Case I,  $\eta = m(dv_z/dx)^{n-1}$  and hence Eq. 4.2-20 becomes

$$\tau_{xz} = -m\left(\frac{dv_z}{dx}\right)^n \quad (4.2-21)$$

Combination of Eqs. 4.2-19 and 4.2-21 gives an equation for  $v_z$  as a function of  $x$ . Integration of this equation and application of the boundary conditions  $v_z = 0$  at  $x = 0$  and  $v_z = V$  at  $x = B$  gives

$$\phi(\xi) = \frac{v_z}{V} = \frac{\beta^{s+1} - (\beta - \xi)^{s+1}}{\beta^{s+1} - (\beta - 1)^{s+1}} \quad (4.2-22)$$

where  $\xi = x/B$ ,  $s = 1/n$ , and  $\beta$  is a dimensionless parameter given by

$$\begin{aligned} \Lambda &\equiv \frac{(p_0 - p_L)B}{mL} \left(\frac{B}{V}\right)^{1/s} \\ &= \left[\frac{s+1}{\beta^{s+1} - (\beta-1)^{s+1}}\right]^{1/s} \quad \text{Case I: } \Lambda \leq (s+1)^{1/s} \end{aligned} \quad (4.2-23)$$

<sup>5</sup> R. W. Flumerfelt, M. W. Pierick, S. L. Cooper, and R. B. Bird, *Ind. Eng. Chem. Fundam.*, **8**, 354-357 (1969); earlier work was done on this problem by F. W. Kroesser and S. Middleman, *Polym. Eng. Sci.*, **5**, 230-234 (1965) and Z. Tadmor, *Polym. Eng. Sci.*, **6**, 203-212 (1966). Annular Couette flow has been studied by S. H. Lin and C. C. Hsu, *Ind. Eng. Chem. Fundam.*, **19**, 421-424 (1980).

Hence, knowing  $\beta = \beta(\Lambda, s)$  from Eq. 4.2-23, one can obtain the velocity profile from Eq. 4.2-22. The volume rate of flow between two planes of width  $W$  is then found to be

$$\begin{aligned} \frac{Q}{WBV} &= \int_0^1 \phi \, d\xi = \phi \xi \Big|_0^1 - \int_0^1 \frac{d\phi}{d\xi} \xi \, d\xi \\ &= -(\beta - 1) + \left( \frac{s+1}{s+2} \right) \frac{\beta^{s+2} - (\beta-1)^{s+2}}{\beta^{s+1} - (\beta-1)^{s+1}} \quad \text{Case I: } \Lambda \leq (s+1)^{1/s} \end{aligned} \quad (4.2-24)$$

with  $\beta$  determined from Eq. 4.2-23.

The results analogous to Eqs. 4.2-23 and 4.2-24 for Case II can be shown to be

$$\Lambda = \left[ \frac{s+1}{\beta^{s+1} - (1-\beta)^{s+1}} \right]^{1/s} \quad \text{Case II: } \Lambda \geq (s+1)^{1/s} \quad (4.2-25)$$

$$\frac{Q}{WBV} = (1-\beta) + \left( \frac{s+1}{s+2} \right) \frac{\beta^{s+2} + (1-\beta)^{s+2}}{\beta^{s+1} - (1-\beta)^{s+1}} \quad \text{Case II: } \Lambda \geq (s+1)^{1/s} \quad (4.2-26)$$

Hence, the choice of Case I or Case II formulas depends on whether  $\Lambda$  is larger or smaller than  $(s+1)^{1/s}$ . A table of  $\beta = \beta(\Lambda, s)$  has been prepared by Flumerfelt *et al.*<sup>5</sup> The dimensionless flow rate  $\Omega = Q/WBV$  is shown in Fig. 4.2-2; this chart is so constructed that it includes the case  $p_0 < p_L$  as well as  $p_0 > p_L$ .

In Case II there is a maximum or a minimum in the velocity profile. Near the maximum or minimum in the velocity the power law will overestimate the viscosity by a large amount. Errors in the volume flow rate  $Q$  may be large unless the bigger of  $|\tau_{xz}(x=0)|$  and  $|\tau_{xz}(x=B)|$  is much greater than  $\eta_0 \dot{\gamma}_0$ , where  $\dot{\gamma}_0$  is that shear rate at which shear thinning of the viscosity begins.

#### EXAMPLE 4.2-4 Axial Annular Flow<sup>6-8</sup>

Obtain the relation between the pressure drop and volume rate of flow for the pressure-driven flow of a power-law fluid through the annular gap between two coaxial cylinders of radii  $\kappa R$  and  $R$  (with  $\kappa < 1$ ). Let the maximum in the velocity distribution be located at  $r = \beta R$ , where  $\beta$  is a constant that has to be determined later.

**SOLUTION** We postulate that  $v_z = v_z(r)$ ,  $v_r = 0$ ,  $v_\theta = 0$ , and  $\mathcal{P} = \mathcal{P}(z)$ . Then the differential equation for  $\tau_{rz}$ , obtained from the  $z$ -component of the equation of motion, is found to be Eq. 4.2-1; this can be integrated to give Eq. 4.2-3, but the constant  $C_1$  cannot now be set equal to zero, because for this problem  $\kappa R \leq r \leq R$ . However we can rewrite Eq. 4.2-3 so that the constant  $\beta$  appears rather than  $C_1$ :

$$\tau_{rz} = \frac{(\mathcal{P}_0 - \mathcal{P}_L)R}{2L} \left( \frac{r}{R} - \beta^2 \frac{R}{r} \right) \quad (4.2-27)$$

<sup>6</sup> A. G. Fredrickson and R. B. Bird, *Ind. Eng. Chem.*, **50**, 347-352 (1958); erratum, *Ind. Eng. Chem. Fundam.*, **3**, 383 (1964).

<sup>7</sup> R. W. Hanks and K. M. Larsen, *Ind. Eng. Chem. Fundam.*, **18**, 33-35 (1979).

<sup>8</sup> For flow in converging annular regions see J. Parnaby and R. A. Worth, *Proc. Inst. Mech. Eng.*, **188**, 357-364 (1974), and J. F. Dijksman and E. P. W. Savenije, *Rheol. Acta*, **24**, 105-118 (1985); in the latter a special toroidal coordinate system is developed and used.

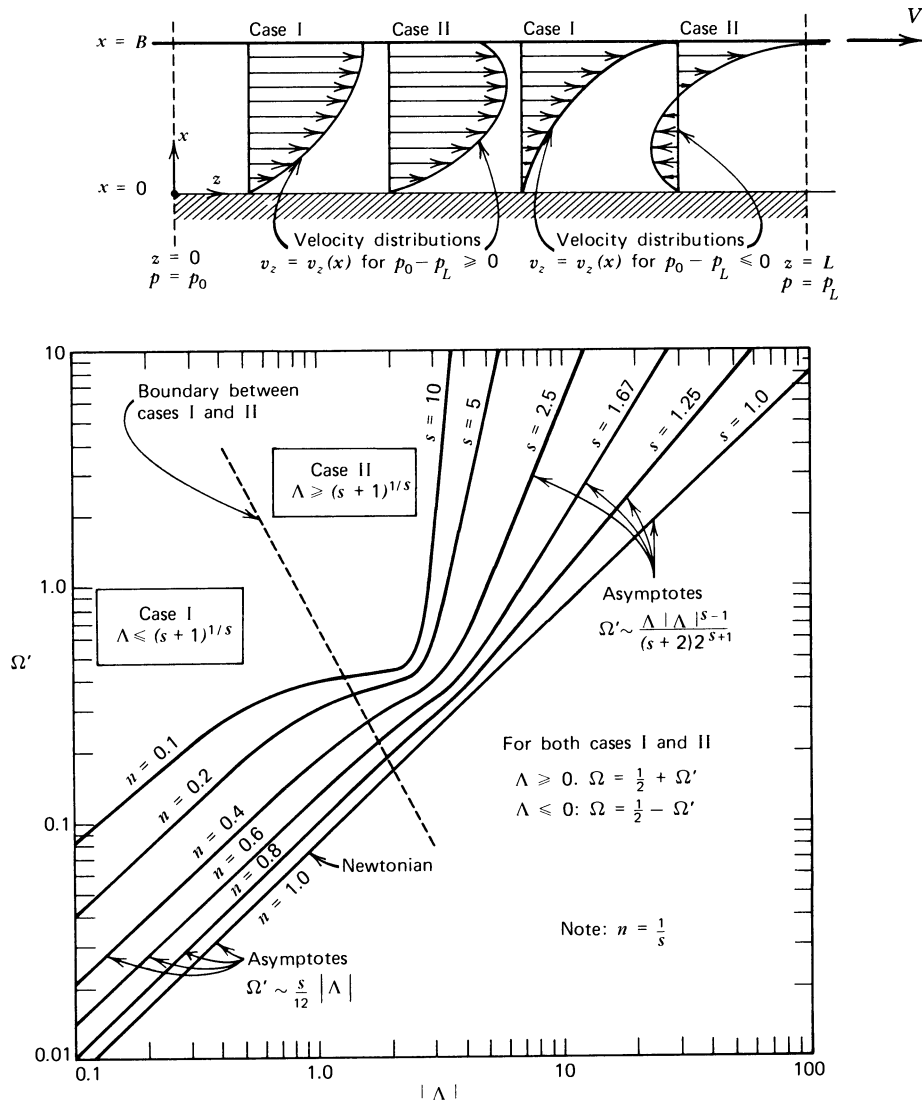


FIGURE 4.2-2. Dimensionless flow rate  $\Omega = Q/WBV$  as a function of  $\Lambda$  and  $n$  (or  $1/s$ ) for generalized Couette flow. [Reprinted with permission from R. W. Flumerfelt, M. W. Pierick, S. L. Cooper, and R. B. Bird, *Ind. Eng. Chem. Fundam.*, **8**, 354-387 (1969). Copyright by the American Chemical Society.]

The parameter  $\beta$  is then regarded as the “constant of integration.” The power-law expression for the shear stress is given by

$$\tau_{rz} = -m \left( \frac{dv_z}{dr} \right)^n, \quad \kappa R \leq r \leq \beta R \quad (4.2-28)$$

$$\tau_{rz} = m \left( -\frac{dv_z}{dr} \right)^n, \quad \beta R \leq r \leq R \quad (4.2-29)$$

Substitution of these expressions into Eq. 4.2-27 leads then to differential equations for the velocity distribution in the two regions. These equations may now be integrated and the boundary conditions used:  $v_z = 0$  at  $r = \kappa R$  and at  $r = R$ . This leads to

$$v_z = R \left[ \frac{(\mathcal{P}_0 - \mathcal{P}_L)R}{2mL} \right]^s \int_{\kappa}^{\xi} \left( \frac{\beta^2}{\xi'} - \xi' \right)^s d\xi', \quad \kappa \leq \xi \leq \beta \tag{4.2-30}$$

$$v_z = R \left[ \frac{(\mathcal{P}_0 - \mathcal{P}_L)R}{2mL} \right]^s \int_{\xi}^1 \left( \xi' - \frac{\beta^2}{\xi'} \right)^s d\xi', \quad \beta \leq \xi \leq 1 \tag{4.2-31}$$

in which  $\xi = r/R$  and  $s = 1/n$ .

Next the constant  $\beta$  is determined by requiring that Eqs. 4.2-30 and 31 match at the location of the velocity maximum; this gives at once

$$\int_{\kappa}^{\beta} \left( \frac{\beta^2}{\xi} - \xi \right)^s d\xi = \int_{\beta}^1 \left( \xi - \frac{\beta^2}{\xi} \right)^s d\xi \tag{4.2-32}$$

This relation gives  $\beta$  as a function of the geometrical quantity  $\kappa$  and the power-law exponent  $n$  (see Table 4.2-2).<sup>7</sup>

The volume rate of flow in the annulus is then<sup>7</sup>

$$\begin{aligned} Q &= 2\pi \int_{\kappa R}^R v_z r dr = \pi R^3 \left[ \frac{(\mathcal{P}_0 - \mathcal{P}_L)R}{2mL} \right]^s \int_{\kappa}^1 |\beta^2 - \xi^2|^{s+1} \xi^{-s} d\xi \\ &= \frac{\pi R^3}{(1/n) + 3} \left( \frac{\mathcal{P}_0 - \mathcal{P}_L}{2mL} \right)^{1/n} [(1 - \beta^2)^{1+(1/n)} - \kappa^{1-(1/n)}(\beta^2 - \kappa^2)^{1+(1/n)}] \end{aligned} \tag{4.2-33}$$

This result follows from substituting  $v_z(r)$  from Eqs. 4.2-30 and 31 into the integral for  $Q$ , and then interchanging the order of integration and performing the inner integrals.

TABLE 4.2-2  
Values of  $\beta(\kappa, n)$  Computed from Eq. 4.2-32<sup>a</sup>

$n$	$\kappa$								
	0.10	0.20	0.30	0.40	0.50	0.60	0.70	0.80	0.90
0.10	0.3442	0.4687	0.5632	0.6431	0.7140	0.7788	0.8389	0.8954	0.9489
0.20	0.3682	0.4856	0.5749	0.6509	0.7191	0.7818	0.8404	0.8960	0.9491
0.30	0.3884	0.4991	0.5840	0.6570	0.7229	0.7840	0.8416	0.8965	0.9492
0.40	0.4052	0.5100	0.5912	0.6617	0.7259	0.7858	0.8426	0.8969	0.9493
0.50	0.4193	0.5189	0.5970	0.6655	0.7283	0.7872	0.8433	0.8972	0.9493
0.60	0.4312	0.5262	0.6018	0.6686	0.7303	0.7884	0.8439	0.8975	0.9494
0.70	0.4412	0.5324	0.6059	0.6713	0.7319	0.7893	0.8444	0.8977	0.9495
0.80	0.4498	0.5377	0.6093	0.6735	0.7333	0.7902	0.8449	0.8979	0.9495
0.90	0.4572	0.5422	0.6122	0.6754	0.7345	0.7909	0.8452	0.8980	0.9495
1.00	0.4637	0.5461	0.6147	0.6770	0.7355	0.7915	0.8455	0.8981	0.9496

<sup>a</sup> This table is abstracted from the more complete Table I in R. W. Hanks and K. M. Larsen, *Ind. Eng. Chem. Fundam.*, **18**, 33-35 (1979).

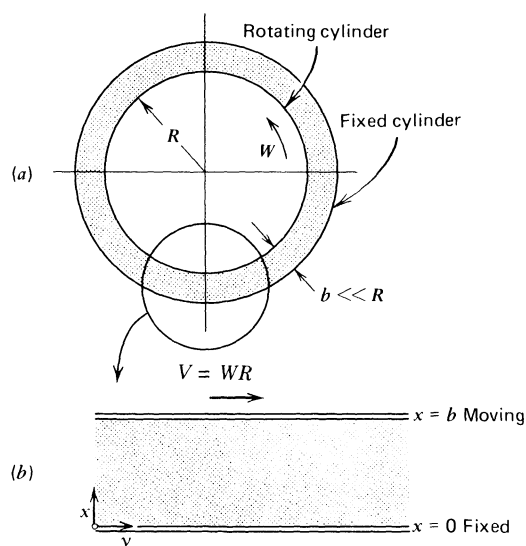


FIGURE 4.2-3. (a) Helical flow in a thin annulus; the fluid flows axially because of a pressure gradient and tangentially because of the rotating inner cylinder. (b) Coordinate system to be used for the equivalent problem neglecting curvature.

In this flow an appreciable portion of the fluid is in a low shear-rate region, namely that which passes through a washer-shaped region about  $r = \beta R$ . The width of this washer-shaped ring increases as the pressure drop decreases, and in that region the viscosity from the power law will be much greater than the experimental value; as a consequence volume flow rates from Eq. 4.2-33 can be expected to be lower than the experimental values. The errors introduced by overestimating the viscosity near  $r = \beta R$  will be negligible if the wall shear stresses at the inner and outer cylinders,  $\tau_{\kappa R}$  and  $\tau_R$ , are both much greater than  $\eta_0 \dot{\gamma}_0$ . This point is pursued further in Example 4.5-2.

#### EXAMPLE 4.2-5 Enhancement of Axial Annular Flow by Rotating Inner Cylinder (Helical Flow of a Power-Law Fluid)<sup>9</sup>

Here we consider the axial flow in a very thin annulus where the inner cylinder radius is  $R$  and the gap width is  $b$ , which is much smaller than  $R$ . The flow is driven by a pressure gradient. We want to investigate the way in which the flow rate changes if the inner cylinder is made to rotate. In this illustrative example we have more than one nonvanishing component of  $\dot{\gamma}$ , so that the flows in the two directions are coupled through the dependence of the non-Newtonian viscosity on the magnitude of  $\dot{\gamma}$  defined in Eq. 4.1-8.

**SOLUTION** The system is sketched in Fig. 4.2-3a. Because of the thinness of the slit, curvature can be neglected and the original problem becomes equivalent to the plane-slit problem shown in Fig. 4.2-3b; in this figure we also show the coordinate system we use. We postulate that  $v_z = v_z(x)$ ,  $v_y = v_y(x)$ ,  $v_x = 0$ , and  $\mathcal{P} = \mathcal{P}(z)$ .

<sup>9</sup> This problem has been studied experimentally and theoretically by A. C. Dierckes, Jr. and W. R. Schowalter, *Ind. Eng. Chem. Fundam.*, **5**, 263-271 (1966); numerical calculations for the Oldroyd model viscosity function (Eq. A of Table 7.3-3) have been made by J. G. Savins and G. C. Wallick, *AIChE J.*, **12**, 357-363 (1966). See also B. D. Coleman, H. Markovitz, and W. Noll, *Viscometric Flows of Non-Newtonian Fluids*, Springer, New York, (1966), pp. 37-41.

For these postulates the equations of motion become:

$$\text{y-component} \quad 0 = -\frac{d}{dx} \tau_{xy} \quad (4.2-34)$$

$$\text{z-component} \quad 0 = \frac{\mathcal{P}_0 - \mathcal{P}_L}{L} - \frac{d}{dx} \tau_{xz} \quad (4.2-35)$$

where  $\mathcal{P}_0 - \mathcal{P}_L$  is the modified pressure drop between  $z = 0$  and  $z = L$ . The components of the stress tensor for the power-law fluid are

$$\tau_{xy} = -\eta(\dot{\gamma})\dot{\gamma}_{xy} = -m\dot{\gamma}^{n-1}\dot{\gamma}_{xy} \quad (4.2-36)$$

$$\tau_{xz} = -\eta(\dot{\gamma})\dot{\gamma}_{xz} = -m\dot{\gamma}^{n-1}\dot{\gamma}_{xz} \quad (4.2-37)$$

in which the magnitude of the rate-of-strain tensor is

$$\dot{\gamma} = \sqrt{\left(\frac{dv_y}{dx}\right)^2 + \left(\frac{dv_z}{dx}\right)^2} \quad (4.2-38)$$

It is convenient to use dimensionless quantities

$$\bar{x} = \frac{x}{b}; \quad \bar{v}_i = \frac{v_i}{V}; \quad a = \frac{(\mathcal{P}_0 - \mathcal{P}_L) b^{n+1}}{mL V^n} \quad (4.2-39)$$

and further to abbreviate  $d\bar{v}_y/d\bar{x}$  by  $Y$  and  $d\bar{v}_z/d\bar{x}$  by  $Z$ . Then the equations of motion, in terms of the velocity gradients, become

$$\frac{d}{d\bar{x}} [(Y^2 + Z^2)^{(n-1)/2} Y] = 0 \quad (4.2-40)$$

$$\frac{d}{d\bar{x}} [(Y^2 + Z^2)^{(n-1)/2} Z] = -a \quad (4.2-41)$$

These equations may be integrated at once, and we use the symbols  $C_1$  and  $C_2$  for the constants of integration that appear on the right side. When these equations are then solved for  $Y$  and  $Z$ , we get

$$Y = \frac{d\bar{v}_y}{d\bar{x}} = C_1 [C_1^2 + (C_2 - a\bar{x})^2]^{(1-n)/2n} \quad (4.2-42)$$

$$Z = \frac{d\bar{v}_z}{d\bar{x}} = (C_2 - a\bar{x}) [C_1^2 + (C_2 - a\bar{x})^2]^{(1-n)/2n} \quad (4.2-43)$$

From this point on we specialize to  $n = 1/3$ , since for this choice an analytical solution can be obtained. The data in §4.1 suggest that  $n = 1/3$  is very nearly appropriate for some polymer solutions.

Integration of Eqs. 4.2-42 and 4.2-43 with  $n = 1/3$  gives

$$\bar{v}_y = \int_0^{\bar{x}} C_1 [C_1^2 + (C_2 - a\bar{x})^2] d\bar{x} \quad (4.2-44)$$

$$\bar{v}_z = \int_0^{\bar{x}} (C_2 - a\bar{x}) [C_1^2 + (C_2 - a\bar{x})^2] d\bar{x} \quad (4.2-45)$$

in which the integration constants have been set equal to zero since both velocity components are zero at  $\bar{x} = 0$ . The boundary condition that  $d\bar{v}_z/d\bar{x} = 0$  at  $\bar{x} = 1/2$  then leads to

$$C_2 = \frac{a}{2} \quad (4.2-46)$$

The boundary condition that  $\bar{v}_y = 1$  at  $\bar{x} = 1$  leads to the cubic equation  $C_1^3 + \frac{1}{12}a^2C_1 - 1 = 0$ , which has only one real root, according to Descartes' rule of signs. That root is

$$C_1 = A_+ + A_- \quad (4.2-47)$$

in which

$$A_{\pm} = \sqrt[3]{\frac{1}{2} \pm \sqrt{\frac{1}{4} + \frac{1}{27}\left(\frac{a^2}{12}\right)^3}} \quad (4.2-48)$$

For large values of  $a$  (i.e., large pressure drop or small angular velocity of the inner cylinder) this last expression can be expanded as

$$C_1 = (12/a^2) - (12/a^2)^4 + \dots \quad (4.2-49)$$

This expansion is used presently.

The integrals in Eqs. 4.2-44 and 45 are now performed to give the velocity profiles (see Fig. 4.2-4):

$$\bar{v}_y = C_1 \left[ C_1^2 \bar{x} + \frac{a^2}{12} (3\bar{x} - 6\bar{x}^2 + 4\bar{x}^3) \right] \quad (4.2-50)$$

$$\bar{v}_z = \frac{a}{2} \left[ \left( C_1^2 + \frac{a^2}{4} \right) \bar{x} - \frac{1}{2} a^2 \bar{x}^2 + \frac{1}{3} a^2 \bar{x}^3 \right] - a \left[ \left( C_1^2 + \frac{a^2}{4} \right) \frac{\bar{x}^2}{2} - \frac{1}{3} a^2 \bar{x}^3 + \frac{1}{4} a^2 \bar{x}^4 \right] \quad (4.2-51)$$

and the axial volume rate of flow through the annulus is

$$\begin{aligned} Q &= 2\pi R \int_0^b v_z dx = 2\pi R^2 b W \int_0^1 \bar{v}_z d\bar{x} \\ &= \frac{\pi R^2 b W a^3}{40} \left[ 1 + \frac{20}{3} \left( \frac{C_1}{a} \right)^2 \right] \end{aligned} \quad (4.2-52)$$

in which  $a = (b\Delta\mathcal{P}/mL)(b/WR)^{1/3}$ . Use of Eq. 4.2-49 then leads to

$$\begin{aligned} Q &= \frac{\pi R^2 b W a^3}{40} \left[ 1 + \frac{960}{a^6} + \dots \right] \\ &= \frac{\pi R b^2}{40} \left( \frac{b\Delta\mathcal{P}}{mL} \right)^3 \left[ 1 + 960 \left( \frac{WR}{b} \right)^2 \left( \frac{mL}{b\Delta\mathcal{P}} \right)^6 + \dots \right] \end{aligned} \quad (4.2-53)$$

in which  $\Delta\mathcal{P} = \mathcal{P}_0 - \mathcal{P}_L$ . This shows that the flow in the axial direction is enhanced because of the imposed shearing in the tangential direction, since this additional shearing causes the viscosity to be lowered. Note that the correction term is very sensitive to the slit width, which enters as the inverse eighth power, and the pressure gradient, which appears to the minus sixth power. This is a good

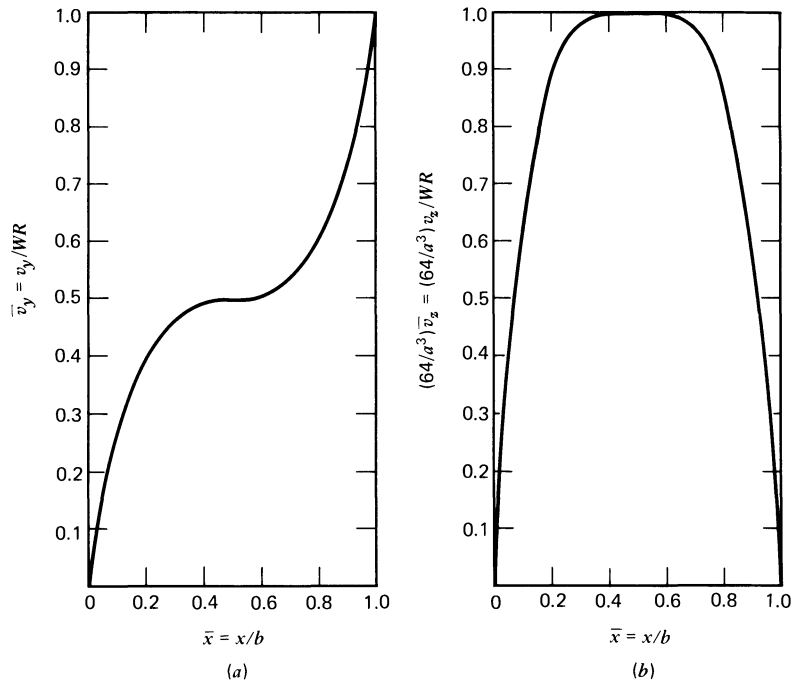


FIGURE 4.2-4. Velocity profiles for helical flow in a thin annular gap. (a) The dimensionless tangential velocity  $\bar{v}_y = v_y/WR$ , given by Eq. 4.2-50, and (b) the dimensionless axial velocity  $\bar{v}_z = v_z/WR$ , given by Eq. 4.2-51. In these velocity expressions  $C_1$  has been taken to be  $12/a^2$  (see Eq. 4.2-49). If there were no axial flow,  $\bar{v}_y$  would be the linear function  $\bar{v}_y = \bar{x}$ ; the deviation from linearity results from the change in viscosity across the cross section, brought about by the axial flow.

illustration of how the power-law model can be used to ascertain the sensitivity of a quantity (e.g.,  $Q$ ) to the key parameters in the system (e.g.,  $b$  and  $\Delta\mathcal{P}$ ).

**EXAMPLE 4.2-6** Flow Enhancement Produced by a Pulsatile Pressure Drop in a Circular Tube (Quasi-Steady-State Approximation)<sup>10</sup>

A polymer is flowing axially in a horizontal circular tube of radius  $R$  and length  $L$  as a result of a sinusoidally varying pressure drop

$$\Delta p = \Delta p_0 \cdot (1 + \varepsilon \Re e\{e^{i\omega t}\}) \tag{4.2-54}$$

in which  $\Delta p = p_0 - p_L$ , and  $\Delta p_0$  is the corresponding quantity for  $\varepsilon = 0$ . The parameter  $\varepsilon$  is presumed to be small with respect to unity.

a. Find the volume rate of flow  $Q(t)$  by applying Eq. B of Table 4.2-1 instantaneously. Then find  $\langle Q \rangle$ , the average value of  $Q$  over one cycle of oscillation; also find the flow-rate enhancement  $(\langle Q \rangle - Q_0)/Q_0$ , where  $Q_0$  is the flow rate with  $\varepsilon = 0$ .

b. Find the power requirement for pumping the material through the circular tube with a pulsatile pressure gradient. What conclusions can you draw?

<sup>10</sup> H. A. Barnes, P. Townsend, and K. Walters, *Rheol. Acta*, **10**, 517-527 (1971); *Nature*, **224**, 585-587 (1969). See also J. M. Davies, S. Bhumeratana, and R. B. Bird, *J. Non-Newtonian Fluid Mech.*, **3**, 237-259 (1977/1978), and N. Phan-Thien and J. Dudek, *J. Non-Newtonian Fluid Mech.*, **11**, 147-161 (1982). Viscoelastic effects are discussed in Example 7.4-2.

**SOLUTION** (a) In the quasi-steady-state approximation

$$Q(t) = \frac{\pi R^3}{(1/n) + 3} \left( \frac{\Delta p_0 R}{2mL} \right)^{1/n} (1 + \varepsilon \Re\{e^{i\omega t}\})^{1/n} \quad (4.2-55)$$

for the power-law fluid model.

Then the time average volume flow rate is

$$\begin{aligned} \frac{\langle Q \rangle}{Q_0} &= \langle (1 + \varepsilon \Re\{e^{i\omega t}\})^{1/n} \rangle \\ &= 1 + \varepsilon \frac{1}{n} \langle \Re\{e^{i\omega t}\} \rangle + \varepsilon^2 \frac{1}{2} \left( \frac{1}{n} \right) \left( \frac{1}{n} - 1 \right) \langle [\Re\{e^{i\omega t}\}]^2 \rangle + \dots \end{aligned} \quad (4.2-56)$$

in which an expansion for small  $\varepsilon$  has been made. The time average of  $\Re\{e^{i\omega t}\}$  is zero, and the time average of its square is<sup>11</sup>

$$\langle [\Re\{e^{i\omega t}\}]^2 \rangle = \frac{1}{2} \langle \Re\{e^{2i\omega t}\} + 1 \rangle = \frac{1}{2} \quad (4.2-57)$$

The flow-rate enhancement is then given by:

$$\frac{\langle Q \rangle - Q_0}{Q_0} = \frac{1}{4} \left( \frac{1-n}{n^2} \right) \varepsilon^2 + O(\varepsilon^4) \quad (4.2-58)$$

The power law thus predicts that the enhancement increases as  $n$  decreases from unity (i.e., as the fluid becomes more non-Newtonian), and that it is independent of the frequency.

(b) The time-averaged power  $\langle P \rangle$  required to pump the fluid is:<sup>12</sup>

$$\begin{aligned} \langle P \rangle &= \left\langle \iint v_z \Delta p \, r dr d\theta \right\rangle \\ &= \langle Q \Delta p \rangle \\ &= Q_0 \Delta p_0 \langle (1 + \varepsilon \Re\{e^{i\omega t}\})^{(1/n)+1} \rangle \\ &= Q_0 \Delta p_0 \left( 1 + \varepsilon^2 \frac{1}{2} \left( \frac{1}{n} + 1 \right) \left( \frac{1}{n} \right) \langle [\Re\{e^{i\omega t}\}]^2 \rangle + \dots \right) \end{aligned} \quad (4.2-59)$$

Hence the fractional increase in power needed is

$$\frac{\langle P \rangle - P_0}{P_0} = \frac{1}{4} \left( \frac{1+n}{n^2} \right) \varepsilon^2 + \dots \quad (4.2-60)$$

<sup>11</sup> The following relation is useful:

$$\Re\{w_1\} \Re\{w_2\} = \frac{1}{2} [\Re\{w_1 w_2\} + \Re\{w_1 \bar{w}_2\}] \quad (4.2-56a)$$

in which  $w_1$  and  $w_2$  are two complex quantities and the overbar indicates a complex conjugate.

<sup>12</sup> S. Middleman, *Fundamentals of Polymer Processing*, McGraw-Hill, New York (1977), p. 114.

Comparison of Eqs. 4.2-58 and 60 shows that the flow-rate enhancement increases less rapidly than the power requirement. Hence there is no energetic advantage to pumping with a sinusoidal pressure gradient.

Flow enhancement under sinusoidal pumping has been observed experimentally; data comparisons are given in Example 7.4-2, where this problem is solved again using a constitutive equation that describes elastic effects, and without the quasi-steady-state assumption. It is found there that the enhancement in Eq. 4.2-58 is exact through order  $\varepsilon^2$  for the power-law viscosity function.

**EXAMPLE 4.2-7** Squeezing Flow between Two Parallel Circular Disks (Lubrication Approximation and Quasi-Steady-State Approximation)

Analyze the flow of a power-law fluid in the gap between two circular disks that approach one another according to some prescribed velocity (see Fig. 4.2-5). The velocity of the upper plate is given by  $\dot{h} = dh/dt$ . Use a lubrication approximation and a quasi-steady-state assumption; that is, assume that the instantaneous volume rate of flow  $Q(r)$  across the cylindrical surface at  $r$  is that for flow through a slit of thickness  $2h$  and width  $2\pi r$ . Equate this  $Q(r)$  to the volumetric flow rate obtained by a conservation-of-mass statement.

Obtain the time required to squeeze out half of the liquid in the gap by the application of a constant force  $F$  on the disks.

**SOLUTION** Conservation of mass states that, for an incompressible fluid, the volume rate at which fluid crosses the cylindrical surface at  $r$  should equal the rate at which the volume between the two plates within the cylindrical surface at  $r$  decreases:

$$Q(r) = 2\pi r^2 (-\dot{h}) \tag{4.2-61}$$

To apply Eq. A of Table 4.2-1 to the flow between the disks in the region between  $r$  and  $r + dr$  we make the following changes of notation:

$$\begin{aligned} W &\rightarrow 2\pi r \\ B &\rightarrow h \\ (\mathcal{P}_0 - \mathcal{P}_L)/L &\rightarrow -dp/dr \\ Q &\rightarrow Q(r) \end{aligned}$$

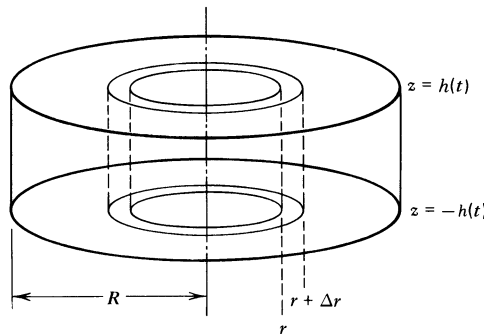


FIGURE 4.2-5. Squeezing flow between two circular disks of radius  $R$ . The instantaneous disk separation is  $2h(t)$ .

Then we get for the volume rate of flow:

$$Q(r) = \frac{2 \cdot 2\pi r \cdot h^2}{(1/n) + 2} \left( -\frac{h}{m} \frac{dp}{dr} \right)^{1/n} \quad (4.2-62)$$

When Eqs. 4.2-61 and 62 are equated, we get an equation for  $p$  as a function of  $r$ . When this is integrated with respect to  $r$ , with the boundary condition  $p = p_a$  at  $r = R$ , we get

$$p - p_a = m \frac{(-\dot{h})^n}{h^{2n+1}} \left( \frac{2n+1}{2n} \right)^n \frac{R^{n+1}}{n+1} \left[ 1 - \left( \frac{r}{R} \right)^{n+1} \right] \quad (4.2-63)$$

where  $p_a$  is the atmospheric pressure.

The force on the upper plate required to move the plate at a speed  $\dot{h}$  is then:

$$F(t) = \int_0^{2\pi} \int_0^R (p - p_a + \tau_{zz}) \Big|_{z=h} r dr d\theta \quad (4.2-64)$$

The normal stress  $\tau_{zz}$  at the upper plate is zero by the same arguments used for Newtonian fluids (see Example 1.2-1). When  $p - p_a$  from Eq. 4.2-63 is substituted into the integral for  $F(t)$  we get

$$F(t) = \frac{(-\dot{h})^n}{h^{2n+1}} \left( \frac{2n+1}{2n} \right)^n \frac{\pi m R^{n+3}}{n+3} \quad (4.2-65)$$

This is the *Scott equation*,<sup>13,14</sup> which was first developed for measuring the non-Newtonian viscosity of unvulcanized rubber stocks.

For a constant force  $F$ , Eq. 4.2-65 is an ordinary differential equation for  $h(t)$ . When this equation is integrated from  $t = 0$  (when  $h = h_0$ ) to  $t = t_{1/2}$  (when  $h = h_0/2$ ), the following equation is obtained for  $t_{1/2}$ :

$$\frac{t_{1/2}}{n} = K_n \left( \frac{\pi R^2 m}{F} \right)^{1/n} \left( \frac{R}{h_0} \right)^{1+(1/n)} \quad (4.2-66)$$

in which  $K_n$  is a constant that depends only on  $n$

$$K_n = \left( \frac{2^{1+(1/n)} - 1}{2n} \right) \left( \frac{2n+1}{n+1} \right) \left( \frac{1}{n+3} \right)^{1/n} \quad (4.2-67)$$

Equation 4.2-66 has been tested by Leider<sup>15</sup> who measured  $t_{1/2}$  and  $F$  in 181 experimental runs. His data are compared with the power-law result in Fig. 4.2-6, where suitably chosen dimensionless groups are used. The characteristic time constant  $\lambda$  for the fluid is defined as

$$\lambda = (m'/2m)^{1/(n'-n)} \quad (4.2-68)$$

<sup>13</sup> J. R. Scott, *Trans. Inst. Rubber Ind.*, **7**, 169-186 (1931); **10**, 481-493 (1935).

<sup>14</sup> S. Oka in F. R. Eirich, ed., *Rheology*, Vol. 3, Academic Press, New York (1960), Chapt. 2, pp. 73-75; A. Cameron, *The Principles of Lubrication*, Longmans, Green, and Co., London (1966), pp. 389-392; D. F. Moore, *The Friction and Lubrication of Elastomers*, Pergamon, Elmsford, NY (1972); A. B. Metzner, *Rheol. Acta*, **10**, 434-444 (1971); M. L. DeMartine and E. L. Cussler, *J. Pharm. Sci.*, **64**, 976-982 (1975); G. Brindley, J. M. Davies, and K. Walters, *J. Non-Newtonian Fluid Mech.*, **1**, 19-37 (1976).

<sup>15</sup> P. J. Leider, *Rheology Research Center Report No. 22*, Nov. 1973, University of Wisconsin, Madison; *Ind. Eng. Chem. Fundam.*, **13**, 342-346 (1974). Additional experimental testing of the squeeze-flow equations and further examination of the theory have been carried out by R. J. Grimm, *AIChE J.*, **24**, 427-439 (1978).

THE GENERALIZED NEWTONIAN FLUID

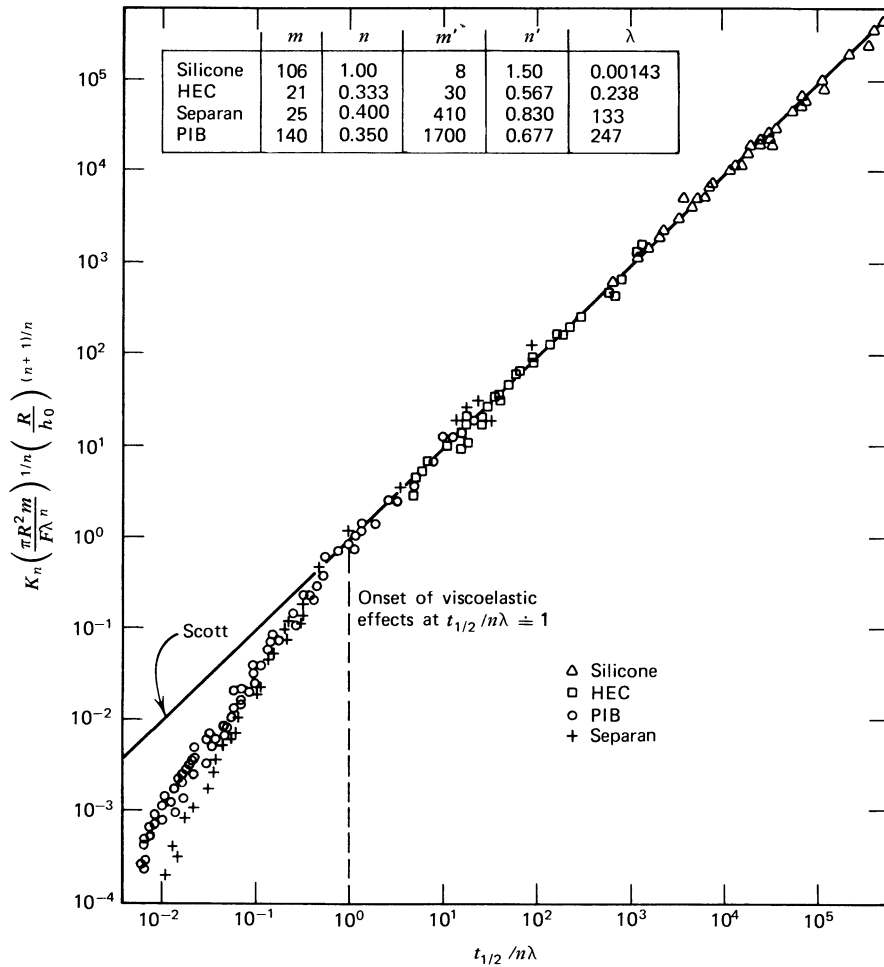


FIGURE 4.2-6. Squeeze flow data of P. J. Leider (University of Wisconsin Rheology Research Center Rept. No. 22, Nov. 1973) along with the Scott equation (Eq. 4.2-66). The fluid parameters for Eq. 4.2-68 are shown in the upper left-hand corner;  $m$  has units of  $\text{Pa} \cdot \text{s}$ ,  $m'$  has units of  $\text{Pa} \cdot \text{s}'$ , and  $\lambda$  is given in seconds. [Reprinted with permission from P. J. Leider, *Ind. Eng. Chem. Fundam.*, **13**, 342-346 (1974). Copyright by the American Chemical Society.]

in which  $m$  and  $n$  are the constants in the power law ( $\eta = m\dot{\gamma}^{n-1}$ ) and  $m'$  and  $n'$  are constants describing the power-law region of the first normal stress coefficient ( $\Psi_1 = m'\dot{\gamma}^{n'-2}$ ). It is seen that for the fluids tested the power-law model describes the data down to  $t_{1/2}/n\lambda = 1$ , but below that value there are marked deviations from the power law because of elastic effects. This point is discussed further in §4.6. The success of the Scott equation indicates that the squeeze-flow experiment may be useful for determining fluid parameters from measurements of  $F$  and  $t_{1/2}$ . From Eq. 4.2-66 we see that a log-log plot of  $(Fh_0/R^3)$  vs.  $(R/h_0 t_{1/2})$  will, for large  $t_{1/2}$ , give  $n$  from the slope of the straight line and  $m$  from an intercept

$$\log \left( \frac{Fh_0}{R^3} \right) = \log [\pi m (n K_n)^n] + n \log \left( \frac{R}{h_0 t_{1/2}} \right) \quad (4.2-69)$$

From a log-log plot of  $(R^2/F)^{1/n} (R/h_0)^{1+(1/n)}$  vs.  $t_{1/2}/n$  one can get  $\lambda$  from the break in the curve at  $t_{1/2}/n = \lambda$ . Explicit illustrations have been given by Leider.<sup>15</sup>

This example has illustrated the use of a generalized Newtonian fluid for a flow that is not a steady-state shear flow. In other words, we have violated the restriction placed on the model. Nonetheless, in the limit of slow squeezing flows, experiments show that we can apply the model. Experimental data were then used to define the limits of applicability of the model in terms of a characteristic time  $\lambda$  for each fluid. Hence the generalized Newtonian fluid model, together with dimensional analysis, has suggested a suitable form for the correlation, and the experimental data have established the correlation quantitatively.

### §4.3 ISOTHERMAL FLOW PROBLEMS BY THE CALCULUS OF VARIATIONS AND WEIGHTED RESIDUAL METHODS<sup>1</sup>

The problems discussed in §4.2 involve flows in simple geometries. To solve the equations of motion for problems of somewhat greater complexity one generally turns to numerical methods. For generalized Newtonian fluids a variational principle is available, and this principle can serve as a basis for the numerical procedures.<sup>2</sup> In addition, the variational principle can be used to obtain approximate analytical solutions; the latter are often useful in those engineering design problems where quick and approximate solutions are needed. A closely related, alternative procedure for obtaining numerical solutions is the method of weighted residuals. We begin this section with a brief introduction to the calculus of variations,<sup>3</sup> illustrating the method for a system with one independent and one dependent variable. Then we give a similar introduction to the method of weighted residuals, followed by a description of the connection between the two methods. We conclude by giving a general variational statement for three-dimensional, creeping flows of generalized Newtonian fluids.

#### a. Introduction to the Variational Method

A functional is a mathematical expression that assigns numbers to functions. As an example of a functional, consider the expression for the distance between two points  $x_1$  and  $x_2$  along the curve defined by a function  $y(x)$ . For fixed endpoints  $x_1, y_1$  and  $x_2, y_2$  the distance depends on the particular function  $y$  chosen and is given by the functional  $J$

$$J\{y(x)\} = \int_{x_1}^{x_2} \sqrt{1 + y'^2} dx \quad (4.3-1)$$

Corresponding to every curve  $y(x)$  we can assign a number  $J$ , the distance between the end-points along the curve. A variational problem arises when we want to find the function  $y$  that gives the shortest distance between the two points  $x_1, y_1$  and  $x_2, y_2$  in the  $xy$ -plane—that is, the smallest value of  $J$ .

<sup>1</sup> This section may be omitted in an introductory course; it is not needed for reading §§4.4 to 4.6.

<sup>2</sup> M. J. Crochet, A. R. Davies, and K. Walters, *Numerical Solution of Non-Newtonian Flow*, Elsevier, Amsterdam (1984).

<sup>3</sup> Very good short introductions to variational methods may be found in I. S. Sokolnikoff and R. M. Redheffer, *Mathematics of Physics and Modern Engineering*, 2nd ed., McGraw-Hill, New York (1966), Chapt. 5, §15; H. Margenau and G. M. Murphy, *The Mathematics of Physics and Chemistry*, 2nd ed., Van Nostrand, Princeton, NJ (1956), Chapt. 6; F. B. Hildebrand, *Methods of Applied Mathematics*, Prentice-Hall, Englewood Cliffs, NJ (1952), Chapt. 2; and V. S. Arpaci, *Conduction Heat Transfer*, Addison-Wesley, Reading, MA (1966), Chapt. 8. For applications to fluid dynamics and transport-phenomena problems see R. S. Schechter, *The Variational Method in Engineering*, McGraw-Hill, New York (1967).

Variational problems such as that of finding the minimum value of  $J$  in Eq. 4.3-1 can be shown to have equivalent statements as differential equations. To demonstrate this let us consider a more general functional  $J$  defined by

$$J\{y(x)\} = \int_{x_1}^{x_2} F(x, y, y') dx + G(x, y) \Big|_{x_1}^{x_2} \quad (4.3-2)$$

in which  $y$  is a function of  $x$ , and the derivative  $dy/dx$  is called  $y'$ ; both  $F$  and  $G$  are presumed to be known functions of their arguments. For each function  $y(x)$  a value of  $J$  can be calculated. We now ask: for what function  $y(x)$  is  $J$  stationary (i.e., a maximum, a minimum, or locally constant)?

Let  $y(x)$  be the function that makes  $J$  stationary, and let  $\bar{y}(x) = y(x) + \varepsilon\eta(x)$  be some "neighboring" function for which  $J$  is not stationary; here  $\eta(x)$  is an arbitrary function (it is presumed that  $\eta$ ,  $\eta'$ , and  $\eta''$  are continuous) and  $\varepsilon$  is a small quantity. Then we require that the function

$$J(\varepsilon) = \int_{x_1}^{x_2} F(x, y + \varepsilon\eta, y' + \varepsilon\eta') dx + G(x, y + \varepsilon\eta) \Big|_{x_1}^{x_2} \quad (4.3-3)$$

be stationary at  $\varepsilon = 0$ . In other words, we require that  $dJ/d\varepsilon$  be zero at  $\varepsilon = 0$ . To do this we expand the functions  $F$  and  $G$  in Taylor series about  $\varepsilon = 0$  in the parameter  $\varepsilon$ :

$$J(\varepsilon) = \int_{x_1}^{x_2} \left[ F(x, y, y') + \varepsilon\eta \frac{\partial F}{\partial y} + \varepsilon\eta' \frac{\partial F}{\partial y'} + \dots \right] dx + \left[ G(x, y) + \varepsilon\eta \frac{\partial G}{\partial y} + \dots \right] \Big|_{x_1}^{x_2} \quad (4.3-4)$$

in which we display only terms through  $\varepsilon$  to the first power. Then

$$\frac{dJ}{d\varepsilon} \Big|_{\varepsilon=0} = \int_{x_1}^{x_2} \left[ \eta \frac{\partial F}{\partial y} + \eta' \frac{\partial F}{\partial y'} \right] dx + \eta \frac{\partial G}{\partial y} \Big|_{x_1}^{x_2} = 0 \quad (4.3-5)$$

When the second term in the integral is integrated by parts, we obtain

$$\int_{x_1}^{x_2} \eta \left[ \frac{\partial F}{\partial y} - \frac{d}{dx} \frac{\partial F}{\partial y'} \right] dx + \left[ \eta \left( \frac{\partial F}{\partial y'} + \frac{\partial G}{\partial y} \right) \right] \Big|_{x_1}^{x_2} = 0 \quad (4.3-6)$$

Therefore, since  $\eta(x)$  is an arbitrary function we can conclude that over the range  $x_1 < x < x_2$ :

$$\boxed{\frac{d}{dx} \frac{\partial F}{\partial y'} - \frac{\partial F}{\partial y} = 0} \quad (4.3-7)$$

and at the end points,  $x = x_1$  and  $x = x_2$ :

$$\boxed{\left( \frac{\partial F}{\partial y'} + \frac{\partial G}{\partial y} \right) \Big|_{x_i} = 0} \quad i = 1, 2 \quad (4.3-8)$$

for the known functions  $F$  and  $G$ . Conversely if a function  $y(x)$  satisfies the differential equation in Eq. 4.3-7 with the boundary conditions in Eq. 4.3-8 then  $y(x)$  has the property of

making  $J$  in Eq. 4.3-2 stationary. Equation 4.3-7 is called the *Euler-Lagrange equation*, which  $y$  must satisfy over the interval  $x_1 < x < x_2$  if  $J$  is to be stationary, and Eqs. 4.3-8 are called the *natural boundary conditions* for the equation.

So far we have not considered any restrictions on the functions  $y(x)$  from which we wish to select the one that makes  $J$  stationary. Now we restrict our attention to functions that have a known value  $y_i$  at one (or both) of the endpoints, so that

$$\boxed{y(x_i) = y_i} \quad (4.3-9)$$

for  $i = 1$  or  $2$  (or both). We then ask: for what function  $y(x)$  that satisfies Eq. 4.3-9 is  $J$  stationary?

To answer this question we again introduce a function  $\bar{y}(x) = y(x) + \epsilon\eta(x)$  that now must satisfy Eq. 4.3-9. This means that  $\eta(x)$  is no longer completely arbitrary since we must have

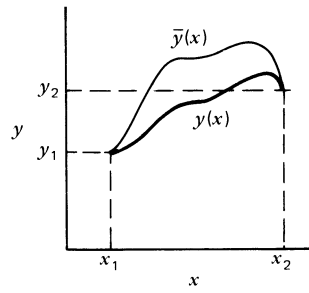
$$\eta(x_i) = 0 \quad (4.3-10)$$

for those end points where  $y$  is given by Eq. 4.3-9. We may then repeat the developments leading to Eq. 4.3-6 and we again arrive at the Euler-Lagrange equation in Eq. 4.3-7, which has to be satisfied by  $y(x)$  in the range  $x_1 < x < x_2$ . At the endpoints  $x = x_1$  and  $x = x_2$ , however, the natural boundary conditions in Eq. 4.3-8 apply only at those points where  $\eta(x) \neq 0$ . At the endpoints where  $\eta(x) = 0$  the natural boundary conditions are replaced by the *essential boundary conditions* in Eq. 4.3-9. In many problems it is necessary to have at least one essential boundary condition in order to specify the function  $y$  completely. In Fig. 4.3-1 the specification of boundary conditions is illustrated in terms of the choice of the function  $\bar{y}(x)$ .

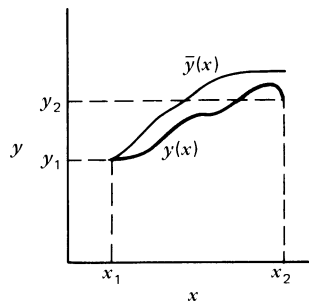
The variational method can be used in problem solving in two ways: (1) If one formulates a problem as the finding of a stationary value of a functional, then one may convert the problem to that of solving a differential equation with boundary conditions using standard procedures. (2) If one is faced with a differential equation and boundary conditions for which a variational functional  $J$  is known, one may obtain an *approximate* solution by substituting a trial function  $y(x)$  containing some arbitrary parameters  $a_1, \dots, a_n$  into the functional  $J$  and then setting  $\partial J / \partial a_j = 0$  for  $j = 1, 2, \dots, n$ . In this way the  $n$  parameters  $a_j$  are determined, and the optimal function of the chosen form for  $y(x)$  is found. Note that the trial function must be chosen to satisfy the essential boundary conditions for all values of the parameters. This means that the approximate solution will satisfy the essential boundary conditions exactly, whereas the differential equation and the natural boundary conditions will in general be satisfied only approximately. It is this second use of the variational method that is of interest here, since it allows us to find approximate solutions to difficult boundary value problems.

To illustrate the use of a variational principle in finding an approximate solution to a differential equation we consider a simple one-dimensional heat-transfer problem.<sup>4</sup> Consider a rod of length  $L$  (see Fig. 4.3-2) that is attached to a wall which is maintained at constant temperature  $T_0$ ; the rod is surrounded by air at temperature  $T_a$ . The loss of heat from the rod to its surroundings is described by a heat-transfer coefficient  $h$ , and we assume the tip of the rod is insulated, so that heat transfer occurs only across the sides.

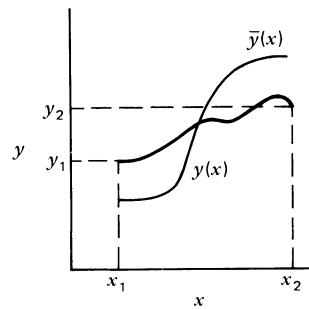
<sup>4</sup> For the derivation of Eq. 4.3-11 see R. B. Bird, W. E. Stewart, and E. N. Lightfoot, *Transport Phenomena*, Wiley, New York (1960), §9.7.



(a)



(b)



(c)

FIGURE 4.3-1. Sketches showing  $y(x)$  and three kinds of “neighboring” functions  $\bar{y}(x)$ . In (a) the function  $y(x)$  is given at both  $x = x_1$  and  $x = x_2$ , whereas in (b)  $y(x)$  is prescribed at  $x = x_1$ , and in (c) no boundary values are given.

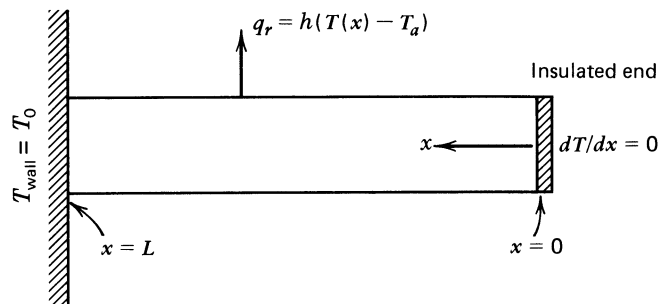


FIGURE 4.3-2. Rod attached to wall at constant temperature  $T_0$ . Heat loss to the surrounding air is given in terms of a heat-transfer coefficient  $h$ .

An energy balance on the rod gives the following differential equation for the temperature profile  $T(x)$ :

$$\frac{d^2 T}{dx^2} - \left( \frac{hP}{kA} \right) (T - T_a) = 0 \quad (4.3-11)$$

where  $P$  and  $A$  are the perimeter and cross-sectional area of the rod, and  $k$  is its thermal conductivity. If we introduce dimensionless variables

$$\Theta = \frac{T - T_a}{T_0 - T_a}; \quad \xi = \frac{x}{L}; \quad N^2 = \frac{hPL^2}{kA} \quad (4.3-12)$$

then the dimensionless form of the differential equation is

$$\Theta'' - N^2 \Theta = 0 \quad (4.3-13)$$

where  $\Theta'' = d^2 \Theta / d\xi^2$ . The boundary conditions become:

$$\text{at } \xi = 0 \quad \Theta' = 0 \quad (4.3-14)$$

$$\text{at } \xi = 1 \quad \Theta = 1 \quad (4.3-15)$$

A variational statement that is equivalent to the problem in Eqs. 4.3-13 through 15 is the following: Find the function  $\Theta(\xi)$  that satisfies Eq. 4.3-15 and makes the following integral stationary:

$$J\{\Theta(\xi)\} = \int_0^1 [(\Theta')^2 + N^2 \Theta^2] d\xi \quad (4.3-16)$$

To see this we note that  $J$  is of the form of Eq. 4.3-2 with

$$F(\xi, \Theta, \Theta') = (\Theta')^2 + N^2 \Theta^2 \quad (4.3-17)$$

and  $G = 0$ . With these forms for  $F$  and  $G$  it is then straightforward to show that the Euler-Lagrange equation (Eq. 4.3-7) is precisely twice Eq. 4.3-13 and that the natural boundary condition (Eq. 4.3-8) is just twice Eq. 4.3-14. It may in addition be shown that the stationary point is a minimum (Problem 4B.14).

We now illustrate how to use the variational principle to get an approximate solution to Eqs. 4.3-13 through 15. The first thing we have to do is to select a trial function for the dimensionless temperature profile  $\Theta(\xi)$ . Instead of picking just one trial function, however, we construct a whole set of trial functions of the form

$$\Theta^{(n)} = 1 + (1 - \xi) \sum_{j=1}^n a_j \xi^{j-1} \quad (n = 1, 2, 3, \dots) \quad (4.3-18)$$

That is, depending on whether  $n$  is 1, 2, 3... we can use a linear, quadratic, cubic, or higher-order trial function. In any event, the trial function satisfies the essential boundary condition in Eq. 4.3-15, but has no other restrictions.

Let us begin by selecting the linear trial function ( $n = 1$ ). When this function is inserted into the functional  $J$  in Eq. 4.3-16 we find<sup>5</sup>:

$$J\{\Theta^{(1)}\} = a_1^2 + N^2(1 + a_1 + \frac{1}{3}a_1^2) \quad (4.3-19)$$

Of all possible linear trial functions the “best” is then the one that minimizes  $J\{\Theta^{(1)}\}$ . This function is obtained by solving the equation  $dJ/da_1 = 0$  to find the optimal value of  $a_1$

$$a_1 = -\frac{3N^2}{2(3 + N^2)} \quad (4.3-20)$$

When this value of  $a_1$  is substituted into Eq. 4.3-18 with  $n = 1$ , the best approximate solution has been obtained that one can get with a linear trial function.

The above process can be repeated for a quadratic trial function by using Eq. 4.3-18 with  $n = 2$ . In this way we get

$$J\{\Theta^{(2)}\} = a_1^2 + \frac{1}{3}a_2^2 + N^2(1 + a_1 + \frac{1}{3}a_1^2 + \frac{1}{6}a_1a_2 + \frac{1}{3}a_2 + \frac{1}{30}a_2^2) \quad (4.3-21)$$

The “best” quadratic trial function is obtained by solving the simultaneous equations  $\partial J/\partial a_1 = 0$  and  $\partial J/\partial a_2 = 0$  to obtain

$$a_1 = -\frac{120N^2 + 2N^4}{240 + 104N^2 + 3N^4}; \quad a_2 = -\frac{120N^2 + 10N^4}{240 + 104N^2 + 3N^4} \quad (4.3-22)$$

When these values are substituted into Eq. 4.3-18 with  $n = 2$ , we have the best approximate solution that is possible with a quadratic trial function. In the same way one can use cubic or higher polynomial trial functions. Of course, functions other than polynomials can also be used.

Now that two approximate solutions have been obtained, it seems reasonable to inquire how “good” the approximations are. For comparison we note that for this problem the exact solution is

$$\Theta = \frac{\cosh N\xi}{\cosh N} \quad (4.3-23)$$

<sup>5</sup> The following integral is useful for polynomial trial functions of the form assumed in Eq. 4.3-18:

$$\int_0^1 x^n(1-x)^m dx = \frac{n! m!}{(n+m+1)!} \quad (4.3-18a)$$

where  $n$  and  $m$  are non-negative integers. For even polynomial trial functions these integrals are useful:

$$\int_0^1 (1-x^2)^m dx = \frac{(2m)!!}{(2m+1)!!} \quad (4.3-18b)$$

$$\int_0^1 x^{2(m+1)}(1-x^2)^n dx = \frac{(2m+1)!! (2n)!!}{(2m+2n+3)!!} \quad (4.3-18c)$$

in which  $m!! = m(m-2)(m-4)\cdots 2$  for  $m$  even and  $m!! = m(m-2)(m-4)\cdots 1$  for  $m$  odd.

TABLE 4.3-1

Minimum Values of the Variational Functional in Eq. 4.3-16 for Linear and Quadratic Trial Functions as well as for the Exact Solution

	$N = \frac{1}{2}$	$N = 1$	$N = 2$	$N = 3$
$J_{\min}^{(1)}$	0.2355768	0.8125000	2.673469	3.937501
$J_{\min}^{(2)}$	0.2310597	0.7617675	1.939394	3.063425
$J_{\min}$	0.2310585	0.7615941	1.928055	2.985165

and the corresponding value of the functional is obtained from Eq. 4.3-16

$$J_{\min} = \frac{N \sinh 2N}{2 \cosh^2 N} \quad (4.3-24)$$

In general it is not a simple matter to make an unambiguous evaluation of different approximate solutions, even when the exact analytical solution is known. For example one could think of comparing the average value of an approximation with the average value of the exact solution. This is not necessarily a meaningful comparison, however, since functions can be constructed that have the same average value as the exact solution, but which otherwise bear little resemblance to the exact solution. With the variational functional available, however, it is possible to make an unambiguous evaluation of various approximations. This is because of our knowledge that the exact solution is the *only* function that will give the value of  $J$  in Eq. 4.3-24 and that all approximations will give higher values of  $J$ . Thus for any fixed value of  $N$  we may define the "best" of two approximations as the one that gives the lowest value of  $J$ . In Table 4.3-1 we show the values of  $J$  obtained for the best linear approximation  $J_{\min}^{(1)}$  and for the best quadratic approximation  $J_{\min}^{(2)}$ . To examine the accuracy of the approximations further we compare in Table 4.3-2 the values of  $\Theta^{(1)}(0)$  and  $\Theta^{(2)}(0)$  with the exact values of  $\Theta(0)$ . We make the comparison at  $\xi = 0$  because  $\Theta$  is not specified here.

Several comments can be made in connection with the trial functions used above. (i) It is interesting that a linear trial function can even be used to obtain an approximate solution of a second-order differential equation. Note however that only first-order derivatives appear in the functional  $J$ . This reduction of order is characteristic for

TABLE 4.3-2

Values of Dimensionless Temperature at  $\xi = 0$  for the Linear and Quadratic Trial Functions as well as for the Exact Solution

	$N = \frac{1}{2}$	$N = 1$	$N = 2$	$N = 3$
$\Theta^{(1)}(0)$	0.884615	0.625000	0.142857	-0.125000
$\Theta^{(2)}(0)$	0.886828	0.648415	0.272727	0.124735
$\Theta(0)$	0.886819	0.648052	0.265802	0.099328

variational principles and also for certain weighted residual methods as explained later. (ii) We see that for small values of  $N$  the coefficients  $a_1$  and  $a_2$  in the second-order solution are nearly equal. Indeed for  $a_2 = a_1$  the natural boundary condition in Eq. 4.3-14 would be satisfied exactly. It is possible to force the quadratic trial function to obey the natural boundary condition exactly by imposing  $a_1 = a_2$ , but this increases the minimum value of  $J$  and is therefore not the best quadratic approximation as defined by the variational statement. (iii) Finally we see that both approximations deteriorate as  $N$  increases. In fact for the linear approximation we see that  $\Theta^{(1)}(0)$  is negative for  $N = 3$ , indicating that the approximation has lost physical significance. Roughly speaking, there are two alternative ways in which further improved approximations can be constructed. One is to keep the polynomial trial function in Eq. 4.3-18, but to use higher values of  $n$ . Another is to replace the trial function in Eq. 4.3-18 by one which is only piecewise polynomial. This latter approach is taken in the method of finite elements.

### b. The Method of Weighted Residuals and Its Relation to Variational Principles

We now turn to another method for obtaining approximate solutions to differential equations. The development of this method does not require that the differential equation have an equivalent variational functional. Rather than give a formal development,<sup>6</sup> however, we just use the simple one-dimensional heat transfer problem, described by Eqs. 4.3-13 through 15, to illustrate the method. Once again we use a trial function  $\Theta^{(n)}$  that depends on a total of  $n$  parameters  $a_j$ . For the differential equation, Eq. 4.3-13, we use the function in Eq. 4.3-18 which automatically satisfies the boundary condition at  $\xi = 1$ . This time, however, the trial function is introduced directly into the differential equation and we then obtain a *residual*

$$R^{(n)}(\xi) = \frac{d^2\Theta^{(n)}}{d\xi^2} - N^2\Theta^{(n)} \quad (4.3-25)$$

since the trial function does not in general satisfy the differential equation. The parameters  $a_j$  are then chosen to make the residual "small." To do this we introduce a set of  $n$  weighting functions  $w_i^{(n)}(\xi)$  where  $i = 1, 2, \dots, n$ . The  $a_j$  are then obtained by requiring that the *weighted residuals*, formed by multiplying the residual with the weighting functions and integrating over the domain of the problem, be zero

$$\int_0^1 \left( \frac{d^2\Theta^{(n)}}{d\xi^2} - N^2\Theta^{(n)} \right) w_i^{(n)} d\xi = 0, \quad i = 1, 2, \dots, n \quad (4.3-26)$$

When the  $w_i^{(n)}$  are chosen to be linearly independent this gives  $n$  equations that may be solved to obtain the parameters  $a_j$ . This is the *method of weighted residuals* for obtaining an approximate solution to a differential equation. A widely used example of this method is the *collocation method*<sup>7</sup> which arises from Eq. 4.3-26 when the weighting functions are chosen to

<sup>6</sup> More extensive descriptions of the method of weighted residuals may be found in B. A. Finlayson, *The Method of Weighted Residuals and Variational Principles*, Academic Press, New York (1972), and J. Villadsen and M. L. Michelsen, *Solution of Differential Equation Models by Polynomial Approximation*, Prentice-Hall, Englewood Cliffs, NJ (1978).

<sup>7</sup> J. Villadsen and W. E. Stewart, *Chem. Eng. Sci.*, **22**, 1483-1501 (1967); J. P. Nirschl and W. E. Stewart, *J. Non-Newtonian Fluid Mech.*, **16**, 233-250 (1984).

be Dirac delta functions. This forces the approximation  $\Theta^{(n)}$  to satisfy the differential equation at selected points, the collocation points. Note however that the collocation method can not be used to obtain a useful approximation  $\Theta^{(1)}$  of the form given by Eq. 4.3-18, since  $d^2\Theta^{(1)}/d\xi^2$  vanishes identically.

We now consider a different weighted residual method which is closely related to the variational method. By integrating the first term in Eq. 4.3-26 by parts, the following alternative weighted residual formulation is obtained for the heat-conduction problem:

$$\left(\frac{d\Theta^{(n)}}{d\xi}\right)w_i^{(n)}\Big|_0^1 - \int_0^1 \left(\frac{d\Theta^{(n)}}{d\xi}\right)\left(\frac{dw_i^{(n)}}{d\xi}\right) d\xi - N^2 \int_0^1 \Theta^{(n)}w_i^{(n)} d\xi = 0, \quad i = 1, 2, \dots, n \quad (4.3-27)$$

Notice that only first-order derivatives appear in this equation; that is, there is the same reduction of order as in the variational formulation of the problem. Despite the fact that we have used Eq. 4.3-26 to derive Eq. 4.3-27, the latter has more general applicability than the former, since lower-order trial functions can be used in Eq. 4.3-27 than in Eq. 4.3-26.

Next we consider a special choice for the weighting function, which leads to *Galerkin's method*:<sup>6</sup>

$$w_i^{(n)} = \frac{\partial}{\partial a_i} \Theta^{(n)} \quad (4.3-28)$$

We illustrate the use of this method in connection with Eq. 4.3-27 to obtain the first-order approximation  $\Theta^{(1)}$  in Eq. 4.3-18. According to Galerkin's method one obtains the single weighting function  $w_1^{(1)} = (1 - \xi)$ . Now  $w_1^{(1)} = 0$  at  $\xi = 1$  and hence the term evaluated at  $\xi = 1$  in Eq. 4.3-27 drops out. Also, in the term at  $\xi = 0$  we insert the natural boundary condition in Eq. 4.3-14 and hence the term at  $\xi = 0$  drops out also. When the remaining integrals in Eq. 4.3-27 are performed we obtain

$$-a_1 - N^2\left(\frac{1}{2} + \frac{1}{3}a_1\right) = 0 \quad (4.3-29)$$

Solving this equation for  $a_1$  gives precisely the same result as in Eq. 4.3-20 obtained by the variational principle. In the same fashion we could go on and derive the coefficients in the second-order approximation and the same coefficients obtained with the variational principle would be found.

For any problem for which there exists a variational principle, it is possible to select a Galerkin formulation that will be equivalent to it.<sup>8</sup> This is illustrated for the heat-conduction problem by substituting Eq. 4.3-28 into Eq. 4.3-27 to obtain

$$\frac{\partial}{\partial a_1} \int_0^1 \left[ \left(\frac{d\Theta^{(n)}}{d\xi}\right)^2 + N^2\Theta^{(n)2} \right] d\xi = 0 \quad (4.3-30)$$

where the terms at  $\xi = 0$  and  $\xi = 1$  have been dropped due to the boundary conditions. Comparison of this equation with the minimization conditions for the variational method ( $\partial/\partial a_i$  of Eq. 4.3-16) shows that the formulations are identical.

Finally we remark that Galerkin formulations as described above have even wider applicability than variational methods, since they can be applied to obtain approximate solutions to many differential equations that have no equivalent variational functional. For

<sup>8</sup> B. A. Finlayson, *op. cit.*, p. 229.

steady creeping flow of generalized Newtonian fluids, however, there is a variational principle, and we proceed now to present the principle and demonstrate its applicability.

### c. Variational Principle for Three-Dimensional Steady Creeping Flow of Generalized Newtonian Fluids

We consider the flow of a generalized Newtonian fluid within a region  $V$  of three-dimensional space; this region is bounded by a surface  $S$ , which is divided into two non-overlapping regions  $S_v$  and  $S_f$ . On the boundary  $S_v$  the velocity  $\mathbf{v}$  is specified, and on  $S_f$  a known external force per unit area  $\mathbf{f}$  is acting on the fluid. In the variational principle the boundary conditions on  $S_v$  are treated as essential boundary conditions and the conditions on  $S_f$  as natural boundary conditions. We define a variational functional by

$$J = \int_V \left[ \int_0^{\dot{\gamma}} \eta(\dot{\gamma}) \dot{\gamma} d\dot{\gamma} - \frac{1}{2} p \operatorname{tr} \dot{\gamma} - \rho(\mathbf{v} \cdot \mathbf{g}) \right] dV - \int_{S_f} (\mathbf{f} \cdot \mathbf{v}) dS \quad (4.3-31)$$

Here  $\eta(\dot{\gamma})$  is the non-Newtonian viscosity and  $\dot{\gamma}$  is the invariant defined by Eq. 4.1-8. For flow in conduits of uniform cross section  $A$ , we can take  $S_v$  to be the conduit wall and  $S_f$  to consist of an upstream plane "1" and a downstream plane "2" both perpendicular to the axis of the conduit. The surface integral in  $J$  then becomes  $-(p_1 - p_2) \int_A v dS$  where  $v$  is the axial velocity and  $(p_1 - p_2)$  is the pressure drop from the upstream to the downstream plane. The variational principle now states the following:<sup>9</sup>

Of all the velocity fields  $\mathbf{v}$  (that satisfy the boundary conditions on  $S_v$ ) and pressure fields  $p$ , the particular pair  $(\mathbf{v}, p)$  that causes  $J$  in Eq. 4.3-31 to have a *stationary* value is also the solution to the incompressible creeping flow equations of continuity and motion with the stated boundary conditions on  $S_v$  and  $S_f$ .

If the velocity fields are restricted a priori to satisfy the incompressibility condition, then the term with  $p$  in Eq. 4.3-31 drops out. It may then be shown that of all the velocity fields  $\mathbf{v}$  (consistent with  $(\nabla \cdot \mathbf{v}) = 0$  and the conditions on  $S_v$ ) the one that satisfies the creeping flow equation of motion with the stated boundary conditions minimizes  $J$  in Eq. 4.3-31.

The variational principle was developed by Pawlowski,<sup>10</sup> Prager,<sup>11</sup> and others.<sup>12-15</sup> The analogous principle for Newtonian fluids was developed by Helmholtz and by Korteweg.<sup>16</sup>

<sup>9</sup> A proof of this principle is outlined in Problems 4D.3 and 4D.4.

<sup>10</sup> J. Pawlowski, *Kolloid-Z.*, **138**, 6-11 (1954).

<sup>11</sup> W. Prager (in *Studies in Mathematics and Mechanics*, R. von Mises Presentation Volume, Academic Press, New York (1954), pp. 208-216) developed a similar variational principle for Bingham fluids.

<sup>12</sup> Y. Tomita, *Bull. Jpn. Soc. Mech. Eng.*, **2**, 469-474 (1959); *Reorogii: Hisenkei Ryūtai no Rikigaku*, Corona, Tokyo (1975), pp. 273-282.

<sup>13</sup> R. B. Bird, *Phys. Fluids*, **3**, 539-541 (1960); comment: **5**, 502 (1962).

<sup>14</sup> M. W. Johnson, Jr., *Phys. Fluids*, **3**, 871-878 (1960); *Trans. Soc. Rheol.*, **5**, 9-21 (1961), has given both minimum and maximum principles. See also J. C. Slattery, *Chem. Eng. Sci.*, **19**, 801-806 (1964); R. W. Flumerfelt and J. C. Slattery, *ibid.*, **20**, 157-163 (1965).

<sup>15</sup> R. S. Schechter, *AIChE J.*, **7**, 445-448 (1961).

<sup>16</sup> H. Lamb, *Hydrodynamics*, 6th ed., Cambridge University Press (1932), §344.

We now present two examples to illustrate the use of this variational principle. We remind the reader that either of these problems could be solved equivalently by forming a weighted residual directly from the governing differential equation. Whether it is easier for a given problem to proceed by forming the weighted residual or by inserting the trial function into the general variational functional depends on the particular problem and also, to some extent, on personal taste.

**EXAMPLE 4.3-1** Axial Annular Flow of a Power-Law Fluid

As in Example 4.2-4 we consider the axial flow of a fluid in a horizontal annulus of length  $L$  formed by cylindrical surfaces at  $r = \kappa R$  and  $r = R$ . Here we study the flow of a power-law fluid for which an analytical solution is known, so that we can have an exact result with which we can compare our approximate variational result. It is desired to find the volume rate of flow  $Q$  for the fluid. Neglect the effect of gravity so that  $\mathcal{P}_0 - \mathcal{P}_L = p_0 - p_L = \Delta p$ .

**SOLUTION** A very simple approximate form for the velocity profile that satisfies the boundary conditions is the expression (see Fig. 4.3-3):

$$v_z = a(1 - |\sigma|^{(1/n)+1}) \tag{4.3-32}$$

where

$$\sigma = \frac{2\xi - (1 + \kappa)}{(1 - \kappa)} \tag{4.3-33}$$

This trial velocity distribution contains  $a$  as the variational parameter;  $\xi = r/R$  is the dimensionless radial coordinate. The quantity  $\dot{\gamma}$  is then

$$\dot{\gamma} = \pm \frac{dv_z}{dr} = \pm \frac{1}{R} \frac{dv_z}{d\xi} = \pm \left( \frac{2/R}{1 - \kappa} \right) \frac{dv_z}{d\sigma} = \mp \frac{2a \left( \frac{1}{n} + 1 \right)}{R(1 - \kappa)} |\sigma|^{1/n} \tag{4.3-34}$$

where the upper sign is for  $\sigma < 0$  and the lower for  $\sigma > 0$ .

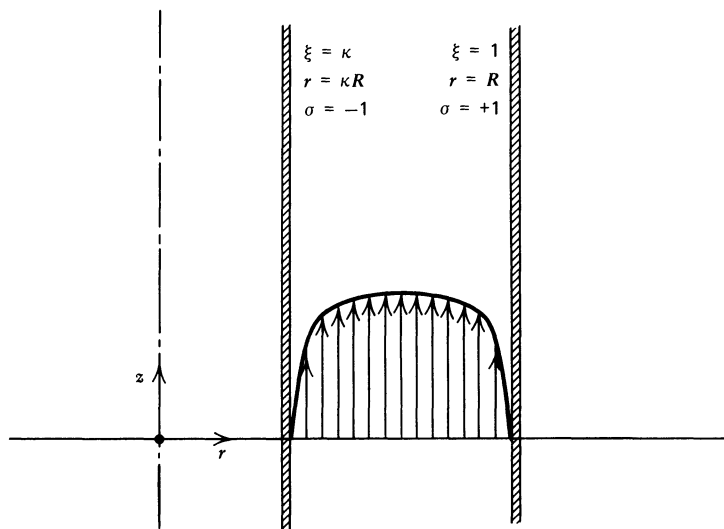


FIGURE 4.3-3. Trial velocity distribution  $v_z = a(1 - |\sigma|^{(1/n)+1})$ .

The variational functional  $J$  for this problem becomes

$$\begin{aligned}
 J &= 2\pi L \int_{\kappa R}^R \frac{m}{n+1} \dot{\gamma}^{n+1} r \, dr - 2\pi \Delta p \int_{\kappa R}^R v_z r \, dr \\
 &= \frac{2\pi L R^2 m}{n+1} \int_{-1}^{+1} \dot{\gamma}^{n+1} \left[ \left( \frac{1-\kappa}{2} \right) \sigma + \left( \frac{1+\kappa}{2} \right) \right] \left( \frac{1-\kappa}{2} \right) d\sigma \\
 &\quad - 2\pi \Delta p R^2 \int_{-1}^{+1} v_z \left[ \left( \frac{1-\kappa}{2} \right) \sigma + \left( \frac{1+\kappa}{2} \right) \right] \left( \frac{1-\kappa}{2} \right) d\sigma \\
 &= \frac{\pi L R^2 m}{n+1} (1-\kappa^2) \left( \frac{2a \left( \frac{1}{n} + 1 \right)}{R(1-\kappa)} \right)^{n+1} \int_0^1 \sigma^{(1/n)+1} d\sigma \\
 &\quad - \pi \Delta p R^2 (1-\kappa^2) a \int_0^1 (1-\sigma^{(1/n)+1}) d\sigma \\
 &= \frac{\pi L R^2 m (1-\kappa^2)}{(n+1) \left( \frac{1}{n} + 2 \right)} \left( \frac{2a \left( \frac{1}{n} + 1 \right)}{R(1-\kappa)} \right)^{n+1} - \left( \frac{1}{n} + 1 \right) \pi \Delta p R^2 (1-\kappa^2) a \quad (4.3-35)
 \end{aligned}$$

The dashed-underlined terms do not contribute since they are odd functions over the interval  $(-1, 1)$ .  
 When we set  $\partial J / \partial a = 0$  and solve for  $a$  we get

$$a = \left( \frac{\Delta p R}{2mL} \right)^{1/n} \frac{R(1-\kappa)^{(1/n)+1}}{2 \left( \frac{1}{n} + 1 \right)} \quad (4.3-36)$$

Then the volumetric flow rate  $Q$  is

$$Q = \pi R^3 \left( \frac{\Delta p R}{2mL} \right)^{1/n} \frac{(1-\kappa)^{(1/n)+2}}{\left( \frac{1}{n} + 2 \right)} \left( \frac{1+\kappa}{2} \right) \quad (4.3-37)$$

Fredrickson and Bird<sup>17</sup> have given a table of exact dimensionless  $Q$  values; when we compare Eq. 4.3-37 with their values we find

		$Q(\pi R^3)^{-1} \left( \frac{\Delta p R}{2mL} \right)^{-1/n} \frac{((1/n) + 2)}{(1-\kappa)^{(1/n)+2}}$	
		Exact	Variational
$n = 0.5$	$\kappa = 0.5$	0.761	0.750
$n = 0.333$	$\kappa = 0.5$	0.765	0.750
$n = 0.333$	$\kappa = 0.2$	0.661	0.600

<sup>17</sup> A. G. Fredrickson and R. B. Bird, *Ind. Eng. Chem.*, **50**, 347-352 (1958); erratum: *Ind. Eng. Chem. Fundam.*, **3**, 383 (1964).

The variational results are within about 2% of the exact results for  $\kappa > 0.5$  and  $n > 0.25$ , but become worse for smaller  $\kappa$  and  $n$  values. Better results could be obtained by using a trial function with two constants  $a_1$  and  $a_2$  instead of the one-constant function in Eq. 4.3-32.

A rather detailed variational calculation for the annular flow of a fluid described by the Sutterby model<sup>18</sup> has been carried out by Mitsuishi, Aoyagi, and Soeda.<sup>19</sup> Extensive comparisons between variational calculations and experimental data have also been made for ducts of elliptical, rectangular, triangular, and eccentric annular cross section.<sup>20</sup> A simple empirical technique for estimating flow rates in channels of unusual cross section has been suggested by Miller<sup>21</sup>. The use of variational methods for flow of various generalized Newtonian fluids around a sphere has been studied by Slattery and co-workers.<sup>22</sup>

#### EXAMPLE 4.3-2 Estimation of Velocity Distribution for Axial Eccentric Annular Flow (e.g., in a Wire-Coating Device)

A wire of radius  $R_1$  is moving axially with speed  $V$  inside a cylindrical cavity of radius  $R_2$  in which a molten polymer is flowing. The wire axis is displaced from the cavity axis by a distance  $\delta$ . It is desired to estimate the velocity distribution and in particular to determine under what conditions the velocity will be significantly dependent on the variable in the tangential direction (i.e., around the wire). This problem was suggested by a recent study on stability of the wire-coating operation.<sup>23</sup>

**SOLUTION** It is appropriate to use bipolar coordinates (see Appendix A). In order to use them it is necessary to relate the geometric quantities  $R_1$ ,  $R_2$ , and  $\delta$  to the quantities  $a$ ,  $\xi_1$ , and  $\xi_2$  used in bipolar coordinates. This is done in the caption for Fig. A.7-1. The quantities  $\xi_1$  and  $\xi_2$  specify the locations of the bounding surfaces.

We now want to estimate the velocity profile. We assume a velocity distribution of the form:

$$\frac{v_z}{V} = \left( \frac{\xi - \xi_2}{\xi_1 - \xi_2} \right) [1 - A(\xi_1 - \xi) \cos \theta] \quad (4.3-38)$$

in which  $A$  will be the variational parameter. This function satisfies the boundary conditions at  $\xi = \xi_1$  and  $\xi = \xi_2$ . For a concentric arrangement  $A$  would be zero, but in an eccentric arrangement it gives the importance of the  $\theta$ -dependence of  $v_z$ . From Fig. A.7-1 it is evident that  $v_z$  should depend on a function of  $\theta$  that is even, and the cosine function satisfies this requirement.

We now wish to determine the optimal value of  $A$  by minimizing  $J$ ; for this problem we are concerned only with the non-Newtonian viscosity term in Eq. 4.3-31. For the flow under consideration (see Table A.7-4):

$$\dot{\gamma} = \sqrt{\frac{1}{2}(\dot{\gamma}:\dot{\gamma})} = \sqrt{\left( \frac{X}{a} \frac{\partial v_z}{\partial \xi} \right)^2 + \left( \frac{X}{a} \frac{\partial v_z}{\partial \theta} \right)^2} \quad (4.3-39)$$

<sup>18</sup> J. L. Sutterby, *Trans. Soc. Rheol.*, **9**:2, 227-241 (1965); *AIChE J.*, **12**, 63-68 (1966). See also Table 4.5-1.

<sup>19</sup> N. Mitsuishi, Y. Aoyagi, and H. Soeda, *Kagaku Kōgaku*, **36**, 186-192 (1972).

<sup>20</sup> N. Mitsuishi, Y. Kitayama, and Y. Aoyagi, *Kagaku Kōgaku*, **31**, 570-577 (1967); N. Mitsuishi and Y. Aoyagi, *Memoirs of the Faculty of Engineering*, Kyūshū University, Vol. 28, No. 3, pp. 223-241 (1969); T. Mizushima, N. Mitsuishi, R. Nakamura, *Kagaku Kōgaku*, **28**, 648-652 (1964); T. L. Guckes, *Trans. ASME, J. Eng. for Industry*, **97B**, 498-506 (1975).

<sup>21</sup> C. Miller, *Ind. Eng. Chem. Fundam.*, **11**, 524-528 (1972); R. W. Hanks, *Ind. Eng. Chem. Fundam.*, **13**, 62-66 (1974).

<sup>22</sup> J. C. Slattery, *AIChE J.*, **8**, 663-667 (1962); M. L. Wasserman and J. C. Slattery, *ibid.*, **10**, 383-388 (1964); S. W. Hopke and J. C. Slattery, *ibid.*, **16**, 224-229, 317-318 (1970).

<sup>23</sup> Z. Tadmor and R. B. Bird, *Polym. Eng. Sci.*, **14**, 124-136 (1974).

in which  $X = \cosh \xi + \cos \theta$ . For a very large wire speed  $V$ , the first term under the square-root sign will surely be much larger than the second term. Hence we write:

$$\dot{\gamma} \doteq + \frac{X}{a} \frac{\partial v_z}{\partial \xi} \quad (4.3-40)$$

The plus sign is chosen since  $\xi$  increases from the outer cylinder to the inner cylinder, as does the axial velocity of the fluid. We shall assume the polymer melt viscosity to be described by a power law so that

$$\begin{aligned} \int_0^{\dot{\gamma}} \eta \dot{\gamma} d\dot{\gamma} &= \frac{m}{n+1} \dot{\gamma}^{n+1} \\ &= \frac{m}{n+1} \left( \frac{X}{a} \frac{\partial v_z}{\partial \xi} \right)^{n+1} \\ &= \frac{m}{n+1} \left[ \frac{X}{a} \frac{V}{\xi_1 - \xi_2} (1 - A(\xi_1 + \xi_2 - 2\xi) \cos \theta) \right]^{n+1} \end{aligned} \quad (4.3-41)$$

Hence the variational integral becomes for a tube of length  $L$

$$\begin{aligned} J &= L \int_0^{2\pi} \int_{\xi_2}^{\xi_1} \frac{m}{n+1} \left( \frac{X}{a} \frac{\partial v_z}{\partial \xi} \right)^{n+1} \left( \frac{a}{X} \right)^2 d\xi d\theta \\ &= \frac{LmV}{(n+1)(\xi_1 - \xi_2)} \int_0^{2\pi} \int_{\xi_2}^{\xi_1} \left( \frac{a}{X} \right)^{n-1} [1 - A(\xi_1 + \xi_2 - 2\xi) \cos \theta]^{n-1} d\xi d\theta \end{aligned} \quad (4.3-42)$$

When  $\delta J / \delta A$  is set equal to zero, it is found that<sup>23</sup> for  $R_1 = 0.317$  mm and  $R_2 = 0.635$  mm:

$\delta$ (mm)	$\xi_1$	$\xi_2$	$a$ (mm)	$A(n = 0.5)$	$A(n = 0.75)$	$A(n = 1)$
0.0237	3.6895	2.9982	6.35	0.025	0.008	0
0.1407	1.8184	1.1948	0.953	0.175	0.060	0
0.261	0.8814	0.4812	0.318	0.73	0.25	0

The values of  $A$  were obtained by numerical integration. It is thus seen that the  $\theta$ -dependence becomes more important as the eccentricity increases and as the index  $n$  decreases.

#### §4.4 NONISOTHERMAL FLOW PROBLEMS<sup>1</sup>

Up to this point we have given examples of flow problems in which it is assumed that the temperature is constant. In most polymer processing applications and in lubrication systems the changes of temperature with position and time are significant and cannot be ignored. In the manufacture of plastic objects one usually starts by melting plastic pellets and then performing a sequence of processing operations on the molten material; finally the

<sup>1</sup> For additional information on heat and mass transfer, we refer the reader to: A. B. Metzner, *Adv. Heat Transfer*, **2**, 357-397 (1965); H. H. Winter, *Adv. Heat Transfer*, **13**, 205-267 (1977); S. Middleman, *Fundamentals of Polymer Processing*, Wiley, New York (1977), Chapt. 13; Z. Tadmor and C. G. Gogos, *Principles of Polymer Processing*, Wiley, New York (1979), Chapt. 9; R. C. Armstrong and H. H. Winter in E. U. Schlünder, ed., *Heat Exchanger Design Handbook*, Hemisphere, New York (1983), §2.5.12; J. R. A. Pearson, *Mechanics of Polymer Processing*, Elsevier, London (1984), Parts III and IV and Appendix 4; J. Laven, Doctoral Dissertation, Delft University Press (1985); J. van Dam and H. Janeschitz-Kriegl, *Int. J. Heat Mass Transfer*, **28**, 395-406 (1985).

material must be cooled in order to obtain the finished product. Clearly heat transfer and phase change play important roles. In high speed processing operations, such as extrusion, and in lubrication problems the temperature rise by viscous heating is appreciable (because of the high viscosity of the polymeric liquids and because of the large velocity gradients); consequently the viscous-heating term must be included in the equation of change for temperature. Moreover, because of the low thermal conductivity of polymers, temperature increases due to viscous heating can be considerable and very nonuniform. The reliable estimation of viscous heating effects and local temperatures is of particular interest in polymer flow problems because of the thermal instability of polymeric liquids; chemical degradation can occur if hot spots develop in the processing line. The description of nonisothermal flows not only requires the simultaneous solution of three equations of change (continuity, motion, and energy) but in addition the temperature dependence of all physical properties (viscosity, thermal conductivity, density, and heat capacity) must in general be taken into account; moreover, for polymeric liquids the shear-rate dependence of the viscosity cannot be ignored.

The equations that will form the starting point for the heat-transfer and fluid-flow discussions here are very similar to those in Table 1.2-1:

<i>Continuity:</i>	$(\nabla \cdot \mathbf{v}) = 0$	(4.4-1)				
	No mass sources within the fluid					
<i>Motion:</i>	$\rho \frac{D\mathbf{v}}{Dt} = -\nabla p + [\nabla \cdot \eta \dot{\gamma}] + \rho \mathbf{g}$	(4.4-2)				
	<table style="width: 100%; border: none;"> <tr> <td style="text-align: center; width: 25%;">Mass per unit volume times acceleration</td> <td style="text-align: center; width: 25%;">Pressure force per unit volume</td> <td style="text-align: center; width: 25%;">Viscous force per unit volume</td> <td style="text-align: center; width: 25%;">Gravitational or external force per unit volume</td> </tr> </table>	Mass per unit volume times acceleration	Pressure force per unit volume	Viscous force per unit volume	Gravitational or external force per unit volume	
Mass per unit volume times acceleration	Pressure force per unit volume	Viscous force per unit volume	Gravitational or external force per unit volume			
<i>Energy:</i>	$\rho \hat{C}_p \frac{DT}{Dt} = (\nabla \cdot k \nabla T) + \frac{1}{2} \eta (\dot{\gamma} : \dot{\gamma})$	(4.4-3)				
	<table style="width: 100%; border: none;"> <tr> <td style="text-align: center; width: 33%;">Rate of increase of internal energy per unit volume</td> <td style="text-align: center; width: 33%;">Rate of addition of energy by heat conduction per unit volume</td> <td style="text-align: center; width: 33%;">Rate of conversion of mechanical to thermal energy per unit volume</td> </tr> </table>	Rate of increase of internal energy per unit volume	Rate of addition of energy by heat conduction per unit volume	Rate of conversion of mechanical to thermal energy per unit volume		
Rate of increase of internal energy per unit volume	Rate of addition of energy by heat conduction per unit volume	Rate of conversion of mechanical to thermal energy per unit volume				

In obtaining Eq. 4.4-3 from Eq. 1.1-13 it has been assumed that  $\hat{U} = \hat{U}(p, T)$ ; that is, we assume that  $\hat{U}$  does not depend explicitly on any kinematic quantities such as strain and rate of strain. This has been a standard assumption in all heat-transfer calculations; although the assumption is generally regarded as reasonable, we know of no thorough experimental study of it.<sup>2</sup>

<sup>2</sup> The review by G. Astarita and G. C. Sarti in J. F. Hutton, J. R. A. Pearson, and K. Walters, eds., *Theoretical Rheology*, Wiley, New York (1974), pp. 123-127, contains a theoretical discussion of the validity of Eq. 4.4-3 for viscoelastic fluids.

TABLE 4.4-1

Scaled Dimensionless Forms of the Equations of Change for the Generalized Newtonian Fluid with Constant  $\rho$  and  $k^{a-d}$

$(\nabla^* \cdot \mathbf{v}^*) = 0$	(A)
$\text{Re} \frac{D\mathbf{v}^*}{Dt^*} = -\nabla^* p^* + \left[ \nabla^* \cdot \frac{\eta}{\eta^0} \nabla^* \mathbf{v}^* \right] + \frac{\text{Re } g}{\text{Fr}} \frac{g}{g}$	(B)
$\text{Pé} \frac{DT^*}{Dt^*} = \nabla^{*2} T^* + \frac{1}{2} \text{Gn} \left( \frac{\eta}{\eta^0} \right) (\dot{\gamma}^* : \dot{\gamma}^*)$	(C)
Dimensionless groups:	
$\text{Re} = HV\rho/\eta^0$	(D)
$\text{Fr} = V^2/gH$	(E)
$\text{Pé} = \rho \hat{C}_p HV/k$	(F)
$\text{Gn} = \eta^0 V^2/k\Delta T_0$	(G)

<sup>a</sup> The dimensionless quantities are defined by

$$\mathbf{v}^* = \mathbf{v}/V, \quad \nabla^* = H\nabla, \quad \frac{D}{Dt^*} = \left( \frac{H}{V} \right) \frac{D}{Dt},$$

$$p^* = \frac{Hp}{\eta^0 V}, \quad T^* = \frac{T - T_0}{\Delta T_0}, \quad \dot{\gamma}^* = \left( \frac{V}{H} \right) \dot{\gamma}$$

<sup>b</sup> To scale length, a characteristic dimension  $H$  is used; for time,  $(H/V)$  is used where  $V$  is a characteristic velocity. A characteristic shear rate and temperature are  $(V/H)$  and  $T_0$ ; the characteristic viscosity  $\eta^0$  is the viscosity evaluated at  $\dot{\gamma} = (V/H)$  and  $T = T_0$ . There are several possibilities for  $\Delta T_0$ :

$$\Delta T_{\text{process}} = |T_w - T_i| \quad \Delta T_{\text{gen}} = \eta^0 V^2/k$$

$$\Delta T_{\text{adiabatic}} = \Delta p/\rho \hat{C}_p \quad \Delta T_{\text{rheol}} = \left| \frac{\eta}{\partial \eta / \partial T} \right|_{\substack{T=T_0 \\ \dot{\gamma}=V/H}}$$

where  $T_i$  and  $T_w$  are two temperatures specified in boundary conditions, say an inlet and a wall temperature.  $\Delta T_{\text{adiabatic}}$  is a characteristic adiabatic temperature rise for the process;  $\Delta T_{\text{gen}}$ , a characteristic temperature change associated with a balance between viscous heating and heat conduction; and  $\Delta T_{\text{rheol}}$  is a characteristic temperature rise necessary to change the viscosity substantially.

<sup>c</sup> If  $\Delta T_0 = \Delta T_{\text{process}}$  then,

$$\text{Gn} = \text{Br} = \eta^0 V^2/k |T_w - T_i|$$

where Br is the Brinkman number. If  $\Delta T_0 = \Delta T_{\text{rheol}}$  then,

$$\text{Gn} = \text{Na} = V^2 |\partial \eta / \partial T| / k$$

where Na is the Nahme-Griffith number.

<sup>d</sup> A thorough discussion of scaling the energy equation is given by J. R. A. Pearson, *Polym. Eng. Sci.*, **18**, 222-229 (1978); see also J. R. A. Pearson, *Mechanics of Polymer Processing*, Elsevier, New York (1985).

The scaled, dimensionless forms of Eqs. 4.4-1 through 3 are listed in Table 4.4-1. There the convection term in the energy equation is seen to be scaled by the Péclet number,  $Pé = \rho \hat{C}_p HV/k$ . Because of the low thermal conductivity of polymer melts and concentrated solutions,  $Pé \gg 1$  in typical nonisothermal flow problems, meaning that heat is convected much more rapidly than it is conducted. The viscous heating term is scaled by a heat generation number  $Gn$ , the form of which depends on the choice of a characteristic temperature difference  $\Delta T_0$  for a problem. If  $\Delta T_{\text{process}} \ll \Delta T_{\text{rheol}}$  then it is reasonable to choose the characteristic  $\Delta T_0$  to be  $\Delta T_{\text{process}}$ . In this case the  $Gn$  number is the Brinkman number introduced in Chapter 1, except that here  $\mu$  is replaced by  $\eta^0$ , the viscosity evaluated at the reference temperature and shear rate. If  $\Delta T_{\text{process}}$  is not small compared with  $\Delta T_{\text{rheol}}$  it is better to use the latter for  $\Delta T_0$ . Then  $Gn$  becomes the Nahme-Griffith<sup>3</sup> number  $Na$ .

Let us now examine the fluid properties that appear in the equations of change and their dependence on temperature. In Table 4.4-2 some sample values of thermal conductivity  $k$ , heat capacity per unit mass  $\hat{C}_p$ , and density  $\rho$ , are given for a number of molten commercial polymers; it should be noted that the  $k$  values all lie within a rather narrow range (0.1–0.3 W/m·K). Then in Table 4.4-3 information is given on the temperature dependence of  $k$ ,  $\hat{C}_p$ , and  $\rho$ . In most flow and heat-transfer calculations we assume that the thermal conductivity, heat capacity, and density of the fluid do not change appreciably with temperature or pressure. The assumption of constant thermal conductivity is not serious since  $k$  does not change much with temperature, nor does it appear to change very much with velocity gradient;<sup>4</sup> in addition there appears to be no need to replace the scalar thermal conductivity by a second-order tensor to account for nonisotropic heat conduction. The assumption of constant density means that our discussion will be restricted to forced convection and that free convection will be omitted.<sup>5</sup>

Although it is reasonable in many calculations to assume that  $k$ ,  $\hat{C}_p$ , and  $\rho$  do not vary with temperature, the same cannot be said of the parameters in the generalized

TABLE 4.4-2

Thermal Conductivity and Heat Capacity of Some Molten Polymers at 150°C<sup>a</sup>

Polymer		$k$ (W/m·K)	$\hat{C}_p$ (kJ/kg·K)	$\rho$ ( $10^{-3}$ kg/m <sup>3</sup> )
LDPE	Low-density polyethylene	0.241	2.57	0.782
HDPE	High-density polyethylene	0.255	2.65	0.782
PP	Polypropylene		2.80	
PVC	Polyvinyl chloride	0.166	1.53	1.31
PS	Polystyrene	0.167	2.04	0.997
PMMA	Polymethylmethacrylate	0.195		1.11

<sup>a</sup> Taken from H. H. Winter, *Adv. Heat Transfer*, **13**, 205–267 (1977).

<sup>3</sup> R. M. Griffith, *Ind. Eng. Chem. Fundam.*, **1**, 180–187 (1962); R. Nahme, *Ingenieur-Archiv.*, **11**, 191–209 (1940).

<sup>4</sup> A. A. Cocci, Jr. and J. J. C. Picot [*Polym. Eng. Sci.* **13**, 337–341 (1973)] have found that the thermal conductivity of polydimethylsiloxane samples increased by about 5% as the shear rate went from 0 to 300 s<sup>-1</sup>.

<sup>5</sup> A theoretical analysis of free-convection heat transfer to non-Newtonian fluids was given by A. Acrivos, *AIChE J.*, **6**, 584–590 (1960). Experimental data were obtained for free convection near a heated vertical plate in an aqueous carboxy-polymethylene solution by I. G. Reilly, C. Tien, and M. Adelman, *Can. J. Chem. Eng.*, **43**, 157–160 (1965). Numerical calculations for the power-law and Ellis models have been made by H. Ozoe and S. W. Churchill, *AIChE J.*, **18**, 1196–1207 (1972).

TABLE 4.4-3

Temperature Dependence of Physical Properties of Polymers<sup>a,b</sup>

Property	Polymer	Temperature Range (°C)	Coefficients in Polynomial Representation					
			A	B	C	D	E	F
$k$ (W/m·K)	HDPE	10-143	0.453	$-8.59 \times 10^{-4}$	$-5.29 \times 10^{-6}$	$4.12 \times 10^{-8}$	$-1.98 \times 10^{-8}$	
		143-200	0.26					
	LDPE	10-126	0.365	$-4.07 \times 10^{-4}$	$-7.34 \times 10^{-6}$	$8.28 \times 10^{-8}$	$-5.53 \times 10^{-8}$	
	PVC	126-200	0.223					
		0-200	0.168					
$\hat{C}_p$ (kJ/kg·K)	HDPE	10-88	1.597	$3.61 \times 10^{-3}$	$5.96 \times 10^{-5}$	$-3.44 \times 10^{-8}$	$9.77 \times 10^{-9}$	
		88-121	$-1.983 \times 10^2$	6.17	$-6.34 \times 10^{-2}$	$2.19 \times 10^{-4}$		
			121-130	$-2.837 \times 10^2$	2.41			
			130-133	$1.208 \times 10^3$	$-9.07$			
			133-200	1.984	$3.88 \times 10^{-3}$			
	LDPE	10-90	1.943	$5.39 \times 10^{-2}$	$2.56 \times 10^{-2}$	$-3.23 \times 10^{-6}$	$3.53 \times 10^{-8}$	
		90-105	$8.497 \times 10^1$	$-1.84$	$1.04 \times 10^{-2}$			
			105-110	$-1.29 \times 10^2$	1.3			
			110-113.5	$3.786 \times 10^2$	$-3.31$			
			113.5-200	1.98	$3.70 \times 10^{-3}$			
PVC		10-67	0.75	$4.66 \times 10^{-3}$				
		67-96	$1.361 \times 10^2$	$-6.64$	$1.21 \times 10^{-1}$	$-9.71 \times 10^{-4}$	$2.90 \times 10^{-6}$	
		96-200	1.208	$2.96 \times 10^{-3}$				
$\rho^{-1}$ (cm <sup>3</sup> /g)	HDPE	10-133	1.033	$17.87 \times 10^{-4}$	$-7.19 \times 10^{-5}$	$16.11 \times 10^{-7}$	$-15.45 \times 10^{-9}$	$5.58 \times 10^{-11}$
		133-200	1.158	$8.09 \times 10^{-4}$				
LDPE		10-113.5	1.078	$1.24 \times 10^{-4}$	$2.68 \times 10^{-5}$	$-3.95 \times 10^{-7}$	$2.35 \times 10^{-9}$	
		113.5-200	1.158	$8.09 \times 10^{-4}$				
PVC		10-110	0.7154	$1.02 \times 10^{-4}$	$0.0781 \times 10^{-5}$	$-0.0167 \times 10^{-7}$	$0.0524 \times 10^{-9}$	
		110-200	0.6791	$5.67 \times 10^{-4}$				

<sup>a</sup> All properties are given as polynomials of the form  $A + BT + CT^2 + DT^3 + \dots$  in which  $T$  is the temperature in degrees centigrade.

<sup>b</sup> The coefficients in this table were taken from U. Kleindienst, Doctoral Dissertation, Universität Stuttgart (1976).

Newtonian model for  $\eta$ . For example, useful empiricisms for the temperature dependence of the power-law parameters  $m$  and  $n$  are<sup>6</sup>

$$m = m^0 e^{-A(T - T_0)} \quad (4.4-4)$$

$$n = n^0 + B(T - T_0) \quad (4.4-5)$$

in which  $T_0$  is a reference temperature, and  $m^0$  and  $n^0$  are the values of the parameters at that temperature; the constants  $A$  and  $B$  are reciprocal characteristic temperature differences and are determined for each fluid from experimental data. As may be seen in Table 4.1-2, the parameter  $m$  is a strong function of temperature. Often  $B$  is found to be quite small; hence assuming  $n$  to be a constant is appropriate.

When the power-law model of Eq. 4.1-10, with the temperature-dependent parameters  $m$  and  $n$  (given, for example, by Eqs. 4.4-4 and 5), is inserted into Eqs. 4.4-2 and 3, then the equations of motion and energy are strongly coupled. In general, then, the solution of the set of equations of change can not be obtained analytically. This means that virtually all realistic nonisothermal polymer flow problems have to be done numerically.

On the other hand a number of analytical solutions to nonisothermal flow problems, with the assumption of constant physical properties, have been given in the engineering literature. These are useful for order-of-magnitude estimates and for checking computer programs in the limit that physical properties do not depend on temperature. We give a few analytical solutions at the end of this section. In addition we give two tables<sup>7</sup> of calculated Nusselt numbers, one for tubes (Table 4.4-4) and one for thin slits (Table 4.4-5). The "constant-wall-temperature" entries for circular tubes are derived in Examples 4.4-1 and 2.

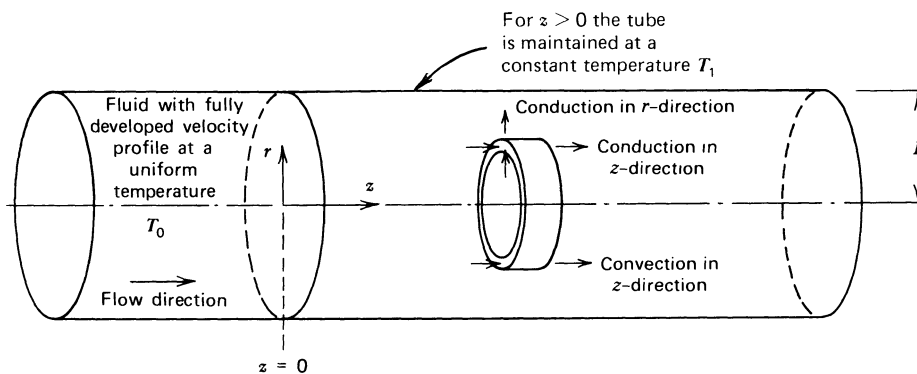


FIGURE 4.4-1. Axial flow in a circular tube with heat transport by conduction and convection. The wall temperature changes from  $T_0$  to  $T_1$  at  $z = 0$ .

<sup>6</sup> R. M. Turian, Ph.D. Thesis, University of Wisconsin, Madison (1964), suggested similar expressions for the power-law, p. 139; see also pp. 161-162 for the corresponding Ellis model results. For some purposes it is convenient to use

$$m^0/m = [1 + C(T - T_0)/T_0]^n \quad (4.4-4a)$$

as suggested by T. Mizushima, R. Itō, Y. Kuriwaki, and K. Yahikozawa, *Kagaku Kōgaku*, **31**, 250-255 (1967); here  $C$  is a constant, and  $n$  is the (constant) exponent in the power-law model.

<sup>7</sup> Tables 4.4-4 and 5 are based on the summary articles (in Dutch) by W. J. Beek and R. Eggink, *De Ingenieur*, **74**, Ch. 81-89 (1962), and J. M. Valstar and W. J. Beek, *ibid.*, **75**, Ch. 1-7 (1963).

The solution techniques needed to solve the “constant-wall-heat-flux” problems are given elsewhere.<sup>8</sup>

**EXAMPLE 4.4-1** Flow in Tubes with Constant Wall Temperature<sup>9-11</sup> (Asymptotic Solution for Small  $z$ )

A polymeric fluid is flowing axially in a circular tube of radius  $R$  (see Fig. 4.4-1). Before the fluid arrives at the plane  $z = 0$ , it is at a uniform temperature  $T_0$  and has the fully developed velocity distribution:

$$v_z = v_{\max} \left[ 1 - \left( \frac{r}{R} \right)^{s+1} \right] \quad (4.4-6)$$

where  $s = 1/n$ , and  $v_{\max}$  is given in Eq. 4.2-8. Then for  $z > 0$  the wall is maintained at a constant temperature  $T_1$ ; if  $T_0 - T_1$  is positive, heat is leaving the tube and the fluid is cooled, whereas if  $T_0 - T_1$  is negative, heat is being added as would be the case if the tube were being heated with steam. Obtain an asymptotic expression for the temperature profile in the fluid for small  $z$  by using the “method of combination of variables.” Then obtain the expression for the local heat-transfer coefficient and the Nusselt number.

**SOLUTION** To obtain an approximate description of this heating or cooling problem, we assume that the power-law constants  $m$  and  $n$  are not dependent on the temperature; also the temperature dependence of  $\rho$ ,  $k$ , and  $\hat{C}_p$  is ignored. The energy equation (Eq. 4.4-3) then becomes, for low flow rates where viscous heating is unimportant:

$$\rho \hat{C}_p v_{\max} \left[ 1 - \left( \frac{r}{R} \right)^{s+1} \right] \frac{\partial T}{\partial z} = k \left[ \frac{1}{r} \frac{\partial}{\partial r} \left( r \frac{\partial T}{\partial r} \right) + \frac{\partial^2 T}{\partial z^2} \right] \quad (4.4-7)$$

Heat convection in the $z$ -direction	Heat conduction in the $r$ -direction	Heat conduction in the $z$ -direction
--	--	--

with boundary conditions:

$$B.C. 1: \quad \text{at } r = 0 \quad T = \text{finite} \quad (4.4-8)$$

$$B.C. 2: \quad \text{at } r = R \quad T = T_1 \quad (4.4-9)$$

$$B.C. 3: \quad \text{at } z \rightarrow -\infty \quad T \rightarrow T_0 \quad (4.4-10)$$

$$B.C. 4: \quad \text{at } z \rightarrow +\infty \quad T \rightarrow T_1 \quad (4.4-11)$$

<sup>8</sup> See, for example, pp. 363–364 and §9.8 of R. B. Bird, W. E. Stewart, and E. N. Lightfoot, *Transport Phenomena*, Wiley, New York (1960). The power-law solution was first given by U. Grigull, *Chem.-Ingen. Techn.*, **28**, 553–556 (1956); see also R. B. Bird, *ibid.*, **31**, 569–572 (1959). The problem has also been solved with  $n = \text{constant}$  and  $m$  varying according to Eq. 4.4-4a by T. Mizushima, R. Itō, Y. Kuriwaki, and K. Yahikozawa, *loc. cit.*; see also T. Mizushima and Y. Kuriwaki, *Mem. Fac. Eng. Kyōto Univ.*, **30**, 511–524 (1968). Further work on the problem has been done by N. Mitsuishi and O. Miyatake, *Kagaku Kōgaku*, **32**, 1222–1227 (1968); *Mem. Fac. Eng., Kyūshū Univ.*, **28**(2), 91–107 (1968). The last four papers listed include experimental data.

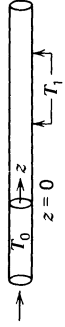

<sup>9</sup> R. B. Bird, W. E. Stewart, and E. N. Lightfoot, *Transport Phenomena*, Wiley, New York (1960), pp. 307–308, 349–350.

<sup>10</sup> R. L. Pigford, *CEP Symp. Ser.*, No. 17, **51**, 79–92 (1955).

<sup>11</sup> The analogous mass-transfer problem was discussed by H. Kramers and P. J. Kreyger, *Chem. Eng. Sci.*, **6**, 42–48 (1956).

TABLE 4.4-4

Asymptotic Results for Nusselt Numbers (Tube Flow)<sup>a, b</sup>;  $Nu = hD/k$

All Values are Local Nu Numbers	Constant wall temperature 	Constant wall heat flux 
Thermal entrance region <sup>c</sup> $\frac{\langle v_z \rangle D^2}{\alpha z} \gg 1$	Plug flow (A) $Nu = \frac{1}{\sqrt{\pi}} \left( \frac{\langle v_z \rangle D^2}{\alpha z} \right)^{1/2}$ (B) $Nu = \frac{2}{9^{1/3} \Gamma(\frac{4}{3})} \left[ \frac{\langle v_z \rangle D^2}{\alpha z} \left( -\frac{1}{4} \frac{d\phi}{d\xi} \Big _{\xi=1} \right) \right]^{1/3}$ (C) $Nu = \frac{2}{9^{1/3} \Gamma(\frac{4}{3})} \left( \frac{\langle v_z \rangle D^2}{\alpha z} \right)^{1/3}$	Plug flow (G) $Nu = \frac{\sqrt{\pi}}{2} \left( \frac{\langle v_z \rangle D^2}{\alpha z} \right)^{1/2}$ (H) $Nu = \frac{2\Gamma(\frac{2}{3})}{9^{1/3}} \left[ \frac{\langle v_z \rangle D^2}{\alpha z} \left( -\frac{1}{4} \frac{d\phi}{d\xi} \Big _{\xi=1} \right) \right]^{1/3}$ (I) $Nu = \frac{2\Gamma(\frac{2}{3})}{9^{1/3}} \left( \frac{\langle v_z \rangle D^2}{\alpha z} \right)^{1/3}$
Thermally fully developed flow $\frac{\langle v_z \rangle D^2}{\alpha z} \ll 1$	Plug flow (D) $Nu = 5.772$ (E) $Nu = \beta_1^2$ , where $\beta_1$ is the lowest eigenvalue of $\frac{1}{\xi} \frac{d}{d\xi} \left( \xi \frac{dX_n}{d\xi} \right) + \beta_n^2 \phi(\xi) X_n = 0;$ $X_n(0) = 0, X_n(1) = 0$	Plug flow (J) $Nu = 8$ (K) $Nu = \left[ 2 \int_0^1 \frac{1}{\xi} \left[ \int_0^\xi \phi(\xi') d\xi' \right]^2 d\xi \right]^{-1}$
	(F) $Nu = 3.657$ Laminar Newtonian flow	(L) $Nu = \frac{48}{11}$ Laminar Newtonian flow

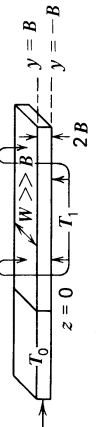
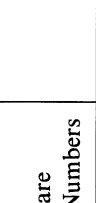
<sup>a</sup> Note:  $\phi(\xi) = v_z/\langle v_z \rangle$  where  $\xi = r/R$  and  $R = D/2$ ; for Newtonian fluids  $\langle v_z \rangle D^2/\alpha z = \text{RePr}(D/2)$  with  $\text{Re} = D\langle v_z \rangle \rho/\mu$ .

<sup>b</sup> W. J. Beek and R. Eggink, *De Ingenieur*, 74, Ch. 85-89 (1962).

<sup>c</sup> The grouping  $\langle v_z \rangle D^2/\alpha z$  is sometimes written as  $Gz \cdot (L/z)$  where  $Gz = \langle v_z \rangle D^2/\alpha L$  is called the Graetz number; here  $L$  is the length of the pipe past  $z = 0$ . Thus the thermal entry region corresponds to large Graetz number.

TABLE 4.4-5

Asymptotic Results for Nusselt Numbers (Thin-Slit Flow)<sup>a, b</sup>,  $Nu = 4hB/k$

All Values are Local Nu Numbers	Constant wall temperature 	Constant wall heat flux 
Thermal entrance region <sup>c</sup>	Plug flow	Plug flow
$\frac{\langle v_z \rangle B^2}{\alpha z} \gg 1$	Laminar non-Newtonian flow	(A) $Nu = \frac{4}{\sqrt{\pi}} \left( \frac{\langle v_z \rangle B^2}{\alpha z} \right)^{1/2}$
	Laminar Newtonian flow	(B) $Nu = \frac{4}{9^{1/3} \Gamma(\frac{4}{3})} \left[ \frac{\langle v_z \rangle B^2}{\alpha z} \left( - \frac{d\phi}{d\sigma} \Big _{\sigma=1} \right) \right]^{1/3}$
	Laminar Newtonian flow	(C) $Nu = \frac{4}{3^{1/3} \Gamma(\frac{4}{3})} \left( \frac{\langle v_z \rangle B^2}{\alpha z} \right)^{1/3}$
	Plug flow	(D) $Nu = \pi^2$
Thermally fully developed flow	Laminar non-Newtonian flow	(E) $Nu = 4\beta_1^2$ , where $\beta_1$ is the lowest eigenvalue of $\frac{d^2 X_n}{d\sigma^2} + \beta_n^2 \phi(\sigma) X_n = 0$ ; $X_n(\pm 1) = 0$
$\frac{\langle v_z \rangle B^2}{\alpha z} \ll 1$	Laminar Newtonian flow	(F) $Nu = 7.54$
	Laminar non-Newtonian flow	(G) $Nu = 2\sqrt{\pi} \left( \frac{\langle v_z \rangle B^2}{\alpha z} \right)^{1/2}$
	Laminar non-Newtonian flow	(H) $Nu = \frac{4\Gamma(\frac{4}{3})}{9^{1/3}} \left[ \frac{\langle v_z \rangle B^2}{\alpha z} \left( - \frac{d\phi}{d\sigma} \Big _{\sigma=1} \right) \right]^{1/3}$
	Laminar Newtonian flow	(I) $Nu = \frac{4\Gamma(\frac{4}{3})}{3^{1/3}} \left( \frac{\langle v_z \rangle B^2}{\alpha z} \right)^{1/3}$
	Plug flow	(J) $Nu = 12$
	Laminar non-Newtonian flow	(K) $Nu = \left[ \frac{1}{4} \int_0^1 \left[ \int_0^\sigma \phi(\sigma') d\sigma' \right]^2 d\sigma \right]^{-1}$
	Laminar Newtonian flow	(L) $Nu = \frac{140}{17}$

<sup>a</sup>Note:  $\phi(\sigma) = v_z/\langle v_z \rangle$  where  $\sigma = y/B$ ; for Newtonian fluids  $\langle v_z \rangle D^2/\alpha z = 4 \text{ RePr}(B/z)$  with  $\text{Re} = 4B\langle v_z \rangle/\mu$ .

<sup>b</sup>J. M. Valstar and W. J. Beek, *De Ingenieur*, 75, Ch. 1-7 (1963).

<sup>c</sup>The grouping  $\langle v_z \rangle B^2/\alpha z$  is sometimes written as  $\text{Gr} (1/z)$  where  $\text{Gr} = \rho \langle v_z \rangle B^2/\eta I$  is the Graetz number; here  $I$  is the length of the slit past  $z = 0$ . Thus the thermal entrance region is large  $\text{Gr} \ll 1$ .

The three terms in Eq. 4.4-7 are represented by arrows in Fig. 4.4-1. Except in unusual problems—mainly in liquid metals—the heat conduction in the  $z$ -direction is much smaller than the heat convection in the  $z$ -direction (the heat transport by fluid flow), so that the axial convection term should be balanced against the radial conduction term. Balancing these two terms allows us to choose an appropriate length scale  $L$  for transport in the  $z$ -direction. Equating the order of magnitude of these two terms gives

$$\rho \hat{C}_p \langle v_z \rangle \Delta T_0 / L = k \Delta T_0 / R^2 \quad (4.4-12)$$

where we have used  $R$  as a length scale for the radial conduction, the average velocity  $\langle v_z \rangle$  as a scale for axial velocity, and  $\Delta T_0 = T_0 - T_1$  as a characteristic temperature difference. From Eq. 4.4-12 we see that  $L = \langle v_z \rangle R^2 / \alpha$  and thus we are led to introduce the following dimensionless quantities:

$$\Theta = \frac{T - T_1}{T_0 - T_1}; \quad \xi = \frac{r}{R}; \quad \zeta = \frac{\alpha z}{\langle v_z \rangle R^2}; \quad \text{Pé} = \frac{\rho \hat{C}_p \langle v_z \rangle R}{k} \quad (4.4-13)$$

We also use a dimensionless velocity profile defined as follows:

$$\phi(\xi) = \frac{v_z}{\langle v_z \rangle} = \frac{v_z}{Q/\pi R^2} = \left( \frac{s+3}{s+1} \right) (1 - \xi^{s+1}) \quad (4.4-14)$$

which follows from Eqs. 4.2-8 and 9. Then the dimensionless form of the differential equation is

$$\phi(\xi) \frac{\partial \Theta}{\partial \zeta} = \frac{1}{\xi} \frac{\partial}{\partial \xi} \left( \xi \frac{\partial \Theta}{\partial \xi} \right) + \frac{1}{\text{Pé}} \frac{\partial^2 \Theta}{\partial \zeta^2} \quad (4.4-15)$$

For large Péclet numbers,<sup>12</sup> typical of polymers because of their low thermal conductivities, the axial conduction (dashed underlined) term can be neglected, and one of the boundary conditions in the  $z$ -direction can be dropped. The dimensionless boundary conditions to be used with Eq. 4.4-15 (with the dashed underlined term omitted) are

$$B.C. 1: \quad \text{at } \zeta = 0 \quad \Theta = 1 \quad (4.4-16)$$

$$B.C. 2: \quad \text{at } \xi = 1 \quad \Theta = 0 \quad (4.4-17a)$$

$$B.C. 3: \quad \text{at } \xi = 0 \quad \Theta = \text{finite} \quad (4.4-17b)$$

For small  $z$  the heat removal (if  $T_0 - T_1 > 0$ ) or the heat penetration (if  $T_0 - T_1 < 0$ ) is restricted to a very thin cylindrical shell near the wall. In this situation the following three approximations lead to results that are accurate in the limit as  $z \rightarrow 0$ :

- i. Curvature effects may be ignored and the problem treated as though the wall were flat; the distance from the wall will be designated by  $y = R - r$ .
- ii. The fluid may be regarded as extending from the (flat) heat-transfer surface,  $y = 0$ , to  $y = \infty$ .
- iii. The velocity profile may be regarded as linear, with a slope given by the velocity gradient at the wall.

<sup>12</sup> See Problem 4D.2 for a discussion of small and moderate Pé.

When we introduce the symbol  $\sigma = y/R = 1 - \zeta$  for the dimensionless distance from the wall, and when the three mathematical approximations above are used, the problem statement becomes

$$\left(\frac{d\phi}{d\sigma}\right)\Big|_{\sigma=0} \sigma \frac{\partial \Theta}{\partial \zeta} = \frac{\partial^2 \Theta}{\partial \sigma^2} \quad (4.4-18)$$

$$B.C. 1: \quad \text{at } \zeta = 0 \quad \Theta = 1 \quad (4.4-19)$$

$$B.C. 2: \quad \text{at } \sigma = 0 \quad \Theta = 0 \quad (4.4-20)$$

$$B.C. 3: \quad \text{at } \sigma = \infty \quad \Theta = 1 \quad (4.4-21)$$

For the power-law fluid  $(d\phi/d\sigma)_{\sigma=0}$  is just  $(s+3)$ , as may be seen from Eq. 4.4-14. We now postulate that a solution can be found of the form  $\Theta = \Theta(\chi)$ , where  $\chi$  is a new variable formed from a combination of the independent variables:

$$\chi = \frac{\sigma}{\sqrt[3]{9\zeta/(s+3)}} \quad (4.4-22)$$

Then the problem becomes

$$\frac{d^2 \Theta}{d\chi^2} + 3\chi^2 \frac{d\Theta}{d\chi} = 0 \quad (4.4-23)$$

with  $\Theta(0) = 0$  and  $\Theta(\infty) = 1$ . The solution is

$$\Theta = \frac{1}{\Gamma(\frac{4}{3})} \int_0^\chi e^{-\bar{x}^3} d\bar{x} \quad (4.4-24)$$

This is the temperature profile in dimensionless form.

For calculating the heat transfer to or from the tube it is convenient to work in terms of the local heat-transfer coefficient  $h$ , defined by

$$q_w = h(T_b - T_w) \quad (4.4-25)$$

in which  $q_w$  is the radial heat flux at the wall,  $T_w$  is the local wall temperature, and  $T_b$  is the bulk temperature, defined by

$$T_b(z) = \frac{\int_0^{2\pi} \int_0^R v_z(r) T(r, z) r dr d\theta}{\int_0^{2\pi} \int_0^R v_z(r) r dr d\theta} \quad (4.4-26)$$

Usually the dimensionless heat-transfer coefficient, or Nusselt number,  $\text{Nu} = 2hR/k$ , is tabulated. For this problem  $T_b \doteq T_0$  and  $T_w = T_1$ , so that the Nusselt number is

$$\text{Nu} = \frac{2q_w R}{k(T_0 - T_1)} = \frac{2R}{k} \frac{(+k \partial T / \partial y)|_{y=0}}{(T_0 - T_1)} = +2 \frac{\partial \Theta}{\partial \sigma} \Big|_{\sigma=0} \quad (4.4-27)$$

When Eq. 4.4-24 is substituted into Eq. 4.4-27 we then get:

$$\text{Nu} = 2 \frac{d\Theta}{d\chi} \Big|_{\chi=0} \left( \frac{\partial \chi}{\partial \sigma} \right) = \frac{2}{\Gamma(\frac{4}{3})} \sqrt[3]{\frac{(s+3)}{9\zeta}} = \frac{2}{\Gamma(\frac{4}{3})} \sqrt[3]{\frac{(s+3)\langle v_z \rangle R^2}{9\alpha z}} \quad (4.4-28)$$

This is just a special case of the result given in Eq. B of Table 4.4-4.

**EXAMPLE 4.4-2.** Flow in Tubes with Constant Wall Temperature (Asymptotic Solution for Large  $z$ )<sup>8,13</sup>

Rework Example 4.4-1 by the “method of separation of variables” and obtain a formal expression for the Nusselt number valid for any value of  $z$ . Show that a particularly simple asymptotic result can be obtained for large  $z$  values.

**SOLUTION** In the method of separation of variables we seek a solution to Eq. 4.4-15 of the form of a product

$$\Theta(\xi, \zeta) = X(\xi)Z(\zeta) \quad (4.4-29)$$

and insert it into the partial differential equation. Then division by  $XZ$  gives

$$\frac{1}{Z} \frac{dZ}{d\zeta} = \frac{1}{\phi X \xi} \frac{d}{d\xi} \left( \xi \frac{dX}{d\xi} \right) \quad (4.4-30)$$

Both sides are equal to a constant, which we denote by  $-\beta^2$ . Hence we get two ordinary differential equations:

$$\frac{dZ}{d\zeta} = -\beta^2 Z \quad (4.4-31)$$

$$\frac{1}{\xi} \frac{d}{d\xi} \left( \xi \frac{dX}{d\xi} \right) + \beta^2 \phi X = 0 \quad (4.4-32)$$

The second of these has boundary conditions:  $X'(0) = 0$  and  $X(1) = 0$ . The  $X$ -equation is a Sturm-Liouville problem, and there is a set of eigenfunctions  $X_i$  corresponding to the set of eigenvalues  $\beta_i$ . The complete solution must then be a linear combination of products of the form given in Eq. 4.4-29:

$$\Theta(\xi, \zeta) = \sum_{i=1}^{\infty} A_i X_i(\xi) e^{-\beta_i^2 \zeta} \quad (4.4-33)$$

The  $A_i$  are determined by the requirement that  $\Theta = 1$  at  $\zeta = 0$ . After Eq. 4.4-33 is written for  $\zeta = 0$ , we multiply both sides by  $X_j(\xi)\phi(\xi)\xi d\xi$  and integrate from  $\xi = 0$  to  $\xi = 1$ . Then when use is made of the fact that the  $X_i(\xi)$  are orthogonal over the range  $\xi = 0$  to  $\xi = 1$  with respect to the weighting function  $\phi(\xi)\xi$  we obtain finally

$$A_i = \frac{\int_0^1 X_i \phi \xi d\xi}{\int_0^1 X_i^2 \phi \xi d\xi} \quad (4.4-34)$$

Equations 4.4-33 and 34 constitute a formal solution to the problem.

We next get an expression for the Nusselt number, which in this case is given by

$$\text{Nu} = \frac{2hR}{k} = \frac{2R(-k\partial T/\partial r)|_{r=R}}{k(T_b - T_w)} = -2 \frac{(\partial\Theta/\partial\xi)|_{\xi=1}}{\Theta_b} \quad (4.4-35)$$

<sup>13</sup> B. C. Lyche and R. B. Bird, *Chem. Eng. Sci.*, **6**, 35-41 (1956), gave the solution for constant  $m$  and  $n$ . The extension to temperature-dependent  $m$  and an associated experimental study were given by E. B. Christiansen and S. E. Craig, Jr., *AIChE J.*, **8**, 154-160 (1962). See also E. B. Christiansen, G. E. Jensen, and F. S. Tao, *ibid.*, **12**, 1196-1202 (1966) and E. B. Christiansen and G. E. Jensen, *ibid.*, **15**, 504-507 (1969).

in which  $T_w = T_1$  and  $\Theta_b = (T_b - T_1)/(T_0 - T_1)$ . From Eq. 4.4-33 we find that

$$\left. \frac{\partial \Theta}{\partial \xi} \right|_{\xi=1} = \sum_{i=1}^{\infty} A_i e^{-\beta_i^2 \zeta} X_i'(1) \tag{4.4-36}$$

$$\begin{aligned} \Theta_b &= \frac{\int_0^1 \phi(\xi) \Theta(\xi, \zeta) \xi \, d\xi}{\int_0^1 \phi(\xi) \xi \, d\xi} = 2 \int_0^1 \phi(\xi) \Theta(\xi, \zeta) \xi \, d\xi \\ &= 2 \sum_{i=1}^{\infty} A_i e^{-\beta_i^2 \zeta} \int_0^1 \phi(\xi) X_i(\xi) \xi \, d\xi \\ &= -2 \sum_{i=1}^{\infty} A_i e^{-\beta_i^2 \zeta} \int_0^1 \frac{1}{\beta_i^2} \frac{d}{d\xi} \left( \xi \frac{dX_i}{d\xi} \right) d\xi \\ &= -2 \sum_{i=1}^{\infty} A_i e^{-\beta_i^2 \zeta} \left. \frac{1}{\beta_i^2} \xi \frac{dX_i}{d\xi} \right|_0^1 = -2 \sum_{i=1}^{\infty} \frac{A_i}{\beta_i^2} e^{-\beta_i^2 \zeta} X_i'(1) \end{aligned} \tag{4.4-37}$$

In going from the second to the third line, use has been made of Eq. 4.4-32. The Nusselt number is then given by

$$\text{Nu} = \frac{\sum_{i=1}^{\infty} A_i e^{-\beta_i^2 \zeta} X_i'(1)}{\sum_{i=1}^{\infty} (A_i/\beta_i^2) e^{-\beta_i^2 \zeta} X_i'(1)} \tag{4.4-38}$$

This expression is the local Nusselt number valid for all values of  $z$ . However, in order to use this result all the eigenvalues and eigenfunctions must be known.

For large values of  $z$  (or  $\zeta$ ) Eq. 4.4-38 can be simplified considerably inasmuch as only the first term in each sum is needed:

$$\lim_{\zeta \rightarrow \infty} \text{Nu} = \beta_1^2 \tag{4.4-39}$$

This is just the result given in Eq. E of Table 4.4-4; according to this result we need calculate only the first eigenvalue for the boundary-value problem in Eq. 4.4-32. There are several ways of doing this; we illustrate here the use of the method of Stodola and Vianello<sup>14</sup> for the particular case of  $n = \frac{1}{2}$  (or  $s = 2$ ).

For  $s = 2$  we have  $\phi(\xi) = \frac{5}{3}(1 - \xi^3)$ . As a first guess for the lowest eigenfunction we try  $X_1(\xi) = 1 - \xi^3$ . Then Eq. 4.4-32 becomes

$$\frac{d}{d\xi} \left( \xi \frac{dX}{d\xi} \right) = -\frac{5}{3} \beta_1^2 \xi (1 - \xi^3)^2 \tag{4.4-40}$$

<sup>14</sup> See, for example, F. B. Hildebrand, *Advanced Calculus for Applications*, Prentice-Hall, Englewood Cliffs, NJ (1962), pp. 200-206. To solve the differential equation

$$\frac{d}{dx} \left[ p(x) \frac{dy}{dx} \right] + \lambda r(x) y = 0 \tag{4.4-39a}$$

with homogeneous boundary conditions at  $x = a$  and  $x = b$ , do the following: (i) in the  $\lambda$ -term, replace  $y(x)$  by a reasonable first guess  $y_1(x)$ ; (ii) solve the resulting differential equation and obtain the solution  $y(x) = \lambda f_1(x)$ ; then repeat (i) with a second guess  $y_2(x) = f_1(x)$ ; solve the resulting differential equation to obtain the solution  $y(x) = \lambda f_2(x)$ , and continue the process as long as desired. At the  $n$ th stage in this process the  $n$ th approximation to the lowest eigenvalue  $\lambda_1$  can be obtained from

$$\lambda_1^{(n)} = \frac{\int_a^b r(x) f_n(x) y_n(x) \, dx}{\int_a^b r(x) [f_n(x)]^2 \, dx} \tag{4.4-39b}$$

This may be integrated to give

$$X(\xi) = \frac{5}{3} \beta_1^2 \left( \frac{297}{64 \cdot 25} - \frac{1}{4} \xi^2 + \frac{2}{25} \xi^5 - \frac{1}{64} \xi^8 \right) \quad (4.4-41)$$

$$\equiv \beta_1^2 f_1(\xi)$$

Then, using Eq. 4.4-39b we find

$$[\beta_1^2]^{(1)} = \frac{\int_0^1 \xi(1-\xi^3) f_1(\xi)(1-\xi^3) d\xi}{\int_0^1 \xi(1-\xi^3) [f_1(\xi)]^2 d\xi} \quad (4.4-42)$$

$$= 3.97$$

This approximate result can be compared with the value  $Nu = 3.95$  obtained by a complete numerical solution to the eigenvalue problem. It should be evident that the method of Stodola and Vianello can provide relatively quick estimates of the Nusselt numbers for large  $z$  for problems of this type.

#### EXAMPLE 4.4-3. Flow in a Circular Die with Viscous Heating<sup>15, 16</sup>

A molten plastic enters a horizontal circular die of radius  $R$  and length  $L$  at a temperature  $T_0$ . The fluid velocity is sufficiently high that viscous heating is known to be important. Find the temperature distribution in the die assuming (i) the die wall is maintained at temperature  $T_0$ ; (ii) the fluid is described adequately by a power-law viscosity with  $m$  and  $n$  independent of temperature; (iii) the fluid has a fully developed velocity profile at the die entrance; and (iv) density, heat capacity, and thermal conductivity do not change with temperature or pressure.

What is the maximum temperature predicted for a polyethylene melt that enters the die at 463 K when the wall shear stress is  $2 \times 10^5$  Pa? The melt has the following physical properties:  $\rho \hat{C}_p = 1.80 \times 10^6$  J/m<sup>3</sup>K;  $k = 0.25$  W/m·K;  $n = 0.50$ ;  $m = 6.9 \times 10^3$  Pa·s<sup>1/2</sup>. The radius and length of the die are 0.0394 and 1.28 cm, respectively.

**SOLUTION** We postulate that  $v_z = v_z(r)$ ,  $p = p(z)$ , and  $T = T(r, z)$ . Then the equation of continuity is satisfied identically and the equation of motion (Eq. 4.4-2) and the equation of energy (Eq. 4.4-3) are

$$\text{Motion:} \quad 0 = -\frac{dp}{dz} + \frac{1}{r} \frac{d}{dr} \left( \eta r \frac{dv_z}{dr} \right) \quad (4.4-43)$$

$$\text{Energy:} \quad \rho \hat{C}_p v_z \frac{\partial T}{\partial z} = k \frac{1}{r} \frac{\partial}{\partial r} \left( r \frac{\partial T}{\partial r} \right) + \eta \left( \frac{dv_z}{dr} \right)^2 \quad (4.4-44)$$

<sup>15</sup> Flow of a Newtonian fluid in a circular tube with viscous heating was first solved according to the method given here by H. C. Brinkman, *Appl. Sci. Res.*, **A2**, 120-124 (1951). The extension to power-law fluids was worked out by R. B. Bird, *J. Soc. Plast. Eng.*, **11**, 35-40 (1955), with later developments by N. Galili, R. Takserman-Krozer, and Z. Rigbi, *Rheol. Acta*, **14**, 550-567 (1975); N. Galili, Z. Rigbi, and R. Takserman-Krozer, *Rheol. Acta*, **14**, 816-831 (1975); and C. A. Hieber, *Rheol. Acta*, **16**, 553-567 (1977). Temperature-dependent viscosity effects were considered by J. B. Lyon and R. E. Gee, *Ind. Eng. Chem.*, **49**, 956-960 (1957), by E. A. Kearsley, *Trans. Soc. Rheol.*, **6**, 253-261 (1962), and by P. C. Sukaneck, *Chem. Eng. Sci.*, **26**, 1775-1776 (1971). In the last two publications cited, analytical solutions are given for large  $z$  for the Newtonian and power-law fluids.

<sup>16</sup> See also S. M. Dinh and R. C. Armstrong, *AIChE J.*, **28**, 294-301 (1982).

Axial heat conduction has been neglected in the energy equation for reasons discussed in Example 4.4-1. For the power-law fluid we have to insert  $\eta = m(-dv_z/dr)^{n-1}$ , and then according to Example 4.2-1

$$v_z = v_{\max} \left[ 1 - \left( \frac{r}{R} \right)^{s+1} \right] \quad (4.4-45)$$

where  $v_{\max} = [(p_0 - p_L)R/2mL]^s [R/(s+1)]$  and  $s = 1/n$ .

It is convenient to rewrite Eq. 4.4-44 in dimensionless form by introducing the following dimensionless quantities:

$$\xi = \frac{r}{R}; \quad \zeta = \frac{\alpha z}{v_{\max} R^2}; \quad \Theta = \frac{T - T_0}{\Delta T_0}; \quad \phi = \frac{v_z}{v_{\max}} \quad (4.4-46)$$

where the scaling for  $z$  is selected as in Example 4.4-1 to correspond to large Péclet number. Here we have chosen to use  $v_{\max}$  as a characteristic velocity. Since in this problem there is no temperature change imposed by the boundary conditions and the viscosity is assumed to be temperature independent, a reasonable choice for  $\Delta T_0$  to scale temperature changes is  $\Delta T_{\text{gen}}$ , the temperature rise associated with a balance between viscous heating and heat conduction. From Table 4.4-1 (footnote *b*) this is

$$\Delta T_{\text{gen}} = \eta^0 V^2/k = \frac{mR^2}{k} \left( \frac{v_{\max}}{R} \right)^{n+1} \quad (4.4-47)$$

where  $\eta^0$  is the viscosity evaluated at a characteristic shear rate ( $v_{\max}/R$ ). Then the dimensionless temperature is

$$\Theta = \frac{(T - T_0)k}{mR^2(v_{\max}/R)^{n+1}} \quad (4.4-48)$$

and the mathematical problem to be solved is

$$(1 - \xi^{s+1}) \frac{\partial \Theta}{\partial \zeta} = \frac{1}{\xi} \frac{\partial}{\partial \xi} \left( \xi \frac{\partial \Theta}{\partial \xi} \right) + (s+1)^{(1/s)+1} \xi^{s+1} \quad (4.4-49)$$

with boundary conditions

$$B.C. 1: \quad \text{at } \zeta = 0 \quad \Theta = 0 \quad (4.4-50)$$

$$B.C. 2: \quad \text{at } \xi = 0 \quad \partial \Theta / \partial \xi = 0 \quad (4.4-51)$$

$$B.C. 3: \quad \text{at } \xi = 1 \quad \Theta = 0 \quad (4.4-52)$$

Because of the heat-production term, Eq. 4.4-49 cannot be directly solved by the method of separation of variables. Intuitively we know that for large distances down the tube a temperature distribution should be attained that depends only on the radial coordinate. Therefore it seems reasonable to postulate a solution of the form

$$\Theta(\xi, \zeta) = \Theta_1(\xi) - \Theta_2(\xi, \zeta) \quad (4.4-53)$$

in which  $\Theta_1$  is the solution for very large  $\zeta$ , and  $\Theta_2$  is a function that just cancels  $\Theta_1$  at  $\zeta = 0$  and which tends to zero as  $\zeta$  becomes very large. The  $\Theta_1$ -part is easily obtained by setting the left side of

## 220 DYNAMICS OF POLYMERIC LIQUIDS

Eq. 4.4-49 equal to zero and solving the remaining ordinary differential equation using the boundary conditions at  $\xi = 0$  and  $\xi = 1$ . This gives

$$\Theta_1(\xi) = \frac{(s+1)^{(1/s)+1}}{(s+3)^2} (1 - \xi^{s+3}) \quad (4.4-54)$$

Now the results in Eqs. 4.4-53 and 54 can be inserted into Eq. 4.4-49, and in this way an equation is obtained for  $\Theta_2$

$$(1 - \xi^{s+1}) \frac{\partial \Theta_2}{\partial \zeta} = \frac{1}{\xi} \frac{\partial}{\partial \xi} \left( \xi \frac{\partial \Theta_2}{\partial \xi} \right) \quad (4.4-55)$$

This equation can be solved by the method of separation of variables. We postulate that  $\Theta_2(\xi, \zeta) = X(\xi)Z(\zeta)$  and this leads to

$$\frac{1}{Z} \frac{dZ}{d\zeta} = \frac{1}{X} \frac{1}{(1 - \xi^{s+1})} \frac{1}{\xi} \frac{d}{d\xi} \left( \xi \frac{dX}{d\xi} \right) = -a \quad (4.4-56)$$

in which  $a$  is the separation constant. This procedure thus leads to two separate ordinary differential equations for  $X(\xi)$  and  $Z(\zeta)$ . The  $X$ -equation has to be solved with the boundary conditions that  $X(\xi) = 0$  at  $\xi = 1$ , and  $X'(\xi) = 0$  at  $\xi = 0$ . This boundary-value problem has an infinite set of solutions  $X_k(\xi)$  corresponding to the infinite set of eigenvalues  $a_k$ . It may be shown directly from the differential equation that the  $X_k(\xi)$  satisfy the orthogonality conditions

$$\int_0^1 (1 - \xi^{s+1}) \xi X_k(\xi) X_l(\xi) d\xi = 0 \quad (k \neq l) \quad (4.4-57)$$

Because of the linearity of the original partial differential equation, the expression for  $\Theta_2(\xi, \zeta)$  must be given by a superposition of products of functions of  $\xi$  and functions of  $\zeta$ . The final expression for  $\Theta$  must therefore have the form

$$\Theta(\xi, \zeta) = \frac{(s+1)^{(1/s)+1}}{(s+3)^2} (1 - \xi^{s+3}) - \sum_{k=1}^{\infty} B_k X_k(\xi) e^{-a_k \zeta} \quad (4.4-58)$$

The  $B_k$  must be determined from the boundary condition at  $\zeta = 0$ . By multiplying Eq. 4.4-58 (with  $\zeta = 0$  and  $\Theta = 0$ ) by  $\xi(1 - \xi^{s+1})X_l$  and integrating over  $\xi$  from 0 to 1, we get

$$B_l = \frac{(s+1)^{(1/s)+1}}{(s+3)^2} \frac{\int_0^1 X_l(1 - \xi^{s+3})(1 - \xi^{s+1}) \xi d\xi}{\int_0^1 X_l^2(1 - \xi^{s+1}) \xi d\xi} \quad (4.4-59)$$

The problem is thus solved once the eigenfunctions  $X_k(\xi)$  and the eigenvalues  $a_k$  are known.

We illustrate here a method that may be used in the instances when  $s = 1/n$  is an integer;<sup>17</sup> in particular we let  $s = 1/n = 2$ . We seek a solution to the  $X(\xi)$ -equation in Eq. 4.4-56 in the form of a

<sup>17</sup> For arbitrary values of  $n$  see C. A. Hieber, *Rheol. Acta*, **16**, 553-567 (1977). A numerical solution for arbitrary  $n$  of the corresponding eigenvalue problem for slit flow is given by R. M. Ybarra and R. E. Eckert, *AIChE J.*, **26**, 751-762 (1980); see also R. A. Mashelkar, V. V. Charan, and N. G. Karanth, *Chem. Eng. J.*, **6**, 75-77 (1973).

**TABLE 4.4-6<sup>a</sup>**  
**Constants for Use in Eq. 4.4-58**  
**When  $n = 1/2$**

$i$	$a_i$	$B_i$
1	6.582	+0.2904
2	39.10	-0.1217
3	99.50	+0.06065
4	187.8	-0.03525

<sup>a</sup> This table is based on C. A. Hieber, *Rheol. Acta*, **16**, 553-567 (1977), Table 4 (with  $a_i = [(s + 3)/(s + 1)] \omega_i$  and  $B_i = -4^{n-1}[(s + 1)/(s + 3)]^{n+1} \tau_i$  where  $\omega_i$  and  $\tau_i$  are the eigenvalues and expansion coefficients in Hieber's notation). This kind of tabulation was first given by R. B. Bird, *SPE J.*, **11**, 35-40 (1955).

power series; the  $i$ th eigenfunction will thus have the form

$$X_i(\xi) = \sum_{k=0}^{\infty} b_{ik} \xi^k \tag{4.4-60}$$

in which  $b_{i0}$  is arbitrarily chosen to be unity, and the  $b_{ik}$  are zero for  $k < 0$ . The coefficient  $b_{i1}$  must be zero to satisfy the boundary condition at  $\xi = 0$ . Substitution of the above postulated solution into the differential equation leads to the following recursion formula:  $b_{ik} = -(a_i/k^2)(b_{i,k-2} - b_{i,k-5})$ . Hence all of the  $b_{ik}$  can be expressed in terms of the eigenvalues  $a_i$ , which are at this point still not known

$$\begin{aligned} b_{i2} &= -\frac{1}{4}a_i & b_{i5} &= +\frac{1}{25}a_i \\ b_{i3} &= 0 & b_{i6} &= -\frac{1}{2304}a_i^3 \\ b_{i4} &= +\frac{1}{64}a_i^2 & b_{i7} &= -\frac{29}{4900}a_i^2, \text{ etc.} \end{aligned} \tag{4.4-61}$$

The boundary condition at  $\xi = 1$  then requires that  $\sum_{k=0}^{\infty} b_{ik} = 0$ . When the  $b$ 's from Eq. 4.4-61 are substituted into this, we get an algebraic equation for  $a_i$ ; since this equation is of infinite order, an infinite number of eigenvalues  $a_1, a_2, a_3, \dots$  will be obtained. The first few of these values are shown in Table 4.4-6. Since the  $X$ -equation is a second-order differential equation, there must be a second solution in addition to that in Eq. 4.4-60, with the  $b$ 's provided by Eq. 4.4-61. It can be shown, however, that the second solution becomes infinite at  $\xi = 0$  and is hence unacceptable here.

Once we have the eigenvalues  $a_i$  and the eigenfunctions  $X_i$ , it is a straightforward matter to get the  $B_i$  from Eq. 4.4-59. The first few  $B_i$  are shown in Table 4.4-6 along with the corresponding eigenvalues.<sup>18</sup> The temperature profiles computed from Eq. 4.4-58 are shown in Fig. 4.4-2. There it can be seen that, at short distances, there is a peak in the temperature profile near the wall where the velocity gradient and also the viscous heating are large. The temperature profiles for a thermally insulated wall are also shown in Fig. 4.4-2 for comparison.

<sup>18</sup> Note that the  $X$ -equations of Eqs. 4.4-32 and 4.4-56 are nearly the same. Since  $\phi = v_z/\langle v_z \rangle$  (rather than  $v_z/v_{z,\max}$ ) in Eq. 4.4-32, the eigenvalues in the two examples bear the relation  $a_j = (v_{z,\max}/\langle v_z \rangle)\beta_j^2$ . Hence the  $a_1 = 6.582$  in Table 4.4-6 corresponds to  $\beta_1^2 = 3.95$  cited just after Eq. 4.4-42.

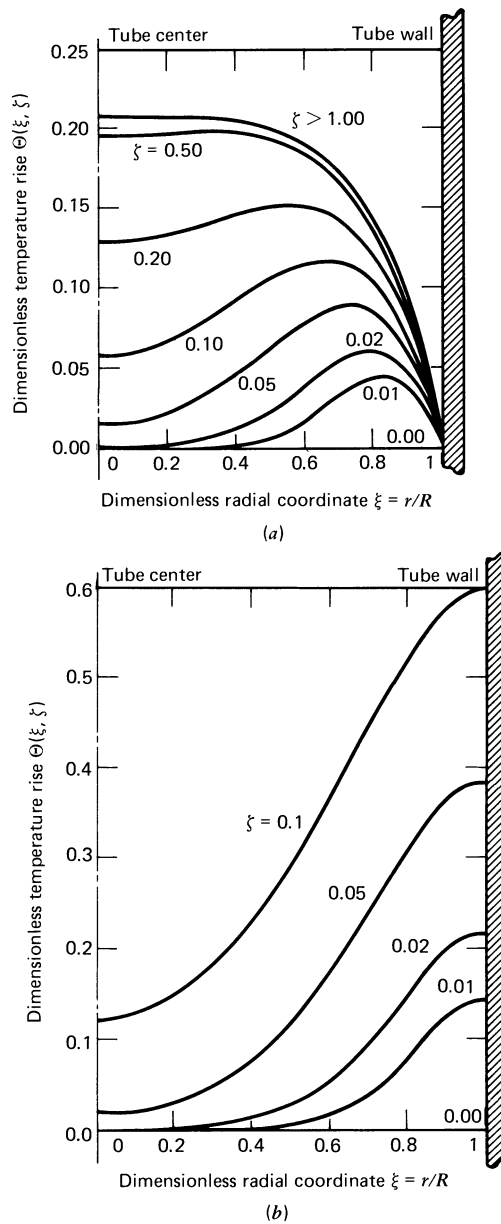


FIGURE 4.4-2. Temperature profiles for tube flow with viscous heating, based on the power-law model with  $n = 1/2$ , and with  $m$  and  $n$  taken to be constant. (a) Constant wall temperature; (b) zero wall heat flux. [After R. B. Bird, *SPE J.*, **11**, 35-40 (1955).]

For the particular experimental data given in the problem statement, the maximum temperature will occur at the tube exit, that is at  $z = 0.0128$  m. The dimensionless axial distance  $\zeta$  divided by Péclet number at the exit is:

$$\begin{aligned}
 \zeta &= \frac{kz}{\rho \hat{C}_p v_{\max} R^2} = \frac{k(s+1)m^s z}{\rho \hat{C}_p \tau_R^s R^3} \\
 &= \frac{(0.25)(3)(6.9 \times 10^3)^2(0.0128)}{(1.80 \times 10^6)(2.0 \times 10^5)^2(3.94 \times 10^{-4})^3} \\
 &= 0.104
 \end{aligned}
 \tag{4.4-62}$$

From Fig. 4.4-2 we find by interpolation that the maximum dimensionless temperature  $\Theta_{\max}$  is about 0.12. Hence from Eq. 4.4-48 we get

$$\begin{aligned}(T - T_0)_{\max} &= \frac{mR^2(\tau_R/m)^{(s+1)}}{(s+1)^{(1/s)+1}k} \Theta_{\max} \\ &= \frac{R^2\tau_R^3\Theta_{\max}}{3^{3/2}km^2} \\ &= \frac{(3.94 \times 10^{-4})^2(2.0 \times 10^5)^3(0.12)}{(6.9 \times 10^3)^2(0.25)(3^{3/2})} \\ &= 2.4 \text{ K}\end{aligned}\tag{4.4-63}$$

For the insulated wall problem, the temperature rise would have been about 12 K. It is thus evident that viscous heating can produce nonignorable temperature rises in extrusion operations.

We emphasize that the development here has been given for temperature-independent physical properties. The temperature dependence of  $m$ , however, cannot really be ignored if the temperature rise is more than a few degrees. Hence the use of the result in Fig. 4.4-2 should really be restricted to estimating flow speeds or pressure drops at which viscous heating just begins to be important.

We conclude with a few comments about the calculation of the eigenvalues  $a_i$ . Obtaining the  $a_i$  for  $i \geq 4$  is tedious by the method outlined above. For  $i \geq 4$  the WKBJ (Wentzel-Kramers-Brillouin-Jeffreys) method, widely used in quantum mechanics, is useful for getting both the eigenvalues and eigenfunctions. Applications to non-Newtonian heat-transfer problems have been given by Whiteman and Drake,<sup>19</sup> by Ziegenhagen,<sup>20</sup> and by Dinh and Armstrong.<sup>21</sup> For the problem at hand the application of the WKBJ method gives for any velocity profile  $v_z$

$$a_i = \left[ \frac{(i - \frac{1}{3})\pi}{\int_0^1 \sqrt{v_z(\xi)/v_{\max}} d\xi} \right]^2\tag{4.4-64}$$

Note that this result is not restricted to integer values of  $s = 1/n$ . For the power law with  $s = 2$  (or  $n = 0.5$ ) we find

$$a_i = \left[ \frac{(i - \frac{1}{3})\pi}{\int_0^1 \sqrt{1 - \xi^3} d\xi} \right]^2 = \left[ \frac{(i - \frac{1}{3})\pi}{\Gamma(\frac{3}{2})\Gamma(\frac{4}{3})/\Gamma(\frac{11}{6})} \right]^2 = \left[ \frac{(i - \frac{1}{3})\pi}{0.841} \right]^2\tag{4.4-65}$$

This gives  $a_1 = 6.202$ ,  $a_2 = 38.8$ ,  $a_3 = 99.2$ , and  $a_4 = 187.6$ ; by comparing with the exact values in Table 4.4-6 we see that for small  $i$ , for which the method is not intended, the results are not too good, but that the error is less than 0.5% for  $i = 3$ .

#### EXAMPLE 4.4-4 Viscous Heating in a Cone-and-Plate Viscometer<sup>22</sup>

Obtain the temperature profile for the flow of a power-law fluid in the parallel-plate system of Fig. 1.3-1 for the special case that there is no superposed pressure gradient. First consider  $m$ ,  $n$ , and  $k$  all to be constants. Then let  $m$  vary with temperature according to Eq. 4.4-4. Finally show how the results can be adapted for use in estimating viscous-heating effects in the cone-and-plate instrument.

<sup>19</sup> I. R. Whiteman and W. B. Drake, *Trans. ASME*, **80**, 728-732 (1958).

<sup>20</sup> A. J. Ziegenhagen, *Int. J. Heat Mass Transfer*, **8**, 499-505 (1965).

<sup>21</sup> S. M. Dinh and R. C. Armstrong, *AIChE J.*, **28**, 294-301 (1982), have obtained the eigenvalues and uniformly valid eigenfunctions for both the tube and slit problems and for wall boundary conditions ranging from insulated to constant temperature.

<sup>22</sup> The perturbation solution presented here is patterned after R. M. Turian, *Chem. Eng. Sci.*, **20**, 771-781 (1965); a closed-form solution was given by J. Gavis and R. L. Laurence, *Ind. Eng. Chem. Fundam.*, **7**, 525-527 (1968). The equation in Turian's paper which corresponds to Eq. 4.4-93 erroneously contains  $(1/20)Na/n$  rather than the correct value  $(1/20)Na$ : note that Turian's  $BrA$  corresponds to  $Na$  in this example.

**SOLUTION** (a) Flow between Parallel Plates with the Assumption of Constant Physical Properties.

We consider the flow in the  $x$ -direction of a fluid between two parallel plates located at  $y = 0$  and  $y = B$  (cf. Fig. 1.3-1); the lower plate is fixed and the upper one is moving in the positive  $x$ -direction with a constant velocity  $V$  and  $\partial p/\partial x = 0$ . For a generalized Newtonian fluid the equations of motion and energy that we need for describing the flow are the following simplifications of Eqs. 4.4-2 and 3:

$$0 = \frac{d}{dy} \left( \eta \frac{dv_x}{dy} \right) \quad (4.4-66)$$

$$0 = \frac{d}{dy} \left( k \frac{dT}{dy} \right) + \eta \left( \frac{dv_x}{dy} \right)^2 \quad (4.4-67)$$

into which, for this problem, we substitute  $\eta = m(dv_x/dy)^{n-1}$ .

We first work through the simplified problem in which  $m$  and  $n$ , as well as the thermal conductivity, are not varying with temperature. The problem can be written in dimensionless form as

$$0 = \frac{d}{d\xi} \left( \frac{d\phi}{d\xi} \right)^n \quad (4.4-68)$$

$$0 = \frac{d^2\Theta}{d\xi^2} + \left( \frac{d\phi}{d\xi} \right)^{n+1} \quad (4.4-69)$$

subject to the boundary conditions

$$\text{at } \xi = 0 \quad \phi = 0, \quad \Theta = 0 \quad (4.4-70)$$

$$\text{at } \xi = 1 \quad \phi = 1, \quad \Theta = 0 \quad (4.4-71)$$

The dimensionless variables are defined by

$$\phi = \frac{v_x}{V}; \quad \Theta = \frac{(T - T_0)}{\Delta T_0}; \quad \xi = \frac{y}{B} \quad (4.4-72)$$

in which  $\Delta T_0$  is a characteristic temperature difference in the problem. Since no reference  $\Delta T$  can be formed from the boundary conditions or the temperature dependence of the viscosity, we choose  $\Delta T_0$  to be the temperature rise necessary for heat conduction to balance heat production by viscous heating. A balance between the order of magnitude of the viscous heating and heat conduction terms in Eq. 4.4-67 gives

$$k \frac{\Delta T_0}{B^2} = \eta \Big|_{\dot{\gamma} = V/B} \left( \frac{V}{B} \right)^2 = m \left( \frac{V}{B} \right)^{n+1} \quad (4.4-73)$$

so that

$$\Delta T_0 = m V^{n+1} / B^{n-1} k \quad (4.4-74)$$

Equations 4.4-68 through 71 are easily solved to give

$$\phi = \xi \quad (4.4-75)$$

$$\Theta = \frac{1}{2}(\xi - \xi^2) \quad (4.4-76)$$

The maximum temperature occurs at the midplane and is given by

$$\Theta_{\max} = \frac{1}{8} \quad (4.4-77)$$

This simple result can be used for making rough estimates of the temperature rise that can be expected in the gap between two moving surfaces in the absence of a pressure gradient.

**(b) Flow Between Parallel Plates with  $m$  Varying with the Temperature, but with  $n$  and  $k$  Constant.** We let  $m$  vary with temperature according to Eq. 4.4-4 and again introduce dimensionless variables defined by Eq. 4.4-72. Now, however, we scale temperature by a characteristic temperature difference required to change the viscosity substantially, since the effects of temperature dependent viscosity are of primary interest here. This  $\Delta T_0$  can be calculated from Eq. 4.4-4 as

$$\Delta T_0 = \left| \frac{\eta}{\partial \eta / \partial T} \right|_{\substack{y=B \\ T=T_0}} = 1/A \quad (4.4-78)$$

and we thus take

$$\Theta = A(T - T_0) \quad (4.4-79)$$

The equations of motion and energy (Eqs. 4.4-66 and 67) become

$$e^{-\Theta} \left( \frac{d\phi}{d\xi} \right)^n = C \quad (4.4-80)$$

$$\frac{d^2\Theta}{d\xi^2} + \text{Na} e^{-\Theta} \left( \frac{d\phi}{d\xi} \right)^{n+1} = 0 \quad (4.4-81)$$

in which  $\text{Na} = m^0 V^{n+1} A / B^{n-1} k$  is the Nahme-Griffith number for the power-law fluid,  $m^0$  is the value of  $m$  at  $T_0$  in Eq. 4.4-4, and  $C$  is an integration constant. The Nahme-Griffith number is a ratio of the temperature rise characteristic of the viscous heating in the problem (Eq. 4.4-74) to the temperature change necessary to alter the viscosity (Eq. 4.4-78). Thus for small values of  $\text{Na}$  the solution of part (a) is expected to be accurate.

From Eq. 4.4-80

$$\frac{d\phi}{d\xi} = C^s e^{s\Theta} = C^s (1 + a_1 \Theta + a_2 \Theta^2 + \dots) \quad (4.4-82)$$

in which  $s = 1/n$  and  $a_j = s^j/j!$ . This can be inserted into the energy equation Eq. 4.4-81 to give

$$\frac{d^2\Theta}{d\xi^2} = -\text{Na} C^{s+1} e^{(s-1)\Theta} = -\text{Na} C^{s+1} (1 + a_1 \Theta + a_2 \Theta^2 + \dots) \quad (4.4-83)$$

Equations 4.4-82 and 83 are solved by a perturbation procedure, using the Nahme-Griffith number as the perturbation parameter. We know that the unperturbed problem discussed in (a) has the solution  $\phi = \xi$  and  $\Theta = (1/2)\text{Na}(\xi - \xi^2)$ . This suggests that we seek a solution of the form:

$$\phi = \xi + \text{Na} \phi_1(\xi) + \text{Na}^2 \phi_2(\xi) + \dots \quad (4.4-84)$$

$$\Theta = \frac{1}{2}\text{Na} (\xi - \xi^2) + \text{Na}^2 \Theta_2(\xi) + \dots \quad (4.4-85)$$

It is also necessary to expand the integration constant in a similar series:

$$C = C_0 + \text{Na}C_1 + \text{Na}^2C_2 + \dots \quad (4.4-86)$$

$$C^s = C_0^s + \text{Na} (sC_0^{s-1}C_1) + \text{Na}^2 (sC_0^{s-1}C_2 + \frac{1}{2}s(s-1)C_0^{s-2}C_1^2) + \dots \quad (4.4-87)$$

When these expansions are substituted into Eqs. 4.4-82 and 83, sets of differential equations are obtained by equating the coefficients of equal powers of Na. The resulting differential equations are solved with the boundary conditions that  $\Theta_j$  and  $\phi_j$  are both zero at  $\xi = 0, 1$ . In this way, we obtain

$$\phi = \xi - \frac{1}{12n} \text{Na} (\xi - 3\xi^2 + 2\xi^3) + \dots \quad (4.4-88)$$

$$\Theta = \frac{1}{2} \text{Na}(\xi - \xi^2) - \frac{1}{24n} \text{Na}^2(n\xi - (n+1)\xi^2 + 2\xi^3 - \xi^4) + \dots \quad (4.4-89)$$

It is not difficult to show that  $\phi(\xi)$  and  $\Theta(\xi)$  are symmetric about the plane  $\xi = 1/2$ .

### (c) Application to the Cone-and-Plate Viscometer

When viscous heating is appreciable, viscometers will give incorrect readings because of the temperature dependence of the rheological properties. We now adapt the above results in an approximate way to the cone-and-plate instrument in order to estimate the influence of viscous heating on the measurement of viscosity.

We can make a table of equivalences between the notation used for the parallel-plate system and that used in Example 1.3-4 for the cone-and-plate system:

Parallel-Plate System	Cone-and-Plate System
$V$	$Wr$
$B$	$\vartheta_0 r$
$\xi = \frac{y}{B}$	$\bar{\xi} = \frac{(\pi/2) - \theta}{\vartheta_0}$
$\phi = \frac{v_x}{V}$	$\bar{\phi} = \frac{v_\phi}{Wr}$
$\text{Na} = \frac{m^0 V^{n+1} A}{kB^{n-1}}$	$\bar{\text{Na}} = \widetilde{\text{Na}} \left(\frac{r}{R}\right)^2 = \frac{m^0 W^{n+1} R^2 A}{k\vartheta_0^{n-1}} \left(\frac{r}{R}\right)^2$

Recall that the torque required to maintain the rotary motion of the cone is, according to Eq. 1.3-35,

$$\mathcal{T} = \int_0^{2\pi} \int_0^R \tau_{\theta\phi} \Big|_{\theta=\pi/2} r^2 dr d\phi = 2\pi \int_0^R \left( -\eta \frac{1}{r} \frac{\partial v_\phi}{\partial \theta} \right) \Big|_{\theta=\pi/2} r^2 dr \quad (4.4-90)$$

Here an approximate form of  $\dot{\gamma}_{\theta\phi}$  is used since  $\theta \doteq \pi/2$  throughout the gap and  $\sin \theta \doteq 1$ .

Now, using the power law gives

$$\begin{aligned} \mathcal{T} &= 2\pi R^3 \int_0^1 \left[ m \left( -\frac{1}{r} \frac{\partial v_\phi}{\partial \theta} \right)^n \right]_{\theta=\pi/2} \left(\frac{r}{R}\right)^2 d\left(\frac{r}{R}\right) \\ &= 2\pi m^0 R^3 \int_0^1 \left[ \left( \frac{d\bar{\phi}}{d\bar{\xi}} \frac{W}{\vartheta_0} \right)^n \right]_{\bar{\xi}=0} \left(\frac{r}{R}\right)^2 d\left(\frac{r}{R}\right) \end{aligned} \quad (4.4-91)$$

We now assume that  $\bar{\phi}$  will be the same function of  $\bar{\xi}$  and  $\bar{Na}$  that  $\phi$  is of  $\xi$  and  $Na$ . Then

$$\mathcal{F} = \frac{2\pi m^0 W^n R^3}{9_0^n} \int_0^1 \left[ 1 - \frac{1}{12n} \widetilde{Na} \left(\frac{r}{R}\right)^2 + \dots \right]^n \left(\frac{r}{R}\right)^2 d\left(\frac{r}{R}\right) \quad (4.4-92)$$

Use of the binomial expansion and integration then finally gives

$$\mathcal{F} = \frac{2\pi m^0 W^n R^3}{39_0^n} \left( 1 - \frac{1}{20} \widetilde{Na} + \dots \right) \quad (4.4-93)$$

This shows how viscous heating reduces the torque below that which one would expect for a power-law fluid with parameters  $m$  and  $n$  independent of temperature (i.e.,  $A = 0$  and  $B = 0$  in Eqs. 4.4-4 and 5). Viscous heating can be a serious problem in interpreting cone-and-plate viscometer data (see §10.2).

#### §4.5 OTHER EMPIRICAL NON-NEWTONIAN VISCOSITY FUNCTIONS FOR USE IN THE GENERALIZED NEWTONIAN FLUID MODEL

In §4.1 we gave two empirical functions  $\eta(\dot{\gamma})$ : the 5-constant Carreau–Yasuda function, which can fit rather accurately many experimental viscosity curves over a wide range of shear rate; and the 2-constant power-law function, which can fit only a linear region of a  $\log \eta$  vs.  $\log \dot{\gamma}$  plot if such exists. Because of the ease with which analytical solutions can be obtained for the power-law function, we used it extensively in §§4.2–4.4. In the engineering literature many other empirical functions have been used, and in this section we introduce a few of them and illustrate their use.

In Table 4.5-1 we give a half dozen expressions for  $\eta(\dot{\gamma})$ . Each of these models has a characteristic time. The three-parameter  $(\eta_0, \dot{\gamma}_0, n)$  *truncated power law* is a discontinuous function that has a zero-shear-rate viscosity up to a critical shear rate  $\dot{\gamma}_0$ , and a power-law region above  $\dot{\gamma}_0$ . The two-parameter  $(\lambda_0, \tau_0)$  *Eyring model* was derived from a molecular theory of liquids,<sup>1</sup> and it has been improved upon by inclusion of additional empirical constants. The three-parameter  $(\eta_0, \tau_{1/2}, \alpha)$  *Ellis model* is an example of a model that gives  $\eta$  in terms of stress rather than velocity gradients; for very high shear stress the model exhibits a power-law region, so that the Ellis-model parameters and the power-law parameters are related by  $m = \eta_0^{1/\alpha} \tau_{1/2}^{1-(1/\alpha)}$  and  $n = 1/\alpha$ . Finally the two-parameter  $(\mu_0, \tau_0)$  *Bingham model* is an illustration of a constitutive equation for a “viscoplastic” material,<sup>2</sup> that is, one with a yield stress,  $\tau_0$ , below which there is no flow. The viscoplastic models are particularly useful for describing liquids with large amounts of suspended solids.

Because of the importance of plane-slit flow and cylindrical-tube flow in engineering applications, we have summarized the results for these two flows for five empirical  $\eta(\dot{\gamma})$ -functions in Table 4.5-2. These results are obtained by following the procedure in Example 4.2-1. In the next two examples we illustrate some other aspects of solving flow problems with generalized Newtonian fluids. Example 4.5-1 shows how to cope with the yield stress in

<sup>1</sup> See, for example, R. B. Bird, W. E. Stewart, and E. N. Lightfoot, *Transport Phenomena*, Wiley, New York (1960), pp. 26–29.

<sup>2</sup> For a literature survey on viscoplastic models (including the Bingham, Casson, and Herschel–Bulkley equations), experimental tests, and solution of flow problems, see R. B. Bird, G. C. Dai, and B. J. Yarusso, *Revs. Chem. Eng.*, **1**, 1–70 (1982). For plastic viscoelastic constitutive equations see J. L. White, *J. Non-Newtonian Fluid Mech.*, **8**, 195–202 (1981).

TABLE 4.5-1

Empirical  $\eta(\dot{\gamma})$  Functions for Use in the Generalized Newtonian Fluid Model<sup>a</sup>

Model	Equation	Time Constant	Comments
Spriggs' truncated power law <sup>b</sup>	$\begin{cases} \eta = \eta_0 & (\dot{\gamma} \leq \dot{\gamma}_0) & \text{(A)} \\ \eta = \eta_0(\dot{\gamma}/\dot{\gamma}_0)^{n-1} & (\dot{\gamma} \geq \dot{\gamma}_0) & \text{(B)} \end{cases}$	$1/\dot{\gamma}_0$	$\dot{\gamma}_0$ is the value of $\dot{\gamma}$ at which "shear thinning" begins
Eyring <sup>c</sup> ( $\eta_1 = 0, \alpha = 1$ ); Powell-Eyring <sup>d</sup> ( $\alpha = 1$ ); Sutterby <sup>e</sup> ( $\eta_1 = 0$ )	$\eta = \lambda_0 \tau_0 \left( \frac{\text{arcsinh } \lambda_0 \dot{\gamma}}{\lambda_0 \dot{\gamma}} \right)^\alpha + \eta_1 \quad \text{(C)}$	$\lambda_0$	The Eyring equation was the first $\eta(\dot{\gamma})$ expression obtained by a molecular theory
Ellis <sup>f</sup>	$\frac{\eta_0}{\eta} = 1 + \left( \frac{\tau}{\tau_{1/2}} \right)^{\alpha-1} \quad \text{(D)}$	$\eta_0/\tau_{1/2}$	$\tau_{1/2}$ is the value of $\tau = \sqrt{(\tau:\tau)/2}$ at which $\eta = \eta_0/2$
Bingham <sup>g</sup>	$\begin{cases} \eta = \infty & (\tau \leq \tau_0) & \text{(E)} \\ \eta = \mu_0 + \frac{\tau_0}{\dot{\gamma}} & (\tau \geq \tau_0) & \text{(F)} \end{cases}$	$\mu_0/\tau_0$	$\tau_0$ is the "yield stress" and $\tau = \sqrt{(\tau:\tau)/2}$ ; Oldroyd <sup>h</sup> has done the most extensive theoretical work for this model

<sup>a</sup> In addition to the Carreau-Yasuda model (Eq. 4.1-9) and the power-law model (Eq. 4.1-10).<sup>b</sup> T. W. Spriggs University of Wisconsin-Madison, unpublished (1965).<sup>c</sup> J. F. Kincaid, H. Eyring, and A. E. Stearn, *Chem. Rev.*, **28**, 301-365 (1941); F. H. Ree, T. Ree, and H. Eyring, *Ind. Eng. Chem.*, **50**, 1036-1040 (1958).<sup>d</sup> R. E. Powell and H. Eyring, *Nature*, **154**, 427-428 (1944); D. L. Salt, N. W. Ryan, and E. B. Christiansen, *J. Colloid Sci.*, **6**, 146-154 (1951). A temperature-dependent Powell-Eyring model has been used by E. B. Christiansen and S. J. Kelsey, *Chem. Eng. Sci.*, **28**, 1099-1113 (1973).<sup>e</sup> J. L. Sutterby, *Trans. Soc. Rheol.*, **9**, 227-241 (1965); *AIChE J.*, **12**, 63-68 (1966).<sup>f</sup> S. B. Ellis [see M. Reiner, *Deformation, Strain, and Flow*, Interscience, New York (1960), p. 246]. S. Matsuhashi and R. B. Bird, *AIChE J.*, **11**, 588-595 (1965).<sup>g</sup> E. C. Bingham, *Fluidity and Plasticity*, McGraw-Hill, New York (1922), pp. 215-218; *U.S. Bur. Stand. Bull.*, **13**, 309-353 (1916). See also W. Prager, *Introduction to Mechanics of Continua*, Ginn, Boston (1961), Chapt. VII.<sup>h</sup> J. G. Oldroyd, *Proc. Camb. Phil. Soc.*, **43**, 100-105, 383-395, 396-405, 521-532 (1947); **44**, 200-213, 214-228 (1948); **45**, 595-611 (1949); **47**, 410-418 (1951).

the Bingham model; Example 4.5-2 demonstrates how to adapt a slit-flow result to an axial annular flow problem in an approximate procedure, and it further illustrates how quantitative limits can be placed on the range of validity of the power-law model.

**EXAMPLE 4.5-1** Tangential Flow of a Bingham Fluid in an Annulus

Determine the velocity distribution for the flow of a Bingham fluid in a coaxial annular region bounded by cylinders of radii  $\kappa R$  and  $R$  (with  $\kappa < 1$ ). The inner cylinder is kept fixed and the outer cylinder has an angular velocity  $W$ . As a result the fluid flows tangentially in the annular region. Obtain the relation between the angular velocity of the outer cylinder and the torque exerted on the outer cylinder.

TABLE 4.5-2

Flow Rates through Slits and Tubes

Model (Constants)	Volume Rate of Flow $Q$ in Thin Slit (Width $W$ , Thickness $2B$ , Length $L$ ) $\tau_{xz} _{x=B} \equiv \tau_B = (\mathcal{P}_0 - \mathcal{P}_L)B/L$	Volume Rate of Flow $Q$ in Circular Tube (Radius $R$ , Length $L$ ) $\tau_{rz} _{r=R} \equiv \tau_R = (\mathcal{P}_0 - \mathcal{P}_L)R/2L$
Power law ( $m, n$ )	$\frac{2WB^2}{(1/n) + 2} \left( \frac{\tau_B}{m} \right)^{1/n}$ (A)	$\frac{\pi R^3}{(1/n) + 3} \left( \frac{\tau_R}{m} \right)^{1/n}$ (F)
Ellis ( $\eta_0, \tau_{1/2}, \alpha$ )	$\frac{2WB^2\tau_B}{3\eta_0} \left[ 1 + \frac{3}{\alpha + 2} \left( \frac{\tau_B}{\tau_{1/2}} \right)^{\alpha-1} \right]$ (B) <sup>a</sup>	$\frac{\pi R^3\tau_R}{4\eta_0} \left[ 1 + \frac{4}{\alpha + 3} \left( \frac{\tau_R}{\tau_{1/2}} \right)^{\alpha-1} \right]$ (G) <sup>a</sup>
Truncated power law ( $\eta_0, \dot{\gamma}_0, n$ )	$\frac{2WB^2\tau_B}{[(1/n) + 2]\eta_0} \left[ \left( \frac{\eta_0\dot{\gamma}_0}{\tau_B} \right)^{1-(1/n)} + \frac{1}{3} \left( \frac{1}{n} - 1 \right) \left( \frac{\eta_0\dot{\gamma}_0}{\tau_B} \right)^3 \right]$ (when $\tau_B \gg \eta_0\dot{\gamma}_0$ ) (C)	$\frac{\pi R^3\tau_R}{[(1/n) + 3]\eta_0} \left[ \left( \frac{\eta_0\dot{\gamma}_0}{\tau_R} \right)^{1-(1/n)} + \frac{1}{4} \left( \frac{1}{n} - 1 \right) \left( \frac{\eta_0\dot{\gamma}_0}{\tau_R} \right)^4 \right]$ (when $\tau_R \gg \eta_0\dot{\gamma}_0$ ) (H)
Eyring ( $\tau_0, \lambda_0$ )	$\frac{2WB^2}{\lambda_0} \left( \frac{\tau_0}{\tau_B} \right)^2 \left[ \frac{\tau_B}{\tau_0} \cosh \frac{\tau_B}{\tau_0} - \sinh \frac{\tau_B}{\tau_0} \right]$ (D)	$\frac{2\pi R^3}{\lambda_0} \left( \frac{\tau_0}{\tau_R} \right)^3 \left[ \frac{1}{2} \left( \frac{\tau_0}{\tau_R} \right)^2 + 1 \right] \cosh \frac{\tau_R}{\tau_0} - \frac{\tau_R}{\tau_0} \sinh \frac{\tau_R}{\tau_0} - 1$ (I)
Bingham ( $\mu_0, \tau_0$ )	$\frac{2WB^2\tau_B}{3\mu_0} \left[ 1 - \frac{3}{2} \left( \frac{\tau_0}{\tau_B} \right) + \frac{1}{2} \left( \frac{\tau_0}{\tau_B} \right)^3 \right]$ (when $\tau_B \geq \tau_0$ ) (E)	$\frac{\pi R^3\tau_R}{4\mu_0} \left[ 1 - \frac{4}{3} \left( \frac{\tau_0}{\tau_R} \right) + \frac{1}{3} \left( \frac{\tau_0}{\tau_R} \right)^4 \right]$ (when $\tau_R \geq \tau_0$ ) (J) <sup>b</sup>

<sup>a</sup> See Problem 4B.9.

<sup>b</sup> Eq. J is called the *Buckingham-Reiner equation*; see E. Buckingham, *Proc. ASTM*, **117**, 1154-1161 (1921), and R. B. Bird, W. E. Stewart, and E. N. Lightfoot, *Transport Phenomena*, Wiley, New York (1960), pp. 48-50.

**SOLUTION** For this system  $v_r = v_z = 0$  and  $v_\theta = v_\theta(r)$ . Hence the only nonvanishing components of  $\boldsymbol{\tau}$  are  $\tau_{r\theta}$  and  $\tau_{\theta r}$ , and the  $\theta$ -equation of motion for steady state is in cylindrical coordinates:

$$0 = \frac{1}{r^2} \frac{d}{dr} (r^2 \tau_{r\theta}) \quad (4.5-1)$$

This may be integrated to give

$$\tau_{r\theta} = \frac{C_1}{r^2} \quad (4.5-2)$$

If the torque at the outer cylinder is known to be  $\mathcal{F}$ , then

$$\mathcal{F} = -\tau_{r\theta}|_{r=R} \cdot 2\pi RL \cdot R \quad (4.5-3)$$

where the minus sign is chosen because the  $\theta$ -momentum flux is in the  $r$ -direction. Hence,  $C_1 = -\mathcal{F}/2\pi L$  and

$$\tau_{r\theta} = -\frac{\mathcal{F}}{2\pi L r^2} \quad (4.5-4)$$

This result, which is valid for any kind of fluid, can also be obtained by recognizing that angular momentum must be transmitted undiminished from the outer to the inner cylinder.

For the Bingham model, the analytical expression to be used depends on the value of  $\tau = \sqrt{(\boldsymbol{\tau}:\boldsymbol{\tau})}/2 = \sqrt{(\sum_i \sum_j \tau_{ij}^2)}/2$ . Because  $\tau_{r\theta}$  and  $\tau_{\theta r}$  are the only nonvanishing components of  $\boldsymbol{\tau}$ , we have

$$\tau = \sqrt{(\boldsymbol{\tau}:\boldsymbol{\tau})}/2 = \sqrt{\tau_{r\theta}^2} = -\tau_{r\theta} \quad (4.5-5)$$

Hence we use Eq. F of Table 4.5-1 when  $\tau \geq \tau_0$  (i.e., when the critical shear stress is exceeded) and Eq. E when  $\tau \leq \tau_0$ . From Eq. 4.5-4, we find that we can define a quantity  $r_0$ , which is the value of  $r$  for which  $\tau = \tau_0$

$$r_0 = \left( \frac{\mathcal{F}}{2\pi\tau_0 L} \right)^{1/2} \quad (4.5-6)$$

We can then discuss three situations:

- a. If  $r_0 \leq \kappa R$ , then there will be no fluid motion at all.
- b. If  $\kappa R < r_0 \leq R$ , then there will be viscous flow in the region  $\kappa R < r < r_0$  and "plug flow" for  $r_0 \leq r \leq R$ .
- c. If  $r_0 \geq R$ , then there is flow throughout.

Next, we write Eq. F of Table 4.5-1 for the system at hand. Inasmuch as

$$\dot{\gamma} = \sqrt{(\dot{\boldsymbol{\gamma}}:\dot{\boldsymbol{\gamma}})}/2 = r \frac{d}{dr} \left( \frac{v_\theta}{r} \right) \quad (4.5-7)$$

we get from Eq. 4.1-4

$$\tau_{r\theta} = - \left\{ \mu_0 + \frac{\tau_0}{r \frac{d}{dr} \left( \frac{v_\theta}{r} \right)} \right\} r \frac{d}{dr} \left( \frac{v_\theta}{r} \right) = -\tau_0 - \mu_0 r \frac{d}{dr} \left( \frac{v_\theta}{r} \right) \quad (4.5-8)$$

Since  $v_\theta/r$  does not decrease with increasing  $r$ , we see that  $\tau_{r\theta}$  is negative as expected.

By substituting Eq. 4.5-8 into Eq. 4.5-4 and integrating, we get for case (b)

$$\frac{v_\theta}{r} = W + \frac{\mathcal{F}}{4\pi L \mu_0 r_0^2} \left[ 1 - \left( \frac{r_0}{r} \right)^2 \right] - \frac{\tau_0}{\mu_0} \ln \frac{r}{r_0} \quad (\text{for } \kappa R \leq r \leq r_0) \quad (4.5-9)$$

$$\frac{v_\theta}{r} = W \quad (\text{for } r_0 \leq r \leq R) \quad (4.5-10)$$

in which the boundary condition  $v_\theta/r = W$  at  $r = r_0$  has been used. For case (c), we use the boundary condition that  $v_\theta/r = W$  at  $r = R$  and get

$$\frac{v_\theta}{r} = W + \frac{\mathcal{F}}{4\pi L \mu_0 R^2} \left[ 1 - \left( \frac{R}{r} \right)^2 \right] - \frac{\tau_0}{\mu_0} \ln \frac{r}{R}, \quad (\text{for } \kappa R \leq r \leq R) \quad (4.5-11)$$

Finally, if in this last equation we set  $v_\theta = 0$  at  $r = \kappa R$ , we can solve for  $W$  to get

$$\text{(case (c) only)} \quad W = \frac{\mathcal{F}}{4\pi L \mu_0 R^2} \left( \frac{1}{\kappa^2} - 1 \right) + \frac{\tau_0}{\mu_0} \ln \kappa \quad (4.5-12)$$

This relation between  $W$  and  $\mathcal{F}$  (known as the *Reiner-Riwlin equation*<sup>3</sup>) gives a means for determining  $\mu_0$  and  $\tau_0$  from a concentric cylinder apparatus.

**EXAMPLE 4.5-2** An Approximate Solution for Axial Annular Flow to Account for the Zero-Shear-Rate Region of the Non-Newtonian Viscosity<sup>4</sup>

At the end of Example 4.2-4 it was pointed out that for slow flow rates the power-law fluid solution for the axial flow in an annulus can be expected to be in error because the power law does not describe the  $\eta(\dot{\gamma})$ -function faithfully for small shear rates. In this example we pursue this point quantitatively and give a comparison with experimental data. We use the Ellis model in this analysis.

Since a completely analytical solution for the Ellis model is not possible, use the following approximate procedure: **a.** Write the expression for volume rate of flow  $Q$  in an annulus for a Newtonian fluid as the expression for  $Q$  for plane slit flow multiplied by a "curvature correction factor;" **b.** Multiply the plane slit flow expression for  $Q$  of an Ellis fluid by the same curvature correction factor as was found in (a).

**SOLUTION (a)** Curvature Correction Factor for Newtonian Fluid

For the Newtonian fluid the volume rate of flow in a coaxial annulus is given by<sup>5</sup>

$$Q_{\text{ann.}} = \frac{\pi(\mathcal{P}_0 - \mathcal{P}_L)R^4}{8\mu L} \left[ (1 - \kappa^4) - \frac{(1 - \kappa^2)^2}{\ln(1/\kappa)} \right] \quad (4.5-13)$$

where  $\mathcal{P}_0 - \mathcal{P}_L$  is the modified pressure drop over a length  $L$  of conduit. For the flow in a slit of width  $W$ , thickness  $2B$ , and length  $L$  ( $B \ll W \ll L$ ) the volume rate of flow is easily found to be (see Eq. 1.3-5)

$$Q_{\text{slit}} = \frac{2(\mathcal{P}_0 - \mathcal{P}_L)WB^3}{3\mu L} \quad (4.5-14)$$

<sup>3</sup> M. Reiner and R. Riwlin, *Kolloid-Z.*, **43**, 1-5 (1927).

<sup>4</sup> E. Ashare, R. B. Bird, and J. A. Lescarbours, *AIChE J.*, **11**, 910-916 (1965).

<sup>5</sup> See, for example, R. B. Bird, W. E. Stewart, and E. N. Lightfoot, *Transport Phenomena*, Wiley, New York (1960), pp. 51-54.

If in Eq. 4.5-14 we replace  $W$  by  $2\pi R$  and  $2B$  by  $R(1 - \kappa)$ , we get

$$Q_{\text{ann. (approximate)}} = \frac{\pi(\mathcal{P}_0 - \mathcal{P}_L)R^4}{6\mu L} (1 - \kappa)^3 \quad (4.5-15)$$

In both Eqs. 4.5-13 and 4.5-15 we set  $1 - \kappa$  equal to the small quantity  $\varepsilon$ . Then we divide one by the other to get the Newtonian curvature correction factor  $C_N$

$$\begin{aligned} C_N &= Q_{\text{ann.}}/Q_{\text{ann. (approximate)}} \\ &= \frac{3}{4\varepsilon^3} \left\{ [1 - (1 - \varepsilon)^4] - \frac{\varepsilon^2(2 - \varepsilon)^2}{\varepsilon + \frac{1}{2}\varepsilon^2 + \frac{1}{3}\varepsilon^3 + \dots} \right\} \\ &= 1 - \frac{1}{2}\varepsilon + \frac{1}{60}\varepsilon^2 + \frac{1}{120}\varepsilon^3 + \dots \end{aligned} \quad (4.5-16)$$

**(b) Approximate Formula for Axial Annular Flow of Ellis Fluid**

We now take the slit flow formula for an Ellis fluid from Eq. B of Table 4.5-2 and replace the slit width

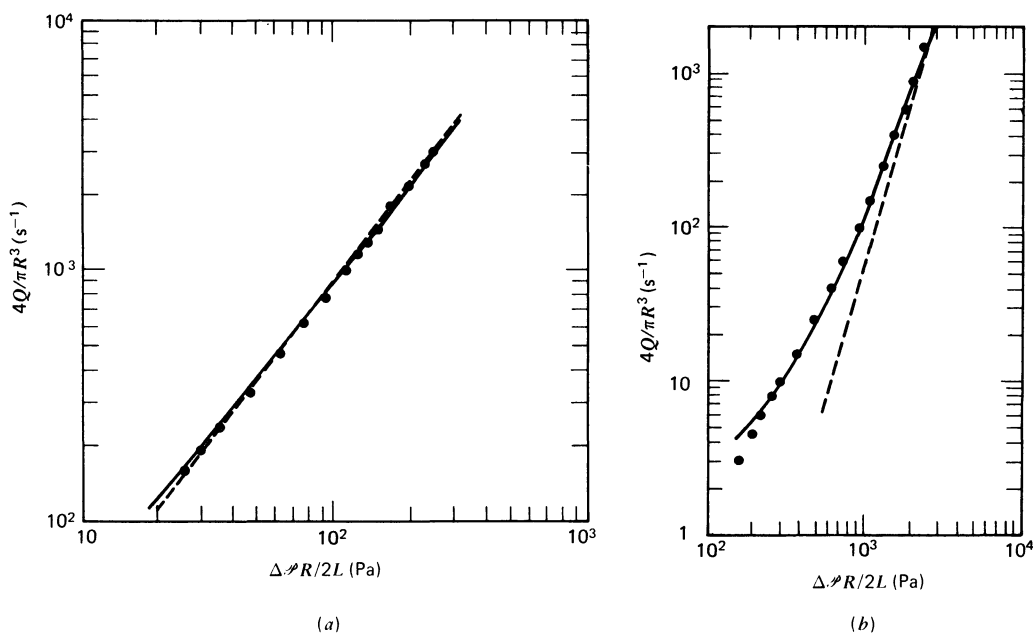


FIGURE 4.5-1. Illustration of the inadequacy of the power-law model in slow annular flow, and the improved description afforded by an  $\eta(\dot{\gamma})$  expression that contains a zero-shear-rate viscosity (the Ellis model of Table 4.5-1). [E. Ashare, R. B. Bird, and J. A. Lescarbours, *AIChE J.*, **11**, 910-916 (1965).] (a) Volume flow rate of 1.0% Natrosol-G in annulus ( $\kappa = 0.5043$ ). Solid curve: approximate equation obtained for the Ellis model (Eq. 4.5-17) ( $\alpha = 1.5$ ,  $\eta_0 = 0.031 \text{ Pa}\cdot\text{s}$ ,  $\tau_{1/2} = 26 \text{ Pa}$ ). Dashed curve: exact solution for the power-law model (Eq. C of Table 4.2-1) ( $n = 0.763$ ,  $m = 0.893 \text{ Pa}\cdot\text{s}^n$ ). Data points are taken from D. W. McEachern, Ph.D. Thesis, University of Wisconsin, Madison (1963). (b) Volume flow rate of 3.5% CMC-70-medium in annulus ( $\kappa = 0.624$ ). Solid curve: Ellis model (Eq. 4.5-17) approximate ( $\alpha = 3.0$ ,  $\eta_0 = 2.27 \text{ Pa}\cdot\text{s}$ ,  $\tau_{1/2} = 152 \text{ Pa}$ ). Dashed curve: power-law (Eq. C of Table 4.2-1) exact ( $n = 0.280$ ,  $m = 60.6 \text{ Pa}\cdot\text{s}^n$ ). Data points are taken from A. G. Fredrickson, Ph.D. Thesis, University of Wisconsin, Madison (1959).

$W$  by  $2\pi R$  and the slit thickness  $2B$  by  $R(1 - \kappa)$  as we did for the Newtonian fluid in (a); we then multiply by  $C_N$ :

$$Q_{\text{ann.}} \doteq \frac{\pi(\mathcal{P}_0 - \mathcal{P}_L)R^4}{6\eta_0 L} (1 - \kappa)^3 \left[ 1 + \frac{3}{\alpha + 2} \left( \frac{(\mathcal{P}_0 - \mathcal{P}_L)R(1 - \kappa)}{2\tau_{1/2}L} \right)^{\alpha-1} \right] \cdot C_N \quad (4.5-17)$$

This is an approximate result because the Newtonian curvature correction  $C_N$  has been applied. It is believed that this approximate procedure is valid<sup>6</sup> for  $\kappa$  greater than about 0.6; this conclusion was drawn by comparing the exact solution for a power-law fluid<sup>7</sup> with the slit approximation for a power-law fluid multiplied by  $C_N$ .

In Fig. 4.5-1 we show annular flow experimental data for aqueous solutions of two different polymers.<sup>7</sup> It can be seen that Eq. 4.5-17 describes the data quite well. The power-law and Ellis models are seen to agree for  $[3/(\alpha + 2)][\Delta\mathcal{P}R(1 - \kappa)/2\tau_{1/2}L]^{\alpha-1} \gg 1$ . Otherwise the Ellis model is appreciably better than the power-law model. This inadequacy has also been pointed out by other authors.<sup>8</sup>

#### §4.6 LIMITATIONS OF GENERALIZED NEWTONIAN FLUID MODELS AND RECOMMENDATIONS FOR THEIR USE

In §4.1 the generalized Newtonian fluid was introduced as a simple empirical modification of the Newtonian fluid that accounts for the experimentally observed dependence of viscosity on shear rate. Because of the empirical nature of the model, the question then arises as to the limits of validity of the formulas developed in this chapter for solving flow problems. To determine these limits we can get some help from the subject of continuum mechanics and some from dimensional analysis, but the ultimate test is, of course, the comparison with experimental data.

In Example 9.6-3, in the chapter on continuum mechanics, it is shown that in steady-state shear flow an extremely wide class of viscoelastic constitutive equations simplifies to the Criminale–Ericksen–Filbey (CEF) equation. The first term of the CEF equation for  $\tau$  is just  $-\eta(\dot{\gamma})\dot{\gamma}$ ; the other two terms, containing  $\Psi_1$  and  $\Psi_2$ , describe the elastic effects associated with the normal stresses. The latter turn out to be unimportant in getting volume-flow-rate versus pressure drop relations in flow in straight, uniform conduits and also in getting torque versus angular velocity relations in tangential or helical annular flows for annuli. In other words for steady-state shear flows the formulas obtained in this chapter for  $Q$  versus  $\Delta\mathcal{P}$  and  $\mathcal{T}$  versus  $W$  are exactly the same as would be obtained for much wider classes of nonlinear viscoelastic constitutive equations. Comparisons with experimental data have furthermore substantiated the conclusion that the methods given in this chapter for  $Q$  versus  $\Delta\mathcal{P}$  and  $\mathcal{T}$  versus  $W$  in steady shear flows are virtually exact, the only limitation resulting from the possible inadequacy of the particular form chosen for  $\eta(\dot{\gamma})$ ; an example of the latter is the failure of the power-law model for the slow axial flow in an annulus (see Example 4.5-2).

In some problems in this chapter we have used the generalized Newtonian fluid to solve flow problems that are not shear flows and/or steady-state flows. In Example 4.2-7 (squeezing flow between parallel disks) we assumed that the flow is locally a *shear* flow—though it is not; in Example 4.2-6 (pulsatile flow in a circular tube) we assumed that the velocity distribution is instantaneously the same as that for a *steady* flow—though it is

<sup>6</sup> S. Matsuhisa and R. B. Bird, *AIChE J.*, **11**, 588–595 (1965).

<sup>7</sup> A. G. Fredrickson and R. B. Bird, *Ind. Eng. Chem.*, **50**, 347–352 (1958); *erratum: Ind. Eng. Chem. Fundam.*, **3**, 383 (1964); R. W. Hanks and K. M. Larsen, *Ind. Eng. Chem. Fundam.*, **18**, 33–35 (1979).

<sup>8</sup> R. D. Vaughn and P. D. Bergman, *Ind. Eng. Chem. Proc. Des. Dev.*, **55**, 44–47 (1966).

not. When is it permissible to make such assumptions? It is permissible if "elastic effects" are not important, and as pointed out in §2.8, this means that the Deborah number<sup>1</sup> in the flow problem must be smaller than some critical value.

We are now faced with the problem of specifying the time constant of the fluid. There are several possibilities: (a) use the time constant in the  $\eta(\dot{\gamma})$  expression (i.e., the  $\lambda$  in the Carreau-Yasuda equation or the time constants in Table 4.5-1); (b) use a time constant constructed from the  $m$  and  $n$  of the power-law viscosity and the  $m'$  and  $n'$  of the power-law expression for  $\Psi_1$  (i.e., the  $\lambda$  in Eq. 4.2-68); or (c) use the time constant provided by linear viscoelasticity (i.e., the time constant from Table 5.3-1). It can be argued that choice (a) is inappropriate, since elastic effects may be unrelated to the viscosity measured in steady shear flow; on the other hand, experimental data, many molecular theories, and many nonlinear viscoelastic constitutive equations do show a connection between the time constant determined from (a) and that determined from (c). We emphasize, however, that the time constants obtained by methods (a), (b), and (c) will not be exactly the same.

Once a choice has been made for the fluid time constant  $\lambda$ , then a comparison of experimental data with the generalized Newtonian fluid flow solution enables one to establish the critical Deborah number above which the generalized Newtonian fluid is inapplicable.<sup>2</sup> For example, in Fig. 4.2-6 it is seen that above  $De \equiv \lambda/t_{1/2}$  of about three elastic effects are important, and the Scott equation, based on the power-law model, is not valid; note further that for very fast squeezing flows the Scott equation may be in error by more than a factor of 10 for the data shown. This should serve as a warning that the appearance of elastic effects can severely limit the usefulness of the generalized Newtonian fluid.

In Example 4.2-6 (pulsatile tube flow) a suitable characteristic time for the flow process would be  $1/\omega$ , where  $\omega$  is the frequency of the sinusoidally varying pressure gradient. Then an appropriate Deborah number would be  $De = \lambda\omega$ . As long as  $De$  is small, we can expect that the flow-enhancement formula in Eq. 4.2-58 will be trustworthy for fluids whose viscosity is well described by the power-law model, but that when  $De$  is much greater than the critical value it will not be able to describe the data.

We have emphasized that the critical Deborah number, which specifies the limit on the range of validity of the generalized Newtonian fluid, has to be determined experimentally. As we shall see in Chapters 6–8, it is also possible to establish the critical Deborah number by using nonlinear viscoelastic models, provided that the model describes experimental material functions well and that the flow problem can be solved for the flow system concerned. In either case experimental data are needed.

In this chapter we have given a sampling of analytical solutions to relatively simple flow problems for the power-law generalized Newtonian fluid. Further examples of analytical solutions can be found in older books on rheology<sup>3–5</sup> and in engineering journals. In some of these references generalized Newtonian fluids are referred to as "purely viscous fluids" or "inelastic fluids." Many other analytical and numerical solutions to

<sup>1</sup> M. Reiner, *Phys. Today*, **17**, 62 (Jan. 1964); R. R. Huilgol, *Continuum Mechanics of Viscoelastic Liquids*, Wiley, New York (1975), pp. 226–228.

<sup>2</sup> The role of the ratio of characteristic times was illustrated by R. B. Bird, *Can. J. Chem. Eng.*, **43**, 161–168 (1965), who documented the importance of this ratio by means of experimental data on flow through porous media, around spheres, in a converging section, and in the oscillating manometer.

<sup>3</sup> M. Reiner, *Deformation, Strain, and Flow*, Wiley-Interscience, New York (1960), Chaps. VIII, XVI, XVII, XVIII, XIX.

<sup>4</sup> W. L. Wilkinson, *Non-Newtonian Fluids: Fluid Mechanics, Mixing and Heat Transfer*, Pergamon Press, New York (1960).

<sup>5</sup> S. Middleman, *The Flow of High Polymers*, Wiley-Interscience, New York (1968), Chapt. 3.

generalized Newtonian flow problems along with applications can be found in books on polymer processing.<sup>6–10</sup>

The engineering and applied science literature abounds with examples of the application of generalized Newtonian fluid models to problems, which are far from being steady-state shear flow problems: boundary-layer flows,<sup>11</sup> complex flows at the entry to tubes,<sup>12</sup> instability problems,<sup>13</sup> turbulent flows,<sup>14</sup> agitation and mixing,<sup>15</sup> fiber spinning,<sup>16</sup> mold filling,<sup>17</sup> films and coatings,<sup>18</sup> flow with pressure-dependent viscosity,<sup>19</sup> and flow around spheres.<sup>20</sup> In some instances there have been no (or very limited) comparisons with experimental data, so that the range of applications of the theoretical calculations is not known. Until such time as these types of problems have been studied with nonlinear viscoelastic models (see Chapters 7 and 8), generalized Newtonian models will continue to be used.

In conclusion, then, we recommend that the generalized Newtonian model be used for calculating  $Q$  vs.  $\Delta\mathcal{P}$  for steady flow in rectilinear conduits of constant cross section, and for getting  $\mathcal{T}$  vs.  $W$  for tangential and helical flow in annuli. Such calculations can be expected to be reliable, provided that the  $\eta(\dot{\gamma})$  function describes the viscosity data well. The power-law viscosity function can be useful in many problems, but caution must be exercised if the flow field puts considerable emphasis on the zero-shear-rate region of the  $\eta(\dot{\gamma})$  curve, where the power law is inadequate. The generalized Newtonian model can also be expected to give good results in systems that deviate somewhat from steady-state shear flows (i.e., they may have some time dependence or some nonshearing velocity gradients), provided that the Deborah number is much less than  $De_{crit}$ ; generally this critical Deborah number

<sup>6</sup> J. M. McKelvey, *Polymer Processing*, Wiley, New York (1962).

<sup>7</sup> S. Middleman, *Fundamentals of Polymer Processing*, McGraw-Hill, New York (1977).

<sup>8</sup> Z. Tadmor and C. G. Gogos, *Principles of Polymer Processing*, Wiley, New York (1979).

<sup>9</sup> R. I. Tanner, *Engineering Rheology*, Oxford University Press (1985).

<sup>10</sup> J. R. A. Pearson, *Mechanics of Polymer Processing*, Elsevier Applied Science, London (1984).

<sup>11</sup> J. G. Oldroyd, *Proc. Camb. Phil. Soc.*, **43**, 383–395 (1947); W. R. Schowalter, *AIChE J.*, **6**, 24–28 (1960), *erratum*: **10**, 597 (1964); A. Acrivos, M. J. Shah, and E. E. Petersen, *ibid.*, **6**, 312–317 (1960); J. L. White and A. B. Metzner, *ibid.*, **11**, 324–330 (1965); S. Y. Lee and W. F. Ames, *ibid.*, **12**, 700–708 (1966); V. G. Fox, L. E. Erickson, and L. T. Fan, *ibid.*, **15**, 327–333 (1969); W. R. Schowalter, *Mechanics of Non-Newtonian Fluids*, Pergamon Press, New York (1978), pp. 205 *et seq.*

<sup>12</sup> S. S. Chen, L. T. Fan, C. L. Hwang, *AIChE J.*, **16**, 293–299 (1970); N. D. Sylvester and S. L. Rosen, *ibid.*, **16**, 964–972 (1970).

<sup>13</sup> J. P. Tordella in F. R. Eirich, ed., *Rheology*, Vol. 5, Academic Press, New York (1969) Chapt. 2; J. R. A. Pearson, *Ann. Rev. Fluid Mech.*, **8**, 163–181 (1976).

<sup>14</sup> A. B. Metzner and J. C. Reed, *AIChE J.*, **1**, 434–440 (1955); R. G. Shaver and E. W. Merrill, *ibid.*, **5**, 181–188 (1959); D. W. Dodge and A. B. Metzner, *ibid.*, **5**, 189–204 (1959); D. W. McEachern, *ibid.*, **15**, 885–889 (1969); H. Rubin and C. Elata, *ibid.*, **17**, 990–996 (1971).

<sup>15</sup> A. B. Metzner and R. E. Otto, *AIChE J.*, **3**, 3–10 (1957); E. S. Godleski and J. C. Smith, *ibid.*, **8**, 617–620 (1961); D. W. Hubbard and F. F. Calvetti, *ibid.*, **18**, 663–665 (1972).

<sup>16</sup> J. R. A. Pearson and Y. T. Shah, *Ind. Eng. Chem. Fundam.*, **13**, 134–138 (1974); J. R. A. Pearson, Y. T. Shah, and R. D. Mhaskar, *ibid.*, **15**, 31–37 (1976); C. J. S. Petrie, *Elongational Flows*, Pitman, London (1979).

<sup>17</sup> J. L. Berger and C. G. Gogos, *Polym. Eng. Sci.*, **13**, 102–112 (1973); P.-C. Wu, C. F. Huang, and C. G. Gogos, *ibid.*, **14**, 223–230 (1974).

<sup>18</sup> C. Gutfinger and J. A. Tallmadge, *AIChE J.*, **11**, 403–413 (1965); J. A. Tallmadge, *ibid.*, **16**, 925–930 (1970); S. A. Jenekhe, *Ind. Eng. Chem. Fundam.*, **23**, 425–432, 432–436 (1984); S. A. Jenekhe and S. B. Schuldt, *Chem. Eng. Commun.*, **33**, 135–147 (1985).

<sup>19</sup> N. Galili, R. Takserman-Krozer, and Z. Rigbi, *Rheol. Acta*, **14**, 550–567 (1975).

<sup>20</sup> A. N. Beris, J. A. Tsamopoulos, R. C. Armstrong, and R. A. Brown, *J. Fluid Mech.*, **158**, 219–244 (1985), (Bingham fluid); K. Adachi, N. Yoshioka, and K. Sakai, *J. Non-Newtonian Fluid Mech.*, **3**, 107–125 (1977/1978), (“extended Williamson model,” i.e., Eq. 4.1-9 with  $n = 1 - a$ ); M. B. Bush and N. Phan-Thien, *J. Non-Newtonian Fluid Mech.*, **16**, 303–313 (1984), (Carreau model, i.e., Eq. 4.1-9 with  $a = 2$ ); Y. I. Cho and J. P. Hartnett, *J. Non-Newtonian Fluid Mech.*, **12**, 243–247 (1983), (power-law model).

must be determined experimentally. In other situations—elongational flows, flows rapidly changing in time, flows with several nonzero velocity components, etc.—the generalized Newtonian fluid should not be used, except as a last resort; good experimental measurements are definitely preferred.

## PROBLEMS

### 4A.1 Pipe Flow of a Polyisoprene Solution

A 13.5% (by weight) solution of polyisoprene in isopentane has the following power-law parameters at 323 K:  $m = 5 \times 10^3 \text{ Pa} \cdot \text{s}^n$ , and  $n = 0.2$ . It is being pumped through a pipe that is 10.2 m long and has an internal diameter of 1.3 cm; the flow is known to be laminar. It is desired to build another pipe with a length of 20.4 m with the same volume rate of flow and the same pressure drop. What should its radius be?

Answer: 1 cm

### 4A.2 Flow of a Carboxymethylcellulose Solution in an Annulus

A 3.5% aqueous carboxymethylcellulose solution has Ellis-model parameters as follows:  $\eta_0 = 2.27 \text{ Pa} \cdot \text{s}$ ,  $\tau_{1/2} = 152 \text{ Pa}$ , and  $\alpha = 3.0$ . Find the flow rate  $Q$  in a horizontal annulus with  $R = 2 \text{ cm}$  and  $\kappa = 0.624$  when  $\Delta p R/2L = 500 \text{ Pa}$ . Use the approximate relation given in Eq. 4.5-17.

Answer:  $154 \text{ cm}^3/\text{s}$

### 4A.3 Pipe Flow of a Polypropylene Melt (Ellis Model)

a. A commercial sample of polypropylene at 403 K has the following Ellis-model parameters:<sup>1</sup>  $\eta_0 = 1.24 \times 10^4 \text{ Pa} \cdot \text{s}$ ,  $\tau_{1/2} = 6.90 \times 10^3 \text{ Pa}$ ,  $\alpha = 2.82$ . Calculate the volume rate of flow  $Q$  for a horizontal pipe, 5 cm internal diameter and length 17 m, when the pressure drop is  $4.5 \times 10^6 \text{ Pa}$ .

b. What would be the power-law constants for the fluid? Repeat the calculations in (a) for the power law. Why are the results in (a) and (b) different? Under what conditions would they be expected to be the same?

Answers: a.  $3.87 \times 10^{-6} \text{ m}^3/\text{s}$   
b.  $5.92 \times 10^{-7} \text{ m}^3/\text{s}$

### 4A.4 Pumping a Nylon Melt through a Capillary (Truncated Power Law)<sup>2</sup>

A nylon-6 melt is to be pumped through a capillary of radius  $5 \times 10^{-4} \text{ m}$  and length  $2.5 \times 10^{-2} \text{ m}$  with pressure drop of  $2.67 \times 10^7 \text{ Pa}$ . What volume rate of flow is expected (neglect viscous dissipation as well as entrance and exit effects)? The viscosity data have been fit with a truncated power law, with the following constants:  $\eta_0 = 2.50 \times 10^2 \text{ Pa} \cdot \text{s}$ ,  $\dot{\gamma}_0 = 800 \text{ s}^{-1}$ , and  $n = 0.5$ .

Answer:  $1.18 \times 10^{-7} \text{ m}^3/\text{s}$

### 4A.5 Squeezing Flow of Polymer Solutions (Power Law)

One of the polymer solutions studied by Leider<sup>3</sup> in his squeezing-flow experiments was a 0.5% solution of polyacrylamide in glycerin for which the power-law parameters had been measured and

<sup>1</sup> N. Yamada, N. Kishi, and H. Iizuka, *Kōbunshi Kagaku*, **22**, 513–519 (1965).

<sup>2</sup> This problem was taken from W. J. Beek and D. B. Holmes, *Fysisch Technologische Aspecten van de Polymeerverwerking*, Laboratorium voor Technische Natuurkunde, Technische Hogeschool, Delft (1965).

<sup>3</sup> P. J. Leider, *Ind. Eng. Chem. Fundam.*, **13**, 342–346 (1974).

found to be:  $m = 25 \text{ Pa} \cdot \text{s}^n$ ,  $n = 1/3$ ; in addition the time constant  $\lambda$ , defined in Eq. 4.2-68, was found to be 129 s.

This fluid was placed between two circular disks with radius 2.54 cm, with an initial disk separation of  $2h_0 = 4.98 \times 10^{-3} \text{ cm}$ . A 4.07 kg mass was placed on the upper disk and it was found that the time for half the material to be squeezed out was 540 s. Compare this value with the value of  $t_{1/2}$  computed from the Scott equation. Verify that the experiment described is indeed within the range of applicability of the Scott equation.

**4A.6** Volume Rate of Flow in a Tube-Disk-Slit Assembly

a. The top curve in Fig. 4.1-2 is for a polystyrene melt at 453 K. Using the graph obtain the  $m$  and  $n$  of the power law appropriate for the power-law region of the data; show all work. Then check the values by obtaining the power-law constants from the Carreau-model parameters given in the figure caption.

b. Derive an equation (based on the power-law model) from which the volume rate of flow  $Q$  can be obtained for the apparatus shown in Fig. 4A.6, when the pressure drop  $p_0 - p_3$  is given. Use the results of Table 4.2-1 and Problem 4B.3 for deriving the expression for  $Q$ .

c. List the assumptions that are implied in the result obtained in (b).

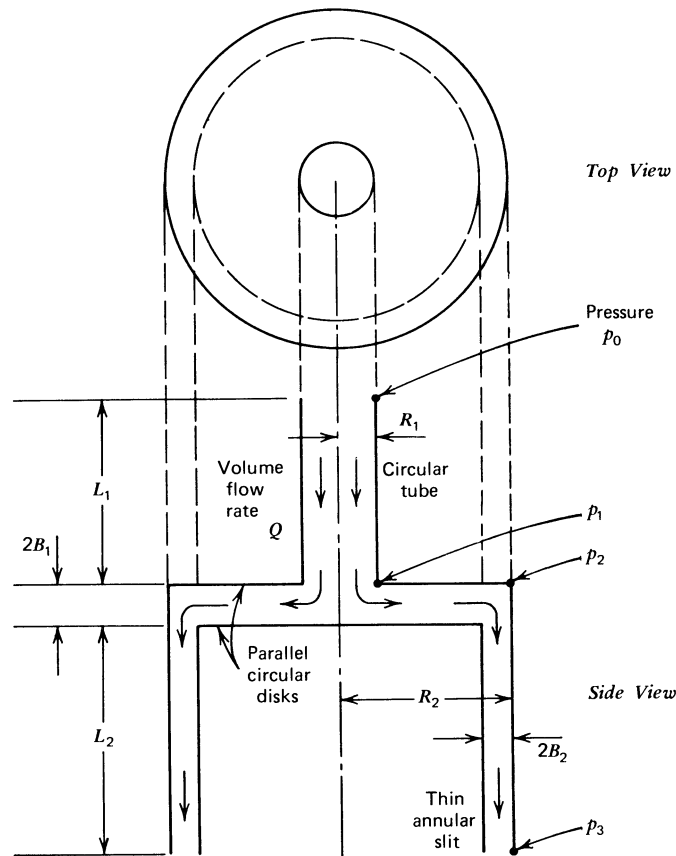


FIGURE 4A.6. Flow downward through a tube, radially between two parallel surfaces and then downward through an annular slit.

## 238 DYNAMICS OF POLYMERIC LIQUIDS

d. Calculate the volume flow rate in  $\text{cm}^3/\text{s}$  for a pressure drop  $p_0 - p_3 = 2.1 \times 10^7 \text{ Pa}$  (which is approximately 210 atm) for the polystyrene melt cited in (a). The dimensions of the device are

$$\begin{array}{lll} R_1 = 0.5 \text{ cm} & L_1 = 11 \text{ cm} & B_1 = 0.2 \text{ cm} \\ R_2 = 7.0 \text{ cm} & L_2 = 9 \text{ cm} & B_2 = 0.15 \text{ cm} \end{array}$$

The fluid density is  $1 \text{ g/cm}^3$ .

Answer:  $75 \text{ cm}^3/\text{s}$  (approximately)

### 4A.7 Tube Flow of a Polystyrene Melt

Viscosity data for a polystyrene melt at 453 K are shown in Fig. 4.1-2. It is desired to pump this melt at 453 K through a tube 8 cm long and with 0.5 cm radius. If a pressure drop of  $5.6 \times 10^6 \text{ Pa}$  is applied, what is the volume flow rate if the fluid is assumed to be described by:

- the power-law model
- the truncated power-law model (cf. Eq. H in Table 4.5-2).

Justify the agreement (or lack of agreement) by comparing the wall shear stress in the tube  $\tau_R$  with the critical shear stress  $\eta_0 \dot{\gamma}_0$  where shear thinning begins in the truncated power law.

Answer: a.  $36.1 \text{ cm}^3/\text{s}$

### 4A.8 Heat Transfer in Mold Filling of a Polystyrene Melt

A molten polystyrene is to be formed into a rectangular shape by injecting it into a cold mold that is 30 cm long, 7.5 cm wide, and 0.2 cm thick.<sup>4</sup> The fluid flow is parallel to the longest dimension of the mold. The time required to fill the mold is 2.5 s with a pressure gradient of  $1.33 \times 10^6 \text{ Pa/m}$ . The temperature of the molten polymer entering the mold is  $250^\circ\text{C}$  and the mold walls are at  $50^\circ\text{C}$ . For polystyrene,<sup>5</sup>  $k = 1.295 \times 10^{-1} \text{ J/K} \cdot \text{m} \cdot \text{s}$  and  $\alpha = 7.05 \times 10^{-8} \text{ m}^2/\text{s}$ . Estimate the local Nusselt number to describe the heat transfer between the polymer and the mold.

### 4A.9 Pipe Flow of a Polymer Solution

A 1% aqueous solution of polyethylene oxide at 333 K has these power-law parameters:  $m = 0.50 \text{ Pa} \cdot \text{s}^n$  and  $n = 0.60$ . The solution is being pumped between two tanks, with Tank 1 at pressure  $p_1$ , and Tank 2 at pressure  $p_2$ ; the pipe carrying the solution has an internal diameter of 27 cm, and a length of 14.7 m.

It has been decided to replace the single pipe by a pair of pipes of the same length, but with smaller diameter. What diameter should these pipes have in order for the volume flow rate to be the same as that in the single pipe?

### 4B.1 Axial Annular Flow with Inner Cylinder Moving Axially (Power-Law)

In the system shown in Fig. 4B.1 it is desired to find the velocity distribution in the annular region between  $A$  and  $B$  for a polymeric fluid. Use the power-law viscosity equation.

- Combine the equation of motion and the power-law equation to obtain a differential equation for  $v_z(r)$ , taking the  $z$ -axis to be coincident with the axis of the moving rod.
- Integrate the equation for  $v_z(r)$  to get the velocity distribution in terms of two constants  $C_1, C_2$ .
- What boundary conditions do you use to determine  $C_1, C_2$ ?

<sup>4</sup> J. L. S. Wales, J. van Leeuwen, and R. van der Vijgh, *Polym. Eng. Sci.*, **12**, 359–363 (1972).

<sup>5</sup> J. Brandrup and E. H. Immergut, *Polymer Handbook*, Wiley Interscience, New York (1966).

d. Use those boundary conditions to find the result

$$\frac{v_z(r)}{V} = \frac{\xi^{1-s} - 1}{\kappa^{1-s} - 1} \quad (4B.1-1)$$

where  $\xi = r/R$  and  $s = 1/n$ .

e. Show how this simplifies, for the Newtonian fluid, to

$$\frac{v_z(r)}{V} = \frac{\ln \xi}{\ln \kappa} \quad (4B.1-2)$$

- f. What is the force acting on the wire in the region between  $A$  and  $B$ ?  
 g. Is this a “shear flow” according to the definition in §3.7?  
 h. Find the volume flow rate  $Q$  of the fluid through the annular region.  
 i. Show how the expression for  $Q$  in (h) simplifies for a Newtonian fluid.

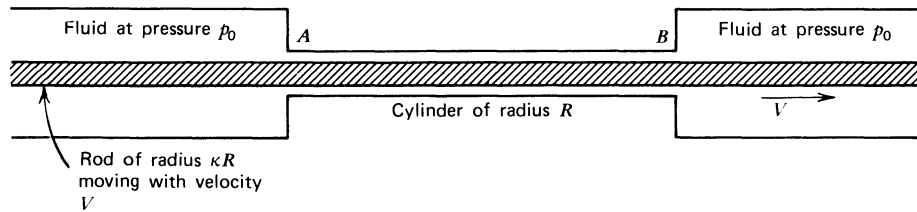


FIGURE 4B.1. Axial annular flow with inner cylinder moving axially.

#### 4B.2 Tangential Annular Flow for a Polymer (Power Law)

A polymeric liquid is being sheared in the annular region between two cylindrical surfaces of length  $L$  and of radii  $\kappa R$  and  $R$  (with  $\kappa < 1$ ). The inner cylinder is rotating with an angular velocity  $W$ , and the outer cylinder is fixed.

a. Show that for this system the  $\theta$ -component of the equation of motion simplifies to

$$0 = -\frac{1}{r^2} \frac{d}{dr} (r^2 \tau_{r\theta}) \quad (4B.2-1)$$

and the  $r\theta$ -component of  $\tau$  for the power-law is

$$\tau_{r\theta} = m \left[ -r \frac{d}{dr} \left( \frac{v_\theta}{r} \right) \right]^n \quad (4B.2-2)$$

b. Show that the equations in (a) along with the appropriate boundary conditions can be solved to give for the velocity distribution

$$\frac{v_\theta}{Wr} = \frac{(R/r)^{2/n} - 1}{(1/\kappa)^{2/n} - 1} \quad (4B.2-3)$$

c. Obtain an expression for the torque required to turn the inner cylinder.

Answer: c.  $\mathcal{T} = 2\pi(\kappa R)^2 m L \left( \frac{2W/n}{1 - \kappa^{2/n}} \right)^n$

4B.3 Radial Flow between Parallel Disks (Power Law)<sup>6</sup>

a. First solve the problem of the power-law fluid flow through a slit of width  $W$  and thickness  $2B$ , and verify the result given in Eq. A of Table 4.2-1.

b. Then solve the problem of slow steady-state radial flow between two fixed parallel disks (see Fig. 4B.3), which are separated by a distance  $2B$ . Let the inner and outer radii of the disks be  $R_1$  and  $R_2$ . Obtain an expression for the volume rate of flow by applying the result of (a) locally in the region between the two disks:

$$Q = \frac{4\pi B^2}{(1/n) + 2} \left( \frac{(p_1 - p_2)B(1-n)}{m(R_2^{1-n} - R_1^{1-n})} \right)^{1/n} \quad (4B.3-1)$$

This equation<sup>7</sup> has been used by several groups of investigators<sup>8-10</sup> to describe radial flow data for some moderately viscoelastic polymer solutions.

- c. Is this a “shear flow” according to the definition in §3.7?  
 d. How does Eq. 4B.3-1 simplify for Newtonian fluids?

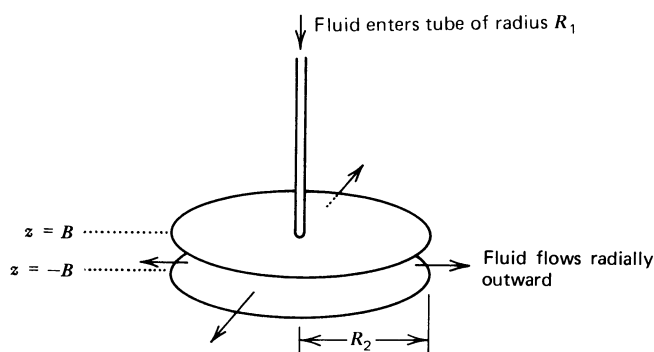


FIGURE 4B.3. Radial flow between two disks of radius  $R_2$  separated by a distance  $2B$ , with  $B \ll R_2$ . Fluid enters the gap from a small tube of radius  $R_1$ .

4B.4 Distributor Design (Power Law)<sup>11</sup>

In this problem we see how the power-law results in Eqs. A and B in Table 4.2-1 can be combined to get an approximate solution to a rather complicated flow problem. In Fig. 4B.4 we see a distributor system that is supposed to deliver a polymeric fluid with a uniform efflux velocity as the fluid leaves the thin slit between parallel plates. The circular pipe and parallel plates are horizontal, and the fluid leaves the pipe and enters the parallel-plate system through a thin slit in the tube. The flow between the plates is in the  $x$ -direction because of the presence of vertical dividers that also serve to maintain the spacing between the plates.

<sup>6</sup> This problem has been solved numerically for the Carreau model by A. Co, *Ind. Eng. Chem. Fundam.*, **20**, 340-348 (1981), for the third-order fluid by A. Co and R. B. Bird, *Appl. Sci. Res.*, **33**, 385-404 (1977), and for a nonlinear differential model by A. Co and W. E. Stewart, *AIChE J.*, **28**, 644-655 (1982).

<sup>7</sup> T. Y. Na and A. G. Hansen, *Int. J. Nonlinear Mech.*, **2**, 261-273 (1967).

<sup>8</sup> B. R. Laurecena and M. C. Williams, *Trans. Soc. Rheol.*, **18**, 331-355 (1974).

<sup>9</sup> H. Amadou, P. M. Adler, and J.-M. Piau, *J. Non-Newtonian Fluid Mech.*, **4**, 229-237 (1978).

<sup>10</sup> L. R. Schmidt, *J. Rheol.*, **22**, 571-588 (1978).

<sup>11</sup> This problem was suggested by a conversation with F. H. Ancker, Union Carbide Co., Bound Brook, NJ, who solved a somewhat similar problem by the method used here.

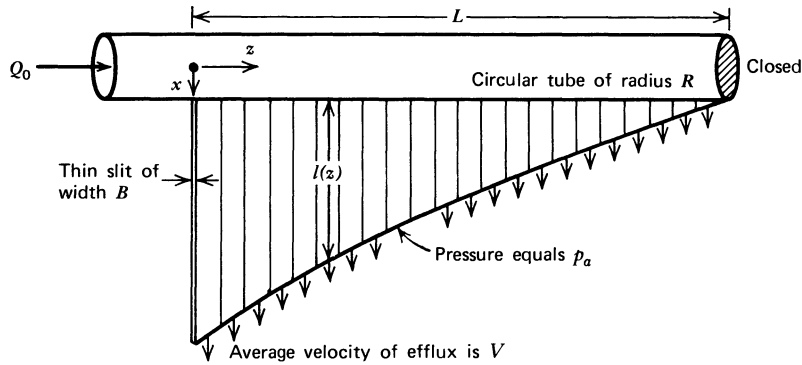


FIGURE 4B.4. Tube of radius  $R$ , with slit of width  $B$  attached, functioning as a distributor.

a. First consider the flow in the cylindrical tube. Verify that if  $Q_0$  is the volume rate of flow entering the tube, then the volume rate of flow across any plane of constant  $z$  will be

$$Q(z) = Q_0 \left(1 - \frac{z}{L}\right) \quad (4B.4-1)$$

Then apply the power-law result for a circular tube (Table 4.2-1) locally to obtain the following differential equation for the pressure:

$$Q_0 \left(1 - \frac{z}{L}\right) = \frac{\pi R^3}{(1/n) + 3} \left(\frac{R}{2m}\right)^{1/n} \left(-\frac{dp}{dz}\right)^{1/n} \quad (4B.4-2)$$

Integrate the differential equation for  $p(z)$  from an arbitrary distance  $z$  to the end of the tube  $z = L$ , and obtain

$$p - p_a = \frac{2mL}{R} \left(\frac{(1/n) + 3}{\pi R^3}\right)^n \frac{Q_0^n}{n + 1} (1 - \zeta)^{n+1} \quad (4B.4-3)$$

where  $\zeta = z/L$ .

b. Next adapt the slit flow result in Table 4.2-1 to the problem at hand to obtain

$$V = \frac{B/2}{(1/n) + 2} \left[\frac{(p - p_a)B}{2ml(\zeta)}\right]^{1/n} \quad (4B.4-4)$$

c. From (a) and (b) find the equation of the curve  $l(\zeta)$  that will ensure uniform efflux:

$$l(\zeta) = \frac{BL}{R(n+1)} \left(\frac{B}{2\pi R^3} \frac{(1/n) + 3}{(1/n) + 2}\right)^n \left(\frac{Q_0}{V}\right)^n (1 - \zeta)^{n+1} \quad (4B.4-5)$$

Note that  $m$  does not appear in the result!

#### 4B.5 Flow in a Tapered Tube (Power Law)

Derive the expression for the relation between  $Q$  and  $p_0 - p_L$  given in Eq. 4.2-10 for a tapered tube. Do this by writing Eq. 4.2-9 over a differential segment of the tube of length  $dz$ . Show how this adaptation of Eq. 4.2-9 can be integrated from  $z = 0$  to  $z = L$  to give Eq. 4.2-10. What limitations have to be placed on the result?

**4B.6** Adjacent Flow of Two Immiscible Fluids (Power Law)<sup>1,2</sup>

a. Two immiscible polymeric fluids are contained in the space between two parallel planes, located at  $x = 0$  and  $x = B$ , the upper one being in motion in the  $z$ -direction with a constant speed  $V$ , as shown in Fig. 4B.6. Both fluids are describable in terms of power-law parameters,  $m_I$  and  $n_I$  for fluid "I", and  $m_{II}$  and  $n_{II}$  for fluid "II." The interface is located at  $x = \lambda B$ , and there is no pressure gradient in the  $z$ -direction. Fluid I is more dense than Fluid II, and it is to be presumed that the flow rate is such that the interface between the fluids remains virtually planar. Find the velocity distribution.

b. (Lengthy!) Repeat the problem in part (a) when the upper plate is fixed, but there is a pressure gradient in the  $z$ -direction.

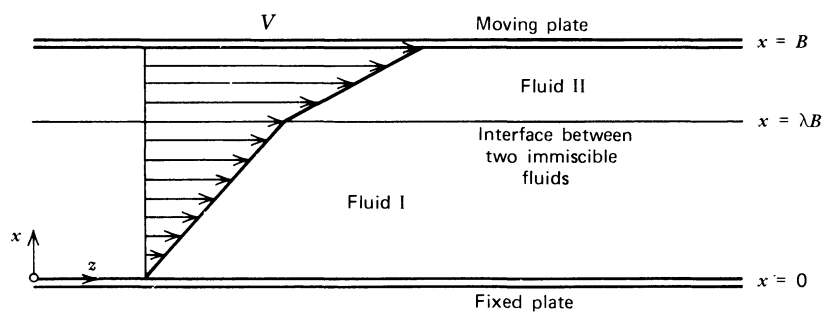


FIGURE 4B.6. Two immiscible power-law fluids being sheared in the region between two parallel plates, one of which is in motion.

**4B.7** Flow in Circular Tubes and Slits (Any Generalized Newtonian Fluid)

In Example 4.2-1 it is shown how to obtain the volume rate of flow for a power-law fluid through circular tubes and the corresponding flow-rate formula for plane slits is given in Eq. A of Table 4.2-1. In Table 4.5-2 results are given for the flow of other kinds of "model" fluids in tubes and thin slits. Actually it is not particularly difficult to obtain formal expressions for the flow rates in tubes and slits for any kind of shear-rate dependence of the viscosity.

a. For circular tubes show that the general expression for volume rate of flow can be integrated by parts twice to obtain

$$\begin{aligned}
 Q &= 2\pi \int_0^R v_z r dr \\
 &= \frac{\pi R^3 \dot{\gamma}_R}{3} - \frac{\pi}{3} \int_0^{\dot{\gamma}_R} r^3 d\dot{\gamma}
 \end{aligned}
 \tag{4B.7-1}$$

in which  $\dot{\gamma} = -dv_z/dr$  and  $\dot{\gamma}_R = -dv_z/dr|_{r=R}$ . Use of Eq. 4.2-4 and the definition of  $\eta$  in Eq. 4.1-4 enables us to make a change of variable:

$$r = (R/\tau_R)\eta\dot{\gamma}
 \tag{4B.7-2}$$

<sup>1,2</sup> For discussions of the problems of multilayered flows with applications to manufacture of laminated sheets and bicomponent filaments and to mixing processes, see W. J. Schrenk, *Plast. Eng.*, **30**, 65-68 (1974); W. J. Schrenk and T. Alfrey, Jr., *SPE J.*, **29**, 38-42, 43-47 (1973); T. Alfrey, Jr., *Polym. Eng. Sci.*, **9**, 400-404 (1969); W. J. Schrenk and T. Alfrey, Jr., *Polym. Eng. Sci.*, **9**, 393-399 (1969); A. E. Everage, Jr., *Trans. Soc. Rheol.*, **17**, 629-646 (1973). Most of the calculations in these papers were made for Newtonian fluids; in the last reference a variational method was employed.

Show that this leads to

$$Q = \frac{\pi R^3 \dot{\gamma}_R}{3} - \frac{\pi}{3} \left( \frac{R}{\tau_R} \right)^3 \int_0^{\dot{\gamma}_R} \eta^3 \dot{\gamma}^3 d\dot{\gamma} \quad (4B.7-3)$$

where  $\dot{\gamma}_R$  is obtained by solving the equation

$$\tau_R = \eta(\dot{\gamma}_R) \dot{\gamma}_R \quad (4B.7-4)$$

Hence, if one knows  $\eta(\dot{\gamma})$  from a cone-and-plate viscometer, for example, then  $\dot{\gamma}_R$  can be obtained from Eq. 4B.7-4 in terms of  $\tau_R$ . When that result is inserted into Eq. 4B.7-3, the integration can be performed to get  $Q$  as a function of  $\tau_R$ . The integrals will have to be performed numerically. Verify Eqs. 4B.7-3 and 4 by inserting the power law and showing that Eq. 4.2-9 is recovered.

**b.** Repeat the procedure outlined in (a), this time for the flow through a plane slit of width  $W$  and thickness  $2B$ . Show that the results corresponding to Eqs. 4B.7-3 and 4 are

$$Q = WB^2 \dot{\gamma}_B - W \left( \frac{B}{\tau_B} \right)^2 \int_0^{\dot{\gamma}_B} \eta^2 \dot{\gamma}^2 d\dot{\gamma} \quad (4B.7-5)$$

$$\tau_B = \eta(\dot{\gamma}_B) \dot{\gamma}_B \quad (4B.7-6)$$

Check these results by inserting the power law and showing that Eq. A in Table 4.5-2 is recovered.

#### 4B.8 Third Invariant of Rate-of-Strain Tensor for Shear Flow

Just after Eq. 4.1-7 it was stated that for shear flows  $III$  is identically zero. Verify this comment by evaluating  $III$  for the flow  $v_x = \dot{\gamma}(t)y$ ,  $v_y = 0$ ,  $v_z = 0$ .

#### 4B.9 Flow in Circular Tubes and Slits (Ellis model)<sup>13</sup>

- a. Verify Eqs. B and G of Table 4.5-2.
- b. Verify that the Ellis and power-law model parameters are related by

$$m = \eta_0^{1/\alpha} \tau_{1/2}^{1-(1/\alpha)}, \quad n = 1/\alpha \quad (4B.9-1)$$

c. How can the Ellis model be used to determine the limits of validity of the power-law model?

#### 4B.10 Flow of Blood in Tubes (Casson Equation)

To describe the flow of pigment-oil suspensions, Casson<sup>14</sup> proposed the following rheological equations for shearing flows:

$$\sqrt{\pm \tau_{yx}} = \sqrt{\tau_0} + \sqrt{\mu_0} \sqrt{\mp dv_x/dy} \quad \text{for } \tau_{yx} > \tau_0 \quad (4B.10-1)$$

$$\dot{\gamma}_{yx} = 0 \quad \text{for } \tau_{yx} < \tau_0 \quad (4B.10-2)$$

in which  $\mu_0$  and  $\tau_0$  are constants; the upper signs in Eq. 4B.10-1 are valid for positive momentum flux, and the lower signs for negative momentum flux.

<sup>13</sup> S. Matsuhisa and R. B. Bird, *AIChE J.*, **11**, 588-595 (1965).

<sup>14</sup> N. Casson in C. C. Mill, ed., *Rheology of Disperse Systems*, Pergamon Press, New York (1959), p. 84.

## 244 DYNAMICS OF POLYMERIC LIQUIDS

The Casson equation has proven useful for the description of the flow of blood on both glass and fibrin surfaces.<sup>15,16</sup> Some information is available on the relation between the model constants and the chemical composition of the blood.<sup>17,18</sup> In addition the Casson equation has been modified for suspensions of spherical particles in polymer solutions.<sup>19</sup>

a. What is the physical significance of the two constants in the equation? To what extent is this equation similar to the Bingham fluid?

b. Show that for the Casson equation the volume flow rate through a circular tube is given by<sup>16</sup>

$$Q = \frac{\pi R^4 (\mathcal{P}_0 - \mathcal{P}_L)}{8\mu_0 L} \left( 1 - \frac{16}{7} \sqrt{\xi} + \frac{4}{3} \xi - \frac{1}{21} \xi^4 \right) \quad (4B.10-3)$$

in which the dimensionless parameter  $\xi$  is

$$\xi = \frac{\tau_0}{(\mathcal{P}_0 - \mathcal{P}_L)R/2L} \quad (4B.10-4)$$

### 4B.11 Flow of a Bingham Fluid in a Tube<sup>20</sup>

a. Show that when a Bingham fluid flows in a tube it will have a “plug flow” region in the center with the radius  $r_0 = 2\tau_0 L/(\mathcal{P}_0 - \mathcal{P}_L)$ .

b. Verify that the velocity distribution is:

$$v_z^> = \frac{(\mathcal{P}_0 - \mathcal{P}_L)R^2}{4\mu_0 L} \left[ 1 - \left( \frac{r}{R} \right)^2 \right] - \frac{\tau_0 R}{\mu_0} \left[ 1 - \left( \frac{r}{R} \right) \right] \quad r \geq r_0 \quad (4B.11-1)$$

$$v_z^< = \frac{(\mathcal{P}_0 - \mathcal{P}_L)R^2}{4\mu_0 L} \left( 1 - \frac{r_0}{R} \right)^2 \quad r \leq r_0 \quad (4B.11-2)$$

c. Obtain the expression for the volume flow rate given in Eq. J of Table 4.5-2.

### 4B.12 Temperature and Shear-Rate Dependence of Viscosity

Derive the *Bestul-Belcher equation*<sup>21</sup> relating various measurable derivatives:

$$\left( \frac{\partial \eta}{\partial T} \right)_{\dot{\gamma}} / \left( \frac{\partial \eta}{\partial T} \right)_{\tau_{yx}} = 1 + \left( \frac{\partial \ln \eta}{\partial \ln \dot{\gamma}} \right)_T \quad (4B.12-1)$$

in a steady shear flow  $v_x = \dot{\gamma}y$ ,  $v_y = 0$ ,  $v_z = 0$ . This equation has been used by Meissner.<sup>22</sup>

<sup>15</sup> V. L. Shah, *Adv. Transport Phenomena*, **1**, 1-57 (1980).

<sup>16</sup> S. Oka in A. L. Copley, ed., *Proceedings of the Fourth International Congress on Rheology*, Wiley, New York (1965), Part 4, pp. 81-92.

<sup>17</sup> E. W. Merrill, W. G. Margetts, G. R. Cokelet, and E. R. Gilliland in A. L. Copley, ed., *Proceedings of the Fourth International Congress on Rheology*, Wiley, New York (1965), Part 4, pp. 135-143.

<sup>18</sup> E. N. Lightfoot, *Transport Phenomena and Living Systems*, Wiley, New York (1974), pp. 35-38, 430, 438, 440; M. M. Lih, *Transport Phenomena in Medicine and Biology*, Wiley, New York (1975), pp. 378-386.

<sup>19</sup> S. Onogi, T. Matsumoto, and Y. Warashina, *Trans. Soc. Rheol.*, **17**, 175-190 (1973).

<sup>20</sup> For other Bingham flow problems see R. B. Bird, G. C. Dai, and B. J. Yarusso, *Rev. Chem. Eng.*, **1**, 1-70 (1982).

<sup>21</sup> A. B. Bestul and H. V. Belcher, *J. Appl. Phys.*, **24**, 696-702 (1953).

<sup>22</sup> J. Meissner in A. L. Copley, ed., *Proceedings of the Fourth International Congress on Rheology*, Wiley, New York (1965), Part 3, pp. 437-453.

**4B.13 Tube Flow for the Truncated Power-Law Fluid**

One way to estimate the importance of the zero-shear-rate viscosity on the volume flow rate in a tube is by using the simple truncated power-law model given in Table 4.5-1, Eqs. A and B. Let  $r_0$  denote the radial position where  $\dot{\gamma} = \dot{\gamma}_0$ , that is where the viscosity changes from the zero-shear-rate value to the power-law function.

- a. How must  $r_0$  be restricted in order to use the truncated power-law model? Show that this corresponds to  $(\eta_0 \dot{\gamma}_0 / \tau_R) < 1$  where  $\tau_R$  is the wall shear stress in the tube.
- b. Solve for the velocity field for  $r \leq r_0$  and  $r \geq r_0$ . Match the results at  $r = r_0$  in order to eliminate the last integration constant.
- c. Show that the volume flow rate is given by Eq. H in Table 4.5-2.
- d. Show that the result in part (c) reduces to the power-law result given in Eq. B of Table 4.2-1 or Eq. F of Table 4.5-2 when  $(\eta_0 \dot{\gamma}_0 / \tau_R) \ll 1$ . Note that the power-law consistency index  $m$  is related to the truncated power-law constants by  $m = \eta_0 \dot{\gamma}_0^{1-n}$ . Where does this come from?

**4B.14 Variational Functional for Rod**

Consider the functional in Eq. 4.3-16 and parallel the development in Eq. 4.3-3 *et seq.* In particular let  $\bar{\Theta}(\xi) = \Theta(\xi) + \varepsilon \eta(\xi)$ , where  $\Theta(\xi)$  is the solution to Eqs. 4.3-13, 14 and 15, and  $\eta(\xi)$  is an arbitrary function with  $\eta(1) = 0$ .

- a. Show that when terms through second order in  $\varepsilon$  are retained one finds:

$$J\{\bar{\Theta}(\xi)\} = J\{\Theta(\xi)\} + \varepsilon^2 J\{\eta(\xi)\} \tag{4B.14-1}$$

- b. Use the above to show that  $\Theta(\xi)$  makes  $J$  a minimum.

**4B.15 Development of Design Equation for Manifold of a “Coat-Hanger” Die (Power Law)<sup>23</sup>**

Plastic sheeting can be made by extruding the molten polymer through a “coat-hanger” die made up of an entry tube, two manifolds, and a slit (see Fig. 4B.15). The manifold is a tube of circular cross section, whose radius  $\bar{R}$  varies in the direction  $\bar{z}$  of the manifold axis. Our object is to design the manifold (i.e., find  $\bar{R}(\bar{z})$ ) so that the flow through the slit will be uniform; that is the volume flow rate of the slit must not vary in the  $x$ -direction.

The slit has a total width  $2W$  and has a thickness  $2B$ . The volume rate of flow into the entry tube is  $2Q_0$ , with half of the fluid going into the left manifold and half into the right manifold.

- a. Consider a width  $\Delta x$  of the slit. What is the volume flow rate through this portion of the slit?
- b. Make a mass balance over a length  $\Delta \bar{z}$  of the manifold tube and then let  $\Delta \bar{z}$  go to zero to get the differential equation:

$$-\frac{d\bar{Q}}{d\bar{z}} = \frac{Q_0}{W} \cos \alpha \tag{4B.15-1}$$

where  $\bar{Q}$  is the volume flow rate at  $\bar{z}$ . Draw a carefully labelled diagram to show how you derive this relation.

- c. Let  $\bar{p}(\bar{z})$  be the pressure as a function of  $\bar{z}$  in the manifold. Let  $p(z)$  be the pressure in the slit. Why is  $p(-L(x)) \doteq \bar{p}(\bar{z})$ ? How are  $x$  and  $\bar{z}$  related? How are  $W$  and  $\bar{L}$  related?

<sup>23</sup> J. R. A. Pearson, *Trans. J. Plast. Inst.*, **32**, 239 (1964); J. R. A. Pearson, *Mechanics of Polymer Processing*, Elsevier Applied Science, New York (1985), §10.2. See also Z. Tadmor and C. G. Gogos, *Principles of Polymer Processing*, Wiley, New York (1979), pp. 545-551.

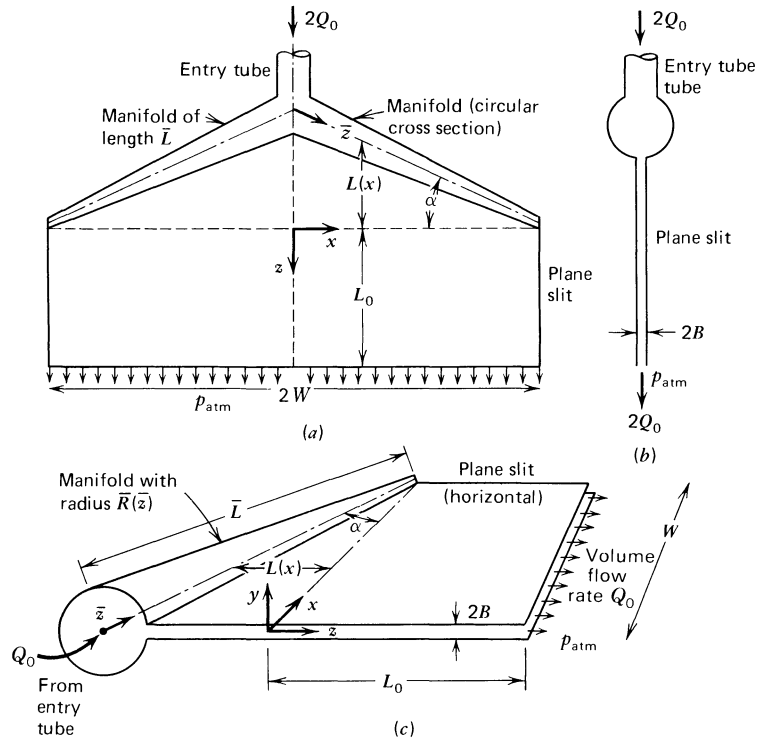


FIGURE 4B.15. The “coat-hanger” die, so named because the entry tube and manifold resemble a coat hanger. (a) Top view; (b) side view (looking in  $x$ -direction at a cut through the apparatus in the  $yz$ -plane); (c) one manifold and half of slit.

d. Adapt the power-law-fluid plane-slit-flow formula to a region of width  $\Delta x$ . Then use the results in (c) to obtain, finally,

$$-\frac{d\bar{p}}{d\bar{z}} = \left[ \frac{Q_0 [(1/n) + 2]}{W 2B^2} \right]^n \frac{m}{B} \sin \alpha \tag{4B.15-2}$$

e. Write the power-law analog of the Hagen–Poiseuille formula locally over a segment  $d\bar{z}$  of the tube. This should contain  $d\bar{p}/d\bar{z}$ .

f. Combine the results of (b), (d), and (e) to get a differential equation for  $\bar{R}$  as a function of  $\bar{z}$ . This should be of the form

$$\bar{R}^{(1/n)+2} d\bar{R}/d\bar{z} = \text{const} \tag{4B.15-3}$$

g. Integrate the differential equation to get  $\bar{R}(\bar{z})$ , the shape of the manifold. Take  $\bar{R}$  to be zero at  $\bar{z} = \bar{L}$  (just to make the problem a little simpler). Find ultimately that the desired design formula is

$$[\bar{R}(\bar{z})]^{3n+1} = \left[ \frac{2 [(1/n) + 3]}{\pi [(1/n) + 2]} \right]^n \frac{2B^{2n+1}}{\sin \alpha} (W - x)^n$$

Show that if  $n = 1/2$ , then  $\bar{R} \propto (W - x)^{1/5}$ .

**4B.16** Tube Flow with Slip at the Wall (Power Law)

Obtain a modification of Eq. B of Table 4.2-1 by using the Navier slip boundary condition at the liquid–solid interface:

$$v_z = \beta \tau_{rz} \quad \text{at } r = R \quad (4B.16-1)$$

in which  $\beta$  is the *slip coefficient*. What is the significance of  $\beta = 0$ ? The boundary condition in Eq. 4B.16-1 may be useful in the description of the “apparent slip” associated with the existence of a non-homogeneous region of fluid near the wall.<sup>24</sup> Instead of using a slip coefficient one can also model the system by postulating a thin film of fluid near the wall with different rheological properties.

**4C.1** Flow out of a Tank with an Exit Tube (Power Law)

The tank-and-tube assembly in Fig. 4C.1 is initially filled with an incompressible non-Newtonian fluid of density  $\rho$ ; the viscosity of the fluid is given by the power-law expression. During the draining

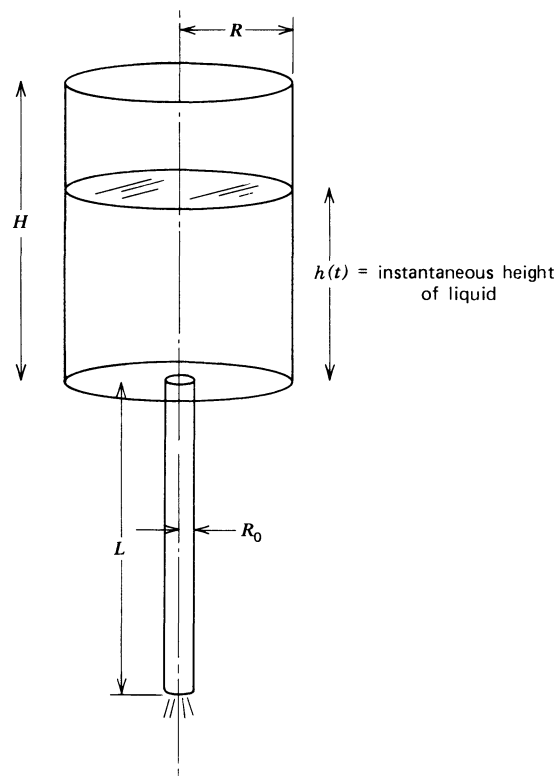


FIGURE 4C.1. Tank with a long tube attached; both the fluid surface and the tube exit are open to the atmosphere.

<sup>24</sup> For some experimental data and further literature references see Y. Cohen and A. B. Metzner, *J. Rheol.*, **29**, 67–102 (1985); see also A. M. Kraynik and W. R. Schowalter, *J. Rheol.*, **25**, 95–114 (1981), and P. J. Carreau, Q. H. Bui, and P. Leroux, *Rheol. Acta*, **18**, 600–608 (1979).

process it is assumed that the flow in the tube is laminar. Show that the time required to drain the tank (but not the pipe),  $t_{\text{efflux}}$ , is given by

$$t_{\text{efflux}} = \left( \frac{2mL}{\rho g R_0} \right)^{1/n} \left( \frac{1}{n} + 3 \right) \frac{R^2}{R_0^3} \left[ \frac{(H+L)^{1-(1/n)} - L^{1-(1/n)}}{1-(1/n)} \right] \quad (4C.1-1)$$

#### 4C.2 Falling Cylinder Viscometer (Power Law)

Rework Problem 1C.2 for a power-law fluid. In order to simplify the development, consider only the situation in which the clearance between the cylinder and tube is extremely small so that curvature effects can be completely neglected.

#### 4C.3 The Rayleigh Problem for a Power-Law Fluid<sup>25</sup>

It is desired to solve the problem given in Problem 1B.6 for a power-law fluid. Use the same dimensionless velocity as before, but define a combined, independent variable appropriate to the power-law fluid

$$\phi_n = \frac{v_x}{V} \quad (4C.3-1)$$

$$r = (n+1)^{-1} y (\rho/mt V^{n-1})^{1/(n+1)} \quad (4C.3-2)$$

and show that the differential equation for the dimensionless velocity distribution is

$$\phi_n'' (-\phi_n')^{n-1} + (n+1)n^{-1} r \phi_n' = 0 \quad (4C.3-3)$$

in which primes denote differentiation with respect to  $r$ . Obtain a formal solution to the problem for a pseudoplastic fluid ( $n < 1$ ). Some sample velocity profiles are given in Fig. 4C.3.

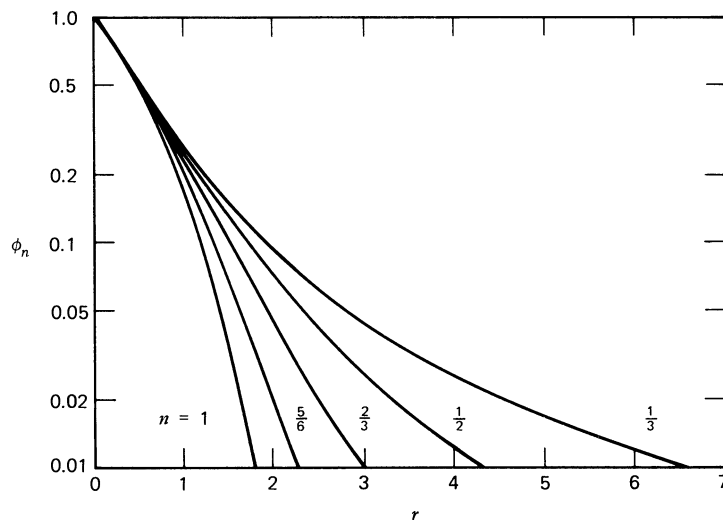


FIGURE 4C.3. Dimensionless velocity profiles for flow of a power-law fluid near a flat surface suddenly set in motion with a constant velocity. [R. B. Bird, *AIChE J.*, **5**, 565-566 (1959).]

<sup>25</sup> R. B. Bird, *AIChE J.*, **5**, 565-566 (1959).

It should be borne in mind that in unsteady-state problems of this type, viscoelastic effects will probably be important, and these are not described by the simple power-law model. See §7.4 for the solution to the Rayleigh problem for a viscoelastic fluid.

$$\text{Answer: } \phi_n = \left[ \frac{(1+n)^n(1-n)}{2n} \right]^{-1/(1-n)} \int_r^\infty (B_n + r^2)^{-1/(1-n)} dr$$

where  $B_n$  is a constant determined by  $\phi_n = 1$  at  $r = 0$ .

#### 4C.4 Axial Annular Flow (Bingham Fluid)

Repeat Example 4.2-4 for the Bingham fluid defined in Table 4.5-1. Use the following dimensionless quantities suggested by Fredrickson and Bird:<sup>26</sup>

$$T = \frac{2\tau_{rz}L}{(\mathcal{P}_0 - \mathcal{P}_L)R}; \quad T_0 = \frac{2\tau_0L}{(\mathcal{P}_0 - \mathcal{P}_L)R} \quad (4C.4-1)$$

$$\phi = \left( \frac{2\mu_0L}{(\mathcal{P}_0 - \mathcal{P}_L)R^2} \right) v_z; \quad \xi = \frac{r}{R} \quad (4C.4-2)$$

a. Show that the momentum flux distribution and the constitutive equation may be written

$$T = \xi - \beta^2 \xi^{-1}; \quad T = \pm T_0 - \frac{d\phi}{d\xi} \quad (4C.4-3)$$

in which the + sign is used when momentum is being transported in the + $r$ -direction and the - sign is used when transport is in the - $r$ -direction. Show further that the bounds on the plug-flow region  $\beta_+$  and  $\beta_-$  are given by

$$\pm T_0 = \beta_\pm - \left( \frac{\beta^2}{\beta_\pm} \right) \quad (4C.4-4)$$

where  $\beta$  is a constant of integration.

b. Obtain the velocity distribution appropriate for each of the three regions:

$$\phi_- = -T_0(\xi - \kappa) - \frac{1}{2}(\xi^2 - \kappa^2) + \beta^2 \ln \frac{\xi}{\kappa}, \quad \kappa \leq \xi \leq \beta_- \quad (4C.4-5)$$

$$\phi_0 = \phi_-(\beta_-) = \phi_+(\beta_+), \quad \beta_- \leq \xi \leq \beta_+ \quad (4C.4-6)$$

$$\phi_+ = -T_0(1 - \xi) + \frac{1}{2}(1 - \xi^2) + \beta^2 \ln \xi, \quad \beta_+ \leq \xi \leq 1 \quad (4C.4-7)$$

c. Verify that the determining equation for  $\beta_+$  is

$$2\beta_+(\beta_+ - T_0) \ln \frac{\beta_+ - T_0}{\beta_+ \kappa} - 1 + (T_0 + \kappa)^2 + 2T_0(1 - \beta_+) = 0 \quad (4C.4-8)$$

<sup>26</sup> A Slibar and P. R. Paslay, *Z. Angew. Math. Mech.*, **37**, 441-449 (1957); A. G. Fredrickson and R. B. Bird, *Ind. Eng. Chem.*, **50**, 347-352 (1958); see also B. E. Anshus, *Ind. Eng. Chem. Fundam.*, **13**, 162-164 (1974). Helical flow of a Bingham fluid in an annulus has been solved approximately by P. R. Paslay and A. Slibar, *Petr. Trans. AIME*, **210**, 310-317 (1957).

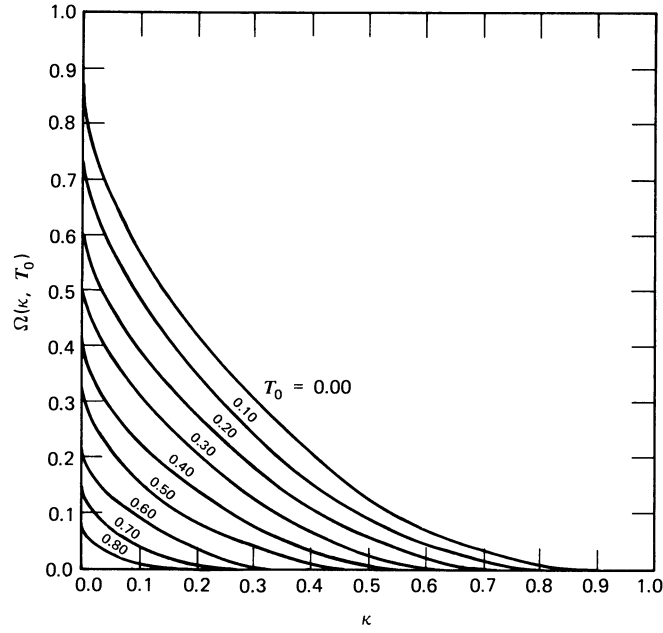


FIGURE 4C.4. The function  $\Omega(\kappa, T_0)$  to be used with Eq. 4C.4-9 for computing Bingham flow in an annulus. A numerical table corresponding to this graph was given by Fredrickson and Bird. [Reprinted with permission from A. G. Fredrickson and R. B. Bird, *Ind. Eng. Chem.*, **50**, 347-352 (1958). Copyright by the American Chemical Society.]

d. Show that the volume rate of flow is

$$\begin{aligned}
 Q &= \frac{\pi R^4(\mathcal{P}_0 - \mathcal{P}_L)}{8\mu_0 L} [(1 - \kappa^4) - 2\beta_+(\beta_+ - T_0)(1 - \kappa^2) \\
 &\quad - \frac{4}{3}(1 + \kappa^3)T_0 + \frac{1}{3}(2\beta_+ - T_0)^3 T_0] \\
 &= \frac{\pi R^4(\mathcal{P}_0 - \mathcal{P}_L)}{8\mu_0 L} \Omega(\kappa, T_0)
 \end{aligned}
 \tag{4C.4-9}$$

In Fig. 4C.4 the function  $\Omega$  is shown as a function of  $\kappa$  and  $T_0$ .

**4C.5** An Empiricism for  $\eta(II, III)$

a. Show that for the elongational flow  $v_z = \dot{\epsilon}z$ ,  $v_x = -(\dot{\epsilon}/2)x$ ,  $v_y = -(\dot{\epsilon}/2)y$ , the invariants of Eqs. 4.1-5 to 7 are

$$I = 0; \quad II = 6\dot{\epsilon}^2; \quad III = 6\dot{\epsilon}^3
 \tag{4C.5-1}$$

b. Now let us require that  $\eta(II, III)$  satisfy the following two limiting expressions:

$$\eta(II, III) = m(\sqrt{II/2})^{n-1}, \quad \text{in steady shear flow}
 \tag{4C.5-2}$$

$$\eta(II, III) = 3\eta_0, \quad \text{in steady elongational flow}
 \tag{4C.5-3}$$

Are these reasonable requirements? Show that the following function has the desired limits:

$$\eta(II, III) = 3\eta_0 \left( \frac{III}{6(II/6)^{3/2}} \right) + m \left( \sqrt{(II - 6(III/6)^{2/3})/2} \right)^{n-1} \quad (4C.5-4)$$

c. What are the dimensions of  $(m/\eta_0)^{1/(n-1)}$ ?

#### 4D.1 Flow of a Polymeric Fluid through a Square Tube<sup>27,28</sup> (Power Law)

Obtain an approximate expression for the volume rate of flow of a power-law fluid through a horizontal tube of square cross section. Let the square be described by the lines  $x = \pm B$ ,  $y = \pm B$ , and let the pressure drop over the tube of length  $L$  be  $p_0 - p_L$ . Use a variational approach and take the trial function to be

$$v_z = A \left[ 1 - \left( \frac{x}{B} \right)^2 \right] \left[ 1 - \left( \frac{y}{B} \right)^2 \right] \quad (4D.1-1)$$

where  $A$  is the variational parameter.

#### 4D.2 Effect of Axial Conduction on Forced Convection Heat Transfer

In Examples 4.4-1 through 3 the axial conduction term in the energy equation was neglected. In this problem we consider its importance on the temperature profiles. Consider the flow of a polymeric fluid between parallel plates separated by a gap  $2B$ . Far upstream the fluid has uniform temperature  $T_0$ , and the walls are also at  $T_0$ ; then at  $z = 0$ , the wall temperature is raised to  $T_1$  and held at that value for all  $z > 0$ . For simplicity assume that the fluid is incompressible and that its physical properties do not depend on temperature. Further assume that the power-law index  $n = 0$  so that the velocity profile is flat with  $v_z = V$ . This latter assumption is clearly a crude approximation for polymeric liquids; it is a good approximation for slurries, foam, and concentrated suspensions.

a. Solve for the temperature profiles in the regions up and downstream of  $z = 0$ . Show that

$$z > 0: \quad \Theta = \sum_{n=0}^{\infty} C_n \cos \lambda_n \eta \exp[-(\text{Pé} - \sqrt{\text{Pé}^2 + 4\lambda_n^2})\zeta/2] \quad (4D.2-1)$$

$$z < 0: \quad \Theta = 1 + \sum_{n=0}^{\infty} D_n \cos \lambda_n \eta \exp[(\text{Pé} + \sqrt{\text{Pé}^2 + 4\lambda_n^2})\zeta/2] \quad (4D.2-2)$$

<sup>27</sup> For a thorough calculation of this type see R. S. Schechter, *AIChE J.*, **7**, 445-448 (1961). For other noncircular conduit calculations see N. Mitsuishi and Y. Aoyagi, *J. Chem. Eng. Jpn.*, **6**, 402-408 (1973), (eccentric annulus); *Chem. Eng. Sci.*, **24**, 309-319 (1969), (rectangular and isosceles triangular ducts); N. Mitsuishi, Y. Kitayama, and Y. Aoyagi, *Kagaku Kōgaku*, **31**, 570-577 (1967), (rectangular and isosceles triangular ducts); N. Mitsuishi, Y. Aoyagi, and H. Soeda, *Kagaku Kōgaku*, **36**, 182-192 (1972), (concentric annulus). In connection with flow through noncircular tubes it must be kept in mind that  $\Psi_2 \neq 0$  is a necessary (but not sufficient) condition for secondary flows to exist [J. G. Oldroyd, *Proc. Roy. Soc.*, **A283**, 115-133 (1965)]; these secondary flows are so weak, however, that they do not appreciably influence the  $Q$  vs.  $\Delta\mathcal{P}$  relation. For application of variational methods to flow around a sphere see A. J. Ziegenhagen, R. B. Bird, and M. W. Johnson, Jr., *Trans. Soc. Rheol.*, **5**, 47-49 (1961); A. J. Ziegenhagen, *Appl. Sci. Res.*, **A14**, 43-56 (1961); S. W. Hopke and J. C. Slattery, *AIChE J.*, **16**, 224-229 (1970); *ibid.*, **16**, 317-318 (1970).

<sup>28</sup> See also T.-J. Liu, *Ind. Eng. Chem. Fundam.*, **22**, 183-186 (1983), for power-law flow in ducts of arbitrary cross section by means of the Galerkin method.

## 252 DYNAMICS OF POLYMERIC LIQUIDS

in which  $\Theta = (T_1 - T)/(T_1 - T_0)$  is the dimensionless temperature,  $\text{Pé} = \rho \hat{C}_p VB/k$  is the Péclet number,  $\eta = y/B$  and  $\zeta = z/B$  are dimensionless position variables, and  $\lambda_n = (n + (1/2))\pi$  for  $n = 0, 1, 2, \dots$  are eigenvalues for the problem.

b. Apply appropriate matching conditions at  $z = 0$  to the two solutions in order to determine the  $C_n$  and  $D_n$  constants.

c. How do these results simplify in the limit of large Pé? Is this consistent with the treatment given in Example 4.4-2?

### 4D.3. Variational Principle for Several Dependent Variables in a Three-Dimensional Space

Consider  $n$  dependent variables  $y_j$  for  $j = 1, 2, \dots, n$  defined in a three-dimensional volume  $V$  bounded by a surface  $S$ . The  $y_j$  are functions of the rectangular coordinates  $x_i$  for  $i = 1, 2, 3$ . The surface  $S$  is divided into two nonoverlapping regions  $S_v$  and  $S_f$ . On  $S_v$  the  $y_j$  satisfy essential boundary conditions

$$y_j = y_{j,c} \quad (4D.3-1)$$

where the  $y_{j,c}$  are known functions defined on  $S_v$ . On  $S_f$  the  $y_j$  satisfy natural boundary conditions. Define a variational functional  $J$  by

$$J = \int_V F_v(x_i, y_j, y_{j,i}) dV + \int_{S_f} F_s(x_i, y_j) dS \quad (4D.3-2)$$

where  $F_v$  and  $F_s$  are known functions of the arguments listed, and  $\partial y_j / \partial x_i$  is denoted  $y_{j,i}$  for brevity.

Prove the following variational principle: The set of functions  $y_j$  that satisfy the essential boundary conditions in Eq. 4D.3-1 and make  $J$  stationary are also the solutions to the partial differential equations

$$\frac{\partial F_v}{\partial y_j} - \sum_{i=1}^3 \frac{\partial}{\partial x_i} \frac{\partial F_v}{\partial y_{j,i}} = 0, \quad \text{for } j = 1, 2, \dots, n \quad (4D.3-3)$$

in the volume  $V$  with the natural boundary conditions

$$\frac{\partial F_s}{\partial y_j} + \sum_{i=1}^3 n_i \frac{\partial F_v}{\partial y_{j,i}} = 0, \quad \text{for } j = 1, 2, \dots, n \quad (4D.3-4)$$

and the essential boundary conditions in Eq. 4D.3-1. In Eq. 4D.3-4 the  $n_i$  are the rectangular components of the outwardly directed unit normal to the surface  $S_f$ .

It is suggested to follow the same outline as in §4.3 part a, and introduce functions  $\bar{y}_j(x) = y_j(x) + \epsilon \eta_j(x)$ . Instead of the integration by parts use the Gauss–Ostrogradskii divergence theorem.

### 4D.4. Variational Principle for Generalized Newtonian Fluids

It is desired to use the general principle derived in Problem 4D.3 to prove the variational principle stated below Eq. 4.3-31. Use rectangular coordinates  $x_i$  with velocity components  $v_i$  for  $i = 1, 2, 3$  and the following outline.

a. Show that

$$\frac{\partial \dot{\gamma}}{\partial v_{j,i}} = \frac{1}{\dot{\gamma}} \dot{\gamma}_{ij} \quad (4D.4-1)$$

where  $v_{j,i} = \partial v_j / \partial x_i$ .

b. Show that the condition that  $J$  in Eq. 4.3-31 is stationary is equivalent to the following differential equation:

$$\sum_{i=1}^3 \frac{\partial}{\partial x_i} (\eta \dot{\gamma}_{ij}) - \frac{\partial}{\partial x_j} p + \rho g_j = 0, \quad \text{for } j = 1, 2, 3 \quad (4D.4-2)$$

with the boundary condition

$$f_j + \sum_{i=1}^3 n_i \eta \dot{\gamma}_{ij} = 0, \quad \text{for } j = 1, 2, 3 \quad (4D.4-3)$$

on  $S_f$  and essential boundary conditions on  $S_v$ .

c. Draw a picture of the control volume  $V$  and explain why the above equations complete the proof. Pay particular attention to Eq. 4D.4-3.



# CHAPTER 5

## THE GENERAL LINEAR VISCOELASTIC FLUID

In Chapter 4 we discussed an expression for the stress tensor that is particularly useful for engineers who must solve problems involving large-deformation flows, both without and with heat transfer. In such problems, as we have seen, the predominant feature of the rheological behavior of the macromolecular fluids is their shear-rate-dependent viscosity.

Although the generalized Newtonian fluid has proven to be of great value in solving problems of engineering interest, its use is strictly speaking limited to steady-state shearing flows. It is generally inappropriate for the description of unsteady flow phenomena, where the elastic response of the polymeric fluid becomes important. In this chapter we introduce a constitutive equation that can describe some of the time-dependent motions of macromolecular fluids, albeit only the restricted class of flows with very small displacement gradients.

Why do we spend a whole chapter on such a restricted class of flows? There are several very good reasons for studying this subject, known as “linear viscoelasticity”: (1) polymer chemists have evolved several experiments that have enabled them to interrelate structure with the linear mechanical responses; (2) the material functions measured in these experiments have proven useful for characterization and quality control; and (3) some background in linear viscoelasticity is helpful to proceed to the subject of “nonlinear viscoelasticity”, which is treated in Chapters 6 through 9 of this volume. It is this last reason that we shall consider the principal motivation here. For the reader interested in the experiments of linear viscoelasticity, their analysis and molecular interpretations, we recommend the outstanding treatise of Ferry,<sup>1</sup> where a wealth of information and an extensive bibliography are to be found.

We begin in §5.1 by comparing and contrasting Newton’s “law” of viscosity and Hooke’s “law” of elasticity, the two limiting idealizations for viscous liquids and elastic solids. Then in §5.2 we show how Maxwell combined the ideas of viscosity and elasticity to arrive at a simple equation for a “viscoelastic fluid”; after that we show how Maxwell’s idea can be extended to obtain the constitutive equation for the *general linear viscoelastic fluid*, which has been widely used for many years to characterize the small-displacement behavior of polymeric liquids. It is this constitutive equation that is the primary subject of study in this chapter.

In §5.3 we use the constitutive equation to obtain expressions for some of the time-dependent material functions defined in Chapter 3. In the highly idealized flows discussed in this section, the velocity distribution is prescribed, and the shear stress is obtained directly from the constitutive equation. By contrast, in §5.4 we solve some linear viscoelastic flow problems that require the simultaneous consideration of the equations of change and the

<sup>1</sup> J. D. Ferry, *Viscoelastic Properties of Polymers*, 3rd ed., Wiley, New York (1980).

constitutive equation. In the final section, §5.5, we point out the limitations of the constitutive equation studied in this chapter.

§5.1 NEWTONIAN FLUIDS AND HOOKEAN SOLIDS

In Chapter 1 a discussion of the constitutive equation for the Newtonian fluid was given. Here we introduce the constitutive equation for the Hookean solid and point out some similarities and differences between these two “classical” constitutive equations. We do this by considering the two idealized experiments shown in Fig. 5.1-1.

The first experiment (Fig. 5.1-1a) is the *shearing motion of a Newtonian fluid* between two planes, the upper one of which moves with a velocity  $V(t)$ . We assume that the viscosity  $\mu$  is so large and that the interplane distance  $B$  is so small that the velocity distribution  $v_x(y, t)$  is a linear function of  $y$ . Then the velocity distribution is:

$$v_x(y, t) = \frac{V(t)}{B} y = \dot{\gamma}_{yx}(t)y \tag{5.1-1}$$

in which  $\dot{\gamma}_{yx}$  is the  $yx$ -component of the *rate-of-strain tensor*

$$\dot{\gamma} = \nabla \mathbf{v} + (\nabla \mathbf{v})^\dagger \quad \left( \text{or } \dot{\gamma}_{ij} = \frac{\partial}{\partial x_i} v_j + \frac{\partial}{\partial x_j} v_i \right) \tag{5.1-2}$$

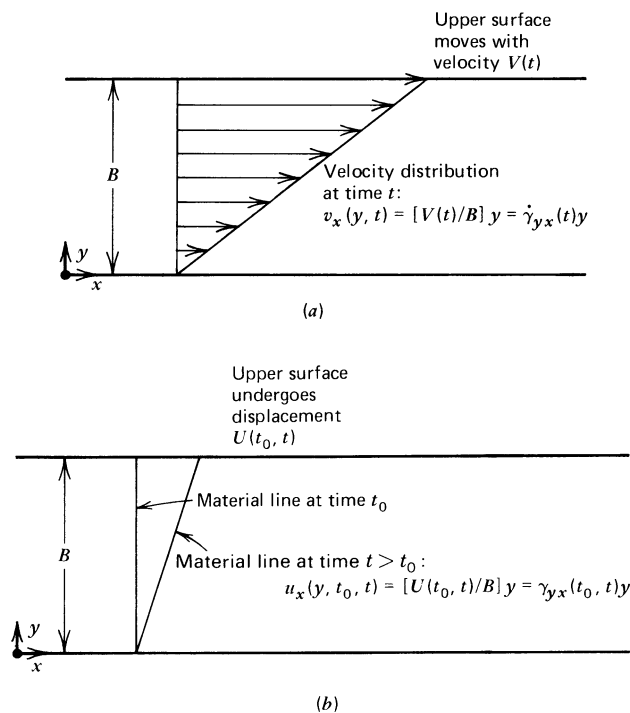


FIGURE 5.1-1. Material being sheared between two parallel planes, the upper one of which moves as a function of time. (a) The *velocity* profile for unsteady shear flow of a Newtonian fluid. (b) The *displacement* profile for the unsteady shearing motion of a Hookean solid. Note: at time  $t_0$  the solid is at rest with no shear stress.

The shear stress is then given for a Newtonian fluid by

$$\tau_{yx}(t) = -\mu \frac{\partial v_x}{\partial y} = -\mu \dot{\gamma}_{yx}(t) \quad (5.1-3)$$

That is, the stress at time  $t$  is proportional to the velocity gradient *at the same time*  $t$ .

The second experiment (Fig 5.1-1b) is the *shearing motion of a Hookean solid* between two parallel planes. At some time  $t_0$  the solid is in an isotropic stress state with no imposed external stresses other than atmospheric pressure. Then the upper plane undergoes an infinitesimal displacement  $U(t_0, t)$ . We assume that the displacement of the material in the gap is a linear function of the distance  $y$  above the lower plane, so that the displacement at any position is:

$$u_x(y, t_0, t) = \frac{U(t_0, t)}{B} y = \gamma_{yx}(t_0, t)y \quad (5.1-4)$$

Here  $\gamma_{yx}(t_0, t)$  is the  $yx$ -component of the *infinitesimal strain tensor*, which is defined in terms of the *displacement gradient tensor*  $\nabla \mathbf{u}$  as follows

$$\boldsymbol{\gamma} = \nabla \mathbf{u} + (\nabla \mathbf{u})^\dagger \quad \left( \text{or } \gamma_{ij} = \frac{\partial}{\partial x_i} u_j + \frac{\partial}{\partial x_j} u_i \right) \quad (5.1-5)$$

Note that the strain tensor depends on two times and that  $\gamma_{yx}(t_0, t_0) = 0$ . Then the shear stress for a Hookean solid is given by

$$\tau_{yx}(t) = -G \frac{\partial u_x}{\partial y} = -G \gamma_{yx}(t_0, t) \quad (5.1-6)$$

where  $G$  is the elastic modulus; that is, the stress at time  $t$  is proportional to the strain at time  $t$ , referred to the isotropic stress state at time  $t_0$ . The Hookean solid “remembers” where it was at time  $t_0$ , in contrast to the Newtonian fluid which has no memory of past events.

The two discussions above are parallel except for two points: (i) in the discussion of solids we must specify a reference time with respect to which strain is measured; strain tensors always depend on two times, and we establish the convention that the first variable listed denotes the reference state; (ii) the stress relation, Eq. 5.1-6, is restricted to infinitesimally small displacement gradients  $\partial u_j / \partial x_i$ ; for large displacement gradients Eq. 5.1-6 ceases to be valid, whereas Eq. 5.1-3 is valid for flow with arbitrarily large displacement gradients. The restriction that is placed on Eq. 5.1-6 has some important implications to be discussed in §5.5.

The kinematic quantities in the two experiments are related to one another. The velocities and displacements are related by:

$$\left\{ \begin{array}{l} v_x(y, t) = \frac{\partial}{\partial t} u_x(y, t_0, t) \\ u_x(y, t_0, t) = \int_{t_0}^t v_x(y, t') dt' \end{array} \right. \quad (5.1-7a)$$

$$\left\{ \begin{array}{l} v_x(y, t) = \frac{\partial}{\partial t} u_x(y, t_0, t) \\ u_x(y, t_0, t) = \int_{t_0}^t v_x(y, t') dt' \end{array} \right. \quad (5.1-7b)$$

Similarly the components of the rate-of-strain and infinitesimal strain tensors are related by:

$$\left\{ \begin{array}{l} \dot{\gamma}_{yx}(t) = \frac{\partial}{\partial t} \gamma_{yx}(t_0, t) \\ \gamma_{yx}(t_0, t) = \int_{t_0}^t \dot{\gamma}_{yx}(t') dt' \end{array} \right. \quad \begin{array}{l} (5.1-8a) \\ (5.1-8b) \end{array}$$

We also point out that for the infinitesimal strain tensor

$$\gamma_{yx}(t_0, t) = \gamma_{yx}(t_0, t^*) + \gamma_{yx}(t^*, t) \quad (5.1-9)$$

That is, the infinitesimal strains are additive. These relations are referred to later.

## §5.2 LINEAR VISCOELASTIC FLUIDS

In Chapter 2 it was found that *polymeric liquids are viscoelastic*. For example, the photographs of §2.5e show how a polymeric liquid recoils because of its elastic properties. Furthermore in §§3.4 and 3.5 several kinds of transient-response experiments were described in which elastic behavior was evident. For example, delayed stress relaxation after cessation of steady flow is an indication of fluid elasticity as is the large recovery following elongational flow. The main thrust of this chapter is to show how the ideas of viscosity and elasticity may be combined into a single constitutive equation that can describe these various elastic effects.

### a. The Maxwell Model

The first attempt to obtain a viscoelastic constitutive equation appears to have been that of Maxwell,<sup>1</sup> who over a century ago developed a theory for viscoelasticity, because he thought that gases might be viscoelastic. He proposed that fluids with both viscosity and elasticity could be described by:

$$\tau_{yx} + \frac{\mu}{G} \frac{\partial \tau_{yx}}{\partial t} = -\mu \dot{\gamma}_{yx} \quad (5.2-1)$$

For steady-state motions this equation simplifies to the Newtonian fluid with viscosity  $\mu$ . For sudden changes in stress, the time derivative term dominates the left side of the equation, and then integration with respect to time (with the help of Eq. 5.1-8b) gives the Hookean solid with elastic modulus  $G$ . This is the simplest expression for the shear stress for a fluid that is both viscous and elastic.

Since Hooke's law is valid only for infinitesimal displacement gradients, it seems reasonable to expect that Maxwell's equation would be subject to the same restriction. We must keep in mind that Newton's and Hooke's "laws" were both proposed empirically; these linear relations were put forward as modest but reasonable suggestions. Subsequent experimentation, coupled with calculations based on the equations of change and the

<sup>1</sup> J. C. Maxwell, *Phil. Trans. Roy. Soc.*, **A157**, 49-88 (1867).

proposed constitutive equations, showed that the linear relations of Newton and Hooke are indeed useful for a wide range of materials. However, it has long been recognized that these “classical” constitutive equations do have their limitations. Many materials require more complex mathematical descriptions.

Maxwell’s proposal was also empirical. Although it turns out that its range of validity is somewhat limited, certain nonlinear generalizations of the Maxwell constitutive equation have proven to be very useful in polymer fluid dynamics, and we will eventually present and evaluate these generalizations in Chapters 7 and 8.

We now look at some alternative forms of the Maxwell model. First we generalize Eq. 5.2-1 to arbitrary, small displacement flows by putting the equation in tensor form. In addition, we adopt new symbols for the constants, since this notation will be more in keeping with subsequent developments: we replace  $\mu$  by  $\eta_0$  (the zero-shear-rate viscosity) and  $\mu/G$  by  $\lambda_1$  (a time constant, often called the “relaxation time”). Then the *Maxwell model* is:

$$\tau + \lambda_1 \frac{\partial}{\partial t} \tau = -\eta_0 \dot{\gamma} \quad (5.2-2)$$

This is more complicated than Newton’s and Hooke’s equations since this is a differential equation for  $\tau$ .

For many purposes it would be preferable to solve Eq. 5.2-2 for the stress tensor. That is easily done by recognizing that Eq. 5.2-2 is a first-order, linear equation<sup>2</sup> for  $\tau$  as a function of  $t$ , which can be integrated at once to give:

$$\tau(t) = e^{-t/\lambda_1} \left[ \int \left( -\frac{\eta_0}{\lambda_1} \dot{\gamma}(t) \right) e^{t/\lambda_1} dt + \kappa \right] \quad (5.2-3)$$

We now affix limits on the integral and write:

$$\tau(t) = - \frac{\int_{-\infty}^t (\eta_0/\lambda_1) \dot{\gamma}(t') e^{t'/\lambda_1} dt'}{e^{t/\lambda_1}} + \kappa e^{-t/\lambda_1} \quad (5.2-4)$$

where primes have been added to  $t$ ’s in the integrand in order to avoid confusion; the choice of  $-\infty$  as the lower limit is arbitrary—some other choice would result in a different value for the integration constant  $\kappa$ . If we prescribe that the stress in the fluid is finite at  $t = -\infty$ , we must choose  $\kappa$  to be zero. But we must also check the first term on the right side of Eq. 5.2-4, since both numerator and denominator tend to zero as  $t$  goes to  $-\infty$ . When we use L’Hôpital’s rule we get:

$$\lim_{t \rightarrow -\infty} \tau(t) = \lim_{t \rightarrow -\infty} - \frac{(\eta_0/\lambda_1) \dot{\gamma}(t) e^{t/\lambda_1}}{(1/\lambda_1) e^{t/\lambda_1}} = -\eta_0 \dot{\gamma}(-\infty) \quad (5.2-5)$$

<sup>2</sup> Recall that the differential equation  $dy/dx + P(x)y = Q(x)$  has the solution:

$$y = e^{-\int P(x)dx} \left[ \int Q(x) e^{+\int P(x)dx} dx + K \right] \quad (5.2-2a)$$

where  $K$  is a constant of integration.

Therefore, if  $\dot{\gamma}(-\infty)$  is finite, the stress is also finite at  $t = -\infty$ . Consequently, the Maxwell constitutive equation can be written in the form

$$\tau(t) = - \int_{-\infty}^t \left\{ \frac{\eta_0}{\lambda_1} e^{-(t-t')/\lambda_1} \right\} \dot{\gamma}(t') dt' \quad (5.2-6)$$

The quantity within the braces is called the *relaxation modulus* for the Maxwell fluid. When written in this form, the Maxwell model says that the stress at the present time  $t$  depends on the rate of strain at time  $t$  as well as on the rate of strain at all past times  $t'$ , with a weighting factor (the relaxation modulus) that decays exponentially as one goes backwards in time. Thus we see that this form of the Maxwell equation contains the notion of a “fading memory”. The fluid remembers very well what it has experienced in the very recent past but has only a hazy recollection of events in the distant past. Sometimes we say that the stress at time  $t$  depends on the “history” of the rate of strain for all past times  $-\infty < t' \leq t$ .

Next, we want to put the Maxwell model into still another form by doing an integration by parts using Eq. 5.1-8b. However, in using the latter equation we have to specify a reference time (there called  $t_0$ ). For fluids there is no unique reference state  $t_0$  to use in describing strains, so that *for fluids it is customary to measure the strain at a past time  $t'$  relative to the configuration of the fluid at the present time  $t$* . Hence, for fluids we generalize Eq. 5.1-8 thus:

$$\frac{\partial \gamma}{\partial t'} = \dot{\gamma}(t') \quad \text{and} \quad \gamma(t, t') = \int_t^{t'} \dot{\gamma}(t'') dt'' \quad (5.2-7)$$

These relations are valid for any flow pattern as long as the displacement gradients are infinitesimally small. Now integration by parts of Eq. 5.2-6 gives

$$\tau(t) = + \int_{-\infty}^t \left\{ \frac{\eta_0}{\lambda_1^2} e^{-(t-t')/\lambda_1} \right\} \gamma(t, t') dt' \quad (5.2-8)$$

The quantity within the braces is called the *memory function* for the Maxwell fluid. In this form the Maxwell model states that the stress at the present time  $t$  depends on the history of the strain for all past times  $-\infty < t' \leq t$ . The exponential factor in the integrand describes the fading memory.

All three forms of Maxwell's constitutive equation—Eqs. 5.2-2, 6, and 8—are equivalent provided that  $\dot{\gamma}$  is finite at  $t = -\infty$  and the displacement gradients are infinitesimally small. Equation 5.2-6 looks like a modified Newton's law and Eq. 5.2-8 like a modified Hooke's law. Maxwell's equation played a key role in the development of linear viscoelasticity, and as we shall see in Chapters 7 and 8, it has also been taken as the starting point for the development of nonlinear viscoelastic models. It is therefore important that the material presented in this section be thoroughly understood before continuing.

The two-constant Maxwell model was found to be inadequate for describing linear viscoelastic data. Therefore, through the years more elaborate equations were suggested; let us look at a few of these.

## b. The Jeffreys Model

The Maxwell equation in Eq. 5.2-2 is a linear relation between  $\tau$  and  $\dot{\gamma}$ . But one can easily invent other linear relations. For example, we can include the time derivative of  $\dot{\gamma}$  and get the constitutive equation

$$\tau + \lambda_1 \frac{\partial \tau}{\partial t} = -\eta_0 \left( \dot{\gamma} + \lambda_2 \frac{\partial \dot{\gamma}}{\partial t} \right) \quad (5.2-9)$$

which is known as the *Jeffreys model*. This equation, containing two time constants  $\lambda_1$  and  $\lambda_2$  (the “relaxation time” and the “retardation time”, respectively), was proposed for the study of wave propagation in the earth’s mantle.<sup>3</sup>

The Jeffreys model can also be put into integral form. When Eq. 5.2-9 is integrated as a first-order differential equation, using the initial condition that  $\tau$  be finite at  $t = -\infty$ , we find that (if  $\dot{\gamma}$  and  $\partial \dot{\gamma} / \partial t$  are both finite at  $t = -\infty$ )

$$\tau(t) = - \int_{-\infty}^t \frac{\eta_0}{\lambda_1} \left( 1 - \frac{\lambda_2}{\lambda_1} \right) e^{-(t-t')/\lambda_1} \dot{\gamma}(t') dt' - \frac{\eta_0 \lambda_2}{\lambda_1} \dot{\gamma}(t) \quad (5.2-10)$$

From this form of the constitutive equation it can be seen that  $\lambda_2 < \lambda_1$ ; otherwise, in stress relaxation after cessation of steady shear flow  $\tau_{yx}$  would have the wrong sign.

We would like to put Eq. 5.2-10 into a form that is the same as Eq. 5.2-6, so that we can identify the relaxation modulus. This is done by using the Dirac delta function:<sup>4</sup>

$$\tau(t) = - \int_{-\infty}^t \left\{ \frac{\eta_0}{\lambda_1} \left( 1 - \frac{\lambda_2}{\lambda_1} \right) e^{-(t-t')/\lambda_1} + 2 \frac{\eta_0 \lambda_2}{\lambda_1} \delta(t-t') \right\} \dot{\gamma}(t') dt' \quad (5.2-11)$$

<sup>3</sup> H. Jeffreys, *The Earth*, Cambridge University Press (1929), p. 265.

<sup>4</sup> P. A. M. Dirac, *The Principles of Quantum Mechanics*, 3rd ed., Oxford University Press (1947), pp. 58-61; M. J. Lighthill, *Fourier Analysis and Generalised Functions*, Cambridge University Press (1964), p. 17. Here we use the definition that:

$$\delta(x) = \lim_{n \rightarrow \infty} \sqrt{\frac{n}{\pi}} e^{-nx^2} \quad (5.2-10a)$$

From this it follows that:

$$\int_{-a}^a f(x) \delta(x) dx = 2 \int_0^a f(x) \delta(x) dx = f(0) \quad (5.2-10b)$$

$$\int_{-a}^a f(x) \delta'(x) dx = -f'(0) \quad (5.2-10c)$$

in which  $a > 0$ , and the prime denotes differentiation with respect to  $x$ . Note particularly the occurrence of the factor of 2 in Eq. 5.2-10b when the integral is over the region from 0 to  $a$ . This explains the occurrence of the factors of 2 in the  $\delta$ -function terms in Eqs. 5.2-11 and 12.

The quantity enclosed in the braces is the relaxation modulus for the Jeffreys model. Integration by parts then gives:

$$\tau(t) = + \int_{-\infty}^t \left\{ \frac{\eta_0}{\lambda_1^2} \left( 1 - \frac{\lambda_2}{\lambda_1} \right) e^{-(t-t')/\lambda_1} + \frac{2\eta_0\lambda_2}{\lambda_1} \frac{\partial}{\partial t'} \delta(t-t') \right\} \gamma(t, t') dt' \quad (5.2-12)$$

The quantity in braces here is the memory function. The Jeffreys model is also used in Chapters 7 and 8 as a point of departure for proposing nonlinear viscoelastic models. Clearly more time derivatives could be added to the left and right sides of Eq. 5.2-9 thereby generating many more linear relations between  $\tau$  and  $\dot{\gamma}$  (see Problem 5C.1).

### c. The Generalized Maxwell Model

Another way to generalize the Maxwell model is to construct a “superposition” of Maxwell models. We can write Eq. 5.2-2 for the  $k$ th partial stress  $\tau_k$  using constants  $\lambda_k$  and  $\eta_k$ ; then we get the total stress by summing the partial stresses. This constitutive equation can be integrated to give equations similar in form to Eqs. 5.2-6 and 5.2-8. To summarize, we have for the *generalized Maxwell model*:

$$\tau(t) = \sum_{k=1}^{\infty} \tau_k(t); \quad \tau_k + \lambda_k \frac{\partial}{\partial t} \tau_k = -\eta_k \dot{\gamma} \quad (5.2-13)$$

$$\tau(t) = - \int_{-\infty}^t \left\{ \sum_{k=1}^{\infty} \frac{\eta_k}{\lambda_k} e^{-(t-t')/\lambda_k} \right\} \dot{\gamma}(t') dt' \quad (5.2-14)$$

$$\tau(t) = + \int_{-\infty}^t \left\{ \sum_{k=1}^{\infty} \frac{\eta_k}{\lambda_k^2} e^{-(t-t')/\lambda_k} \right\} \gamma(t, t') dt' \quad (5.2-15)$$

We adopt the convention that  $\lambda_1 > \lambda_2 > \lambda_3 \dots$ . This model contains infinitely many constants  $\lambda_k$  and  $\eta_k$ , thus allowing for a spectrum of relaxation times and viscosities. (Of course, one can set  $\lambda_k = 0$  and  $\eta_k = 0$  for  $k$  greater than some finite number  $K$ .) For some purposes it may be desirable to reduce the total number of parameters to three by use of the following empiricisms:<sup>5</sup>

$$\eta_k = \eta_0 \frac{\lambda_k}{\sum_k \lambda_k}; \quad \lambda_k = \frac{\lambda}{k^\alpha} \quad (5.2-16,17)$$

where  $\eta_0$  is the zero-shear-rate viscosity,  $\lambda$  is a time constant, and  $\alpha$  is a dimensionless quantity, which describes the slope of  $\eta'$  versus  $\omega$  on a log-log plot at high  $\omega$  (for large  $\omega$ ,  $\eta' \propto \omega^{(1/\alpha)-1}$ ). The relations above are not entirely empirical. The *Rouse molecular theory for dilute polymer solutions*<sup>6</sup> gives very nearly Eqs. 5.2-16,17 with  $\alpha = 2$ ; in this theory the polymer molecules are modeled as freely jointed chains made up of beads connected linearly by Hookean springs. Experimental data for concentrated polymer situations and polymer melts seem to be portrayed reasonably well by Eqs. 5.2-16,17 with  $\alpha$  in the range 2 to 4. On the other hand, the *Doi and Edwards molecular theory for polymer melts*<sup>7</sup> suggests an

<sup>5</sup> T. W. Spriggs, *Chem. Eng. Sci.*, **20**, 931-940 (1965).

<sup>6</sup> P. E. Rouse, Jr., *J. Chem. Phys.*, **21**, 1272-1280 (1953); see also Chapter 15.

<sup>7</sup> M. Doi and S. F. Edwards, *J. Chem. Soc. Faraday Trans. II*, **74**, 1789-1832 (1978); **75**, 38-54 (1979); see also Chapter 19.

empiricism with  $\lambda_k$  replaced by  $\lambda_k^2$  in Eq. 5.2-16, and  $k$  taking on odd values only. Still other possibilities for describing  $G(s)$  are the three-parameter empiricism in Problem 5B.2 and the finite sum of exponentials used in Example 5.3-7.

d. The General Linear Viscoelastic Model

When we compare Eq. 5.2-6 (for the Maxwell model), Eq. 5.2-11 (for the Jeffreys model), and Eq. 5.2-14 (for the generalized Maxwell model) we find that they are all of the same form: an integral over all past times of a relaxation modulus multiplied by a rate-of-deformation tensor. The only physical ideas that have been included in these models of varying degrees of complexity are those of viscosity and elasticity. An equation that includes all of these models, and many more of course, is the *general linear viscoelastic model*, which may be written in either of two equivalent forms:

$$\tau = - \int_{-\infty}^t G(t-t') \dot{\gamma}(t') dt' \tag{5.2-18}$$

$$\tau = + \int_{-\infty}^t M(t-t') \gamma(t, t') dt' \tag{5.2-19}$$

in which  $G(t-t')$  is the *relaxation modulus* and  $M(t-t') = \partial G(t-t')/\partial t'$  is the *memory function*. This model is the starting point for most of the development in this chapter and will be referred to in connection with nonlinear constitutive equations and molecular theories. Of course, for getting quantitative answers to problems we shall have to use some specific expression for  $G(t-t')$ , such as the expression between braces in Eqs. 5.2-6, 11, or 14. It should be kept in mind that Eqs. 5.2-18 and 19 are equivalent only if  $\dot{\gamma}$  is finite at  $t = -\infty$  and if the displacement gradients are infinitesimally small.

Equations 5.2-18 and 19 have an important feature: the integrands consist of the product of two functions, *the first depending on the nature of the fluid* (since material parameters, such as  $\eta_k$  and  $\lambda_k$ , appear in  $G(t-t')$  or  $M(t-t')$ ) and *the second depending on the nature of the flow* (since the kinematics is described by  $\dot{\gamma}(t')$  or  $\gamma(t, t')$ ). In Chapter 8 we discuss nonlinear viscoelastic constitutive equations that have this same “factorized” structure.

In Eqs. 5.2-18 and 19 the functions  $G(s)$  and  $M(s)$  are positive functions which decrease monotonically to zero as  $s = t - t'$  goes to infinity. Such viscoelastic fluids are often said to have “fading memory”. If  $G(s)$  has the form given by the generalized Maxwell model, the duration of the memory is governed by the largest relaxation time,  $\lambda_{\max}$ . Although Eqs. 5.2-18 and 19 are strictly applicable only to flows with infinitesimally small displacement gradients, we can in some instances apply them outside this region because of the rapidly fading memory. For example, in steady shear flow with shear rate  $\dot{\gamma} \ll 1/\lambda_{\max}$ , the memory of the large strains is negligible and does not contribute to the stress.

The general linear viscoelastic model in Eq. 5.2-18 may also be derived by more formal arguments.<sup>8</sup> One assumes that the stress at time  $t$  resulting from a step strain at time  $t'$  is linear in the strain and multiplied by a decaying function of the elapsed time  $t - t'$ . An actual flow history may then be regarded as made up of a number of small step strains. By *Boltzmann’s superposition principle*<sup>9</sup> it is assumed that the stress contributions from the

<sup>8</sup> A. C. Pipkin, *Lectures on Viscoelasticity Theory*, Springer, New York (1972), pp. 7-12.

<sup>9</sup> L. Boltzmann, *Pogg. Ann. Phys.*, 7, 624-654 (1876).

individual small step strains at past times  $t'$  may be added to give the stress at time  $t$ . This results in the integral in Eq. 5.2-18. In the linear limit considered in this chapter the Boltzmann superposition principle seems reasonable inasmuch as coupling effects between two past deformations must be of second order in the applied deformations and hence negligible.

Equation 5.2-18 (or Eq. 5.2-19) is generally accepted as the correct starting point for the description of the rheology of incompressible viscoelastic fluids for small-displacement-gradient motions. In Chapters 7, 8, and 9 large-displacement-gradient flows are considered and equations more general than Eq. 5.2-18 are given.

### §5.3 LINEAR VISCOELASTIC RHEOLOGICAL PROPERTIES

In the foregoing section it was shown that the elementary concepts of viscosity and elasticity can be combined in a number of ways to develop equations of increasing complexity, culminating with Eq. 5.2-18, which is the most general equation of linear viscoelasticity. In this section we illustrate the use of this equation by obtaining expressions for the time-dependent material functions in terms of the relaxation modulus  $G(t - t')$ .

Before discussing the transient-response phenomena, we mention briefly how Eq. 5.2-18 simplifies for steady-state shear flow. When the fluid has been flowing between parallel plates for a long time with constant velocity gradient  $\dot{\gamma}_{yx}$  (where  $\lambda_{\max} |\dot{\gamma}_{yz}| \ll 1$ ), then Eq. 5.2-18 becomes

$$\begin{aligned}\tau_{yx} &= - \int_{-\infty}^t G(t - t') \dot{\gamma}_{yx} dt' \\ &= - \left[ \int_0^{\infty} G(s) ds \right] \dot{\gamma}_{yx} \\ &\equiv -\eta_0 \dot{\gamma}_{yx}\end{aligned}\tag{5.3-1}$$

Here the change of variables  $s = t - t'$  has been made. We see that the viscosity is just equal to the integral over the relaxation modulus. The subscript "0" on  $\eta_0$  indicates that this is the zero-shear-rate viscosity. In the theory of linear viscoelasticity we are able to obtain the viscosity only in this limit of vanishingly small velocity gradients.

#### EXAMPLE 5.3-1 Small-Amplitude Oscillatory Motion

A polymeric fluid is located in the space between two parallel plates, the upper one of which is made to oscillate with frequency  $\omega$  in its own plane in the  $x$ -direction. As shown in Figure 3.4-1b the velocity profile is assumed to be instantaneously linear,<sup>1</sup> which is a good assumption for highly viscous materials in very narrow slits (cf. Problem 1D.1). Therefore the velocity gradient is changing with time in the following way:

$$\dot{\gamma}_{yx}(t) = \dot{\gamma}_{yx}^0 \cos \omega t\tag{5.3-2}$$

in which we take  $\dot{\gamma}_{yx}^0$  to be real and positive. In order to satisfy the small-displacement-gradient restriction on Eq. 5.2-18, we require that  $\dot{\gamma}_{yx}^0/\omega \ll 1$ . Find the time-dependent shear stress  $\tau_{yx}$  that is needed to maintain this oscillatory motion, and obtain expressions for the real and imaginary parts of the complex viscosity.

<sup>1</sup> Inertial effects have been considered by K. Walters and R. A. Kemp in *B. E. Whetton and R. W. Whorlow, eds., Polymer Systems*, Macmillan, London (1968), pp. 237-250, and *Rheol. Acta*, **7**, 1-8 (1968).

**SOLUTION** Substitution of the velocity gradient of Eq. 5.3-2 into the constitutive equation in Eq. 5.2-18 gives:

$$\begin{aligned}
 \tau_{yx} &= - \int_{-\infty}^t G(t-t') \dot{\gamma}_{xy}^0 \cos \omega t' dt' \\
 &= - \dot{\gamma}_{yx}^0 \int_0^\infty G(s) \cos \omega(t-s) ds \\
 &= - \left[ \int_0^\infty G(s) \cos \omega s ds \right] \dot{\gamma}_{yx}^0 \cos \omega t \\
 &\quad - \left[ \int_0^\infty G(s) \sin \omega s ds \right] \dot{\gamma}_{yx}^0 \sin \omega t
 \end{aligned} \tag{5.3-3}$$

Comparison of this result with the definitions of  $\eta'(\omega)$  and  $\eta''(\omega)$  in Eq. 3.4-3b shows that:

$$\eta'(\omega) = \int_0^\infty G(s) \cos \omega s ds \tag{5.3-4}$$

$$\eta''(\omega) = \int_0^\infty G(s) \sin \omega s ds \tag{5.3-5}$$

or, alternatively, we may write the results in terms of the “complex viscosity”

$$\eta^* = \eta' - i\eta'' = \int_0^\infty G(s) e^{-i\omega s} ds \tag{5.3-6}$$

The relaxation modulus  $G(s)$  can be eliminated between Eqs. 5.3-4 and 5 to give the Kramers–Kronig relations (see Problem 5D.2), which interrelate  $\eta'(\omega)$  and  $\eta''(\omega)$ . Finally, we note for future reference that:

$$\lim_{\omega \rightarrow 0} \frac{\eta''(\omega)/\omega}{\eta'(\omega)} = \frac{\int_0^\infty G(s) s ds}{\int_0^\infty G(s) ds} \tag{5.3-7}$$

We shall find as we go through this section that several other limiting quantities are also equal to the same ratio of integrals.

Let us now see what the expressions for  $\eta'(\omega)$  and  $\eta''(\omega)$  look like for the particular choice of relaxation modulus given by the generalized Maxwell model (quantity in braces in Eq. 5.2-14)

$$\eta'(\omega) = \sum_{k=1}^{\infty} \frac{\eta_k}{1 + (\lambda_k \omega)^2} \tag{5.3-8}$$

$$\frac{\eta''(\omega)}{\omega} = \sum_{k=1}^{\infty} \frac{\eta_k \lambda_k}{1 + (\lambda_k \omega)^2} \tag{5.3-9}$$

If, in addition, we introduce the expressions for  $\eta_k$  and  $\lambda_k$  given in Eqs. 5.2-16 and 17, these results become

$$\frac{\eta'}{\eta_0} = \frac{1}{\zeta(\alpha)} \sum_{k=1}^{\infty} \frac{k^\alpha}{k^{2\alpha} + (\lambda \omega)^2} \tag{5.3-10}$$

$$\frac{\eta''}{\eta_0} = \frac{\lambda \omega}{\zeta(\alpha)} \sum_{k=1}^{\infty} \frac{1}{k^{2\alpha} + (\lambda \omega)^2} \tag{5.3-11}$$

in which  $\zeta(\alpha)$  is the Riemann zeta function.<sup>2</sup> These expressions are not particularly appropriate for computation of the functions  $\eta'(\omega)$  and  $\eta''(\omega)$ . Instead we have available<sup>3</sup> an alternative pair of expressions useful for low frequencies ( $\omega \ll \lambda^{-1}$ )

$$\frac{\eta'}{\eta_0} = 1 - \left[ \frac{(\lambda\omega)^2}{\zeta(\alpha)} \sum_{k=1}^{\infty} \frac{1}{k^{2\alpha}(k^{2\alpha} + (\lambda\omega)^2)} \right] \quad (5.3-12)$$

$$\frac{\eta''}{\eta_0} = \lambda\omega \left[ \frac{\zeta(2\alpha)}{\zeta(\alpha)} - \frac{(\lambda\omega)^2}{\zeta(\alpha)} \sum_{k=1}^{\infty} \frac{1}{k^{2\alpha}(k^{2\alpha} + (\lambda\omega)^2)} \right] \quad (5.3-13)$$

and another pair of asymptotic expressions that is excellent for high frequencies ( $\omega \gg \lambda^{-1}$ )

$$\frac{\eta'}{\eta_0} \sim \frac{1}{\zeta(\alpha)} \left[ \frac{\pi(\lambda\omega)^{(1/\alpha)-1}}{2\alpha \sin((\alpha+1)\pi/2\alpha)} \right] \quad (5.3-14)$$

$$\frac{\eta''}{\eta_0} \sim \frac{1}{\zeta(\alpha)} \left[ \frac{\pi(\lambda\omega)^{(1/\alpha)-1}}{2\alpha \sin(\pi/2\alpha)} - \frac{(\lambda\omega)^{-1}}{2} \right] \quad (5.3-15)$$

These large-frequency expressions are obtained by using the Euler-Maclaurin expansion to convert the sums into integrals (see Problem 5B.5). Equations 5.3-10 and 11 (and their low- and high-frequency equivalents) are useful for curve-fitting data for the small-amplitude oscillatory experiment. In addition, in Example 5.3-7 it is shown how  $\eta_k$  and  $\lambda_k$  can be chosen so that Eqs. 5.3-8 and 9 accurately fit experimental data for  $\eta'$  and  $\eta''$ .

We conclude this illustrative example by reminding the reader that for a Newtonian fluid  $\eta'$  is just a constant (the viscosity), and that  $\eta''$  is zero; that is, for the Newtonian fluid the shear stress is in phase with the velocity gradient.

### EXAMPLE 5.3-2 Stress Relaxation after a Sudden Shear $\gamma$ Displacement

The purpose of this example is to show why the function  $G(t-t')$  is called the "relaxation modulus". A polymeric liquid is at rest in the region between two parallel plates for time  $t < t_0$ . At time  $t = t_0$  the upper plate is instantaneously moved slightly in the  $x$ -direction, as shown in Fig. 3.4-1e. Find the expression for the shear stress at time  $t > t_0$ , for a sudden shear strain  $\gamma_0 \ll 1$ .

**SOLUTION** To solve this problem we first imagine that the displacement actually occurs during the finite time interval from  $t_0 - \varepsilon$  to  $t_0$ , and then later we let  $\varepsilon$  go to zero. That is, the  $yx$ -components of the infinitesimal strain tensor and of the rate-of-strain tensor are as shown in Fig. 5.3-1.

For the displacement occurring in the finite time interval  $\varepsilon$ , Eq. 5.2-18 becomes (for  $t > t_0$ )

$$\begin{aligned} \tau_{yx}(t) &= - \int_{-\infty}^{t_0-\varepsilon} G(t-t') \dot{\gamma}_{yx}(t') dt' - \int_{t_0-\varepsilon}^{t_0} G(t-t') \dot{\gamma}_{yx}(t') dt' - \int_{t_0}^t G(t-t') \dot{\gamma}_{yx}(t') dt' \\ &= - \frac{\gamma_0}{\varepsilon} \int_{t_0-\varepsilon}^{t_0} G(t-t') dt' \end{aligned} \quad (5.3-16)$$

<sup>2</sup> The Riemann zeta function is defined as:

$$\zeta(\alpha) = \sum_{k=1}^{\infty} k^{-\alpha}, \quad \alpha > 1 \quad (5.3-11a)$$

a few sample values being  $\zeta(2) = \pi^2/6$ ,  $\zeta(4) = \pi^4/90$ ,  $\zeta(6) = \pi^6/945$  (see M. Abramowitz and I. A. Stegun, eds., *Handbook of Mathematical Functions*, Nat. Bur. Stds. Appl. Math. Series No. 55, U.S. Govt. Ptg. Off., Washington, D.C. (1964), p. 807).

<sup>3</sup> T. W. Spriggs, *Chem. Eng. Sci.* **20**, 931-940 (1965).

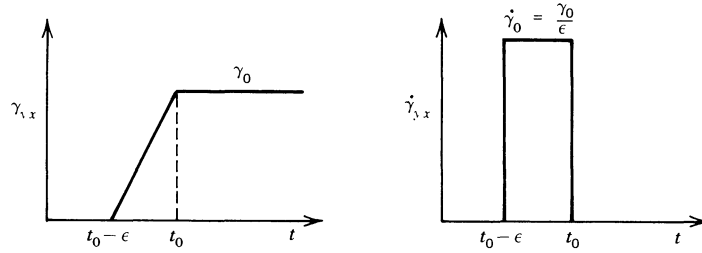


FIGURE 5.3-1. Time-dependent behavior of  $\gamma_{yx}$  and  $\dot{\gamma}_{yx}$  in the sudden shear strain stress-relaxation experiment.

since the velocity gradient is zero except during the middle time interval. Now we take the limit as  $\epsilon$  approaches zero using L'Hôpital's rule:

$$\begin{aligned} \tau_{yx}(t) &= \lim_{\epsilon \rightarrow 0} (-\gamma_0) \left[ \frac{\frac{d}{d\epsilon} \int_{t_0-\epsilon}^{t_0} G(t-t') dt'}{\frac{d}{d\epsilon} \epsilon} \right] \\ &= -\gamma_0 G(t-t_0) \end{aligned} \quad (5.3-17)$$

Thus the function  $G(t-t_0)$  describes the way in which the shear stress relaxes after the sudden shearing displacement. The top curve in either Fig. 3.4-15 or Fig. 3.4-16a gives a direct experimental measurement of  $G$ . If we insert the expression for the relaxation modulus for the generalized Maxwell fluid, we see that the stress dies out as a sum of exponentials. Keep in mind that for a Newtonian fluid there is no delayed stress relaxation—the stress drops instantly to zero as soon as the motion stops.

### EXAMPLE 5.3-3 Stress Relaxation after Cessation of Steady Shear Flow

Next we turn our attention to the stress relaxation that occurs in a different type of experiment. Here we envisage a steady shear flow with shear rate  $\dot{\gamma}_0 \ll 1/\lambda_{\max}$ , for time  $t < 0$  (see Fig. 3.4-1d). Then at time  $t = 0$  the flow is stopped suddenly. It is desired to describe the way in which the stress decays with time after the cessation of the steady shear flow. It is also desired to find the area under the  $\eta^-(t)$  curve.

**SOLUTION** For this experiment Eq. 5.2-18 gives for  $t < 0$  and  $t > 0$

$$\tau_{yx}(t < 0) = -\eta_0 \dot{\gamma}_0 = -\dot{\gamma}_0 \int_{-\infty}^t G(t-t') dt' \quad (5.3-18)$$

$$\tau_{yx}(t > 0) = -\eta^- \dot{\gamma}_0 = -\dot{\gamma}_0 \int_{-\infty}^0 G(t-t') dt' \quad (5.3-19)$$

We now take the ratio of the above two expressions and then integrate it from  $t = 0$  to  $t = \infty$ . This gives for the area under the stress-relaxation curve

$$\begin{aligned} \int_0^{\infty} \frac{\eta^-(t)}{\eta_0} dt &= \int_0^{\infty} \frac{\int_{-\infty}^0 G(t-t') dt'}{\int_{-\infty}^t G(t-t') dt'} dt \\ &= \frac{\int_0^{\infty} \int_t^{\infty} G(s) ds dt}{\int_0^{\infty} G(s) ds} \\ &= \frac{\int_0^{\infty} \int_0^s G(s) dt ds}{\int_0^{\infty} G(s) ds} \\ &= \frac{\int_0^{\infty} s G(s) ds}{\int_0^{\infty} G(s) ds} \end{aligned} \quad (5.3-20)$$

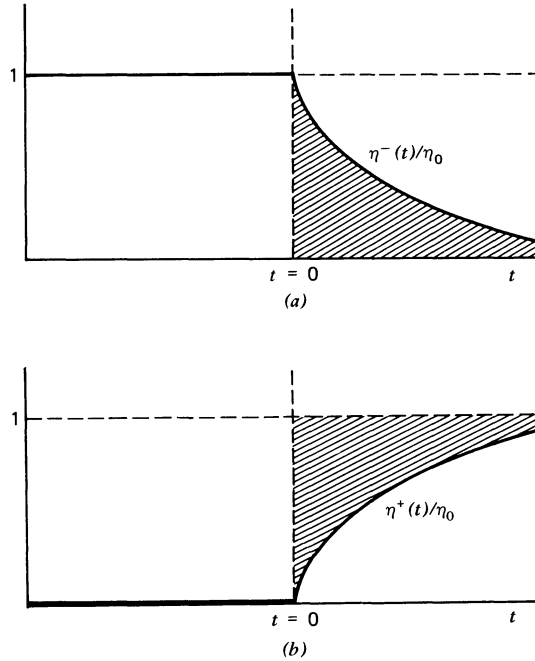


FIGURE 5.3-2. Integrals evaluated in Examples 5.3-3 and 4. (a) Integral in Eq. 5.3-20 for stress relaxation is given by the shaded area; (b) integral in Eq. 5.3-24 for stress growth is given by the shaded area.

In going from the second to the third line, we interchanged the order of integration so that one integration could be performed. See Fig. 5.3-2a for the graphical interpretation of this integral.

Note further that if we use the relaxation modulus for the generalized Maxwell model, then we find

$$\frac{\eta^-}{\eta_0} = \frac{\sum_k \eta_k e^{-t/\lambda_k}}{\sum_k \eta_k} \tag{5.3-21}$$

This result describes the top curve of the set of curves in Fig. 3.4-11, that is, the limiting curve for vanishingly small  $\dot{\gamma}_0$ . The linear theory cannot describe the dependence of the lower curves on  $\dot{\gamma}_0$ . To describe those curves we need a nonlinear viscoelastic theory, such as one of those described in Chapters 7 and 8.

**EXAMPLE 5.3-4** Stress Growth at Inception of Steady Shear Flow

The next flow situation we examine is that shown in Fig. 3.4-1c where a fluid at rest is suddenly made to undergo steady-state shear flow after  $t = 0$ . Let the velocity gradient for  $t > 0$  be  $\dot{\gamma}_0$ , where  $\lambda_{\max} \dot{\gamma}_0 \ll 1$ . Find  $\eta^+(t)$  and the area under the curve of  $1 - (\eta^+/\eta_0)$ .

**SOLUTION** For this experiment Eq. 5.2-18 gives for  $t < 0$  and  $t > 0$

$$\tau_{yx}(t < 0) = 0 \tag{5.3-22}$$

$$\begin{aligned} \tau_{yx}(t > 0) &= -\eta^+ \dot{\gamma}_0 \\ &= -\dot{\gamma}_0 \int_0^t G(t-t') dt' \end{aligned} \tag{5.3-23}$$

The area between the stress growth curve and its asymptote (see Fig. 5.3-2b) is given by

$$\begin{aligned} \int_0^\infty \left(1 - \frac{\eta^+(t)}{\eta_0}\right) dt &= \int_0^\infty \frac{\int_{-\infty}^0 G(t-t') dt'}{\int_{-\infty}^t G(t-t') dt'} dt \\ &= \frac{\int_0^\infty \int_t^\infty G(s) ds dt}{\int_0^\infty G(s) ds} \\ &= \frac{\int_0^\infty sG(s) ds}{\int_0^\infty G(s) ds} \end{aligned} \quad (5.3-24)$$

Thus the area between the stress-growth curve and its asymptote is the same as the area between the stress-relaxation curve and its asymptote.

When the relaxation modulus is specified as that for the generalized Maxwell model, then the stress-growth function is

$$\frac{\eta^+}{\eta^0} = \frac{\sum_k \eta_k (1 - e^{-t/\lambda_k})}{\sum_k \eta_k} \quad (5.3-25)$$

Note that this curve is monotonically increasing with  $t$ ; it gives the upper “envelope” in Fig. 3.4-7. We cannot, by means of the linear viscoelastic theory, describe the “overshoot effect” shown in Figs. 3.4-7 and 8.

#### EXAMPLE 5.3-5 Constrained Recoil after Cessation of Steady Shear Flow

Next we investigate the system depicted in Fig. 3.4-18. Prior to  $t = 0$  the fluid between the two parallel plates is undergoing steady shear flow with velocity gradient  $\dot{\gamma}_0 \ll 1/\lambda_{\max}$ . After  $t = 0$ , the shear stress is removed so that  $\tau_{yx} = 0$ . The fluid then recoils and the strain  $\gamma_{yx}(0, t)$  can be followed as a function of time. It is presumed that the plate spacing is small enough and the fluid viscous enough that a linear velocity profile is maintained throughout the experiment; that is, inertial effects can be neglected. We wish to find the “ultimate recoil,”  $\gamma_\infty = \gamma_{yx}(0, t)|_{t=\infty} = \int_0^\infty \dot{\gamma}_{yx}(t) dt$  (see Fig. 3.4-18). (*Note:* In this problem it is convenient to take  $t = 0$  to be the reference time for the measurement of strain!)

**SOLUTION** Application of Eq. 5.2-18 to this problem for  $t > 0$  gives

$$0 = - \int_{-\infty}^0 G(t-t') \dot{\gamma}_0 dt' - \int_0^t G(t-t') \dot{\gamma}_{yx}(t') dt' \quad (5.3-26)$$

or, in terms of the variable  $s = t - t'$

$$0 = -\dot{\gamma}_0 \int_t^\infty G(s) ds - \int_0^t G(s) \dot{\gamma}_{yx}(t-s) ds \quad (5.3-27)$$

Next we integrate over the time from  $t = 0$  to  $t = \infty$ , and this gives

$$0 = -\dot{\gamma}_0 \int_0^\infty \int_t^\infty G(s) ds dt - \int_0^\infty \int_0^t G(s) \dot{\gamma}_{yx}(t-s) ds dt \quad (5.3-28)$$

Next interchange the order of integration to get

$$0 = -\dot{\gamma}_0 \int_0^\infty \left[ \int_0^s dt \right] G(s) ds - \int_0^\infty \left[ \int_s^\infty \dot{\gamma}_{yx}(t-s) dt \right] G(s) ds \quad (5.3-29)$$

or

$$0 = -\dot{\gamma}_0 \int_0^\infty s G(s) ds - \int_0^\infty \left[ \int_0^\infty \dot{\gamma}_{yx}(t') dt' \right] G(s) ds \quad (5.3-30)$$

The quantity in brackets in Eq. 5.3-30 is just the ultimate recoil  $\gamma_\infty$ , for which we then have the final result

$$\frac{-\gamma_\infty}{\dot{\gamma}_0} = \frac{\int_0^\infty s G(s) ds}{\int_0^\infty G(s) ds} \quad (5.3-31)$$

Notice that we did not actually solve the integral equation for  $\dot{\gamma}_{yx}(t)$  in Eq. 5.3-26, but we were able to extract an integral of the solution, namely the ultimate recoil. This problem can also be solved by using Laplace transforms, as indicated in Problem 5D.1.

A quantity  $J_e^0$ , the steady-state compliance, is defined by Eq. 3.4-11

$$\gamma_\infty = J_e^0 \tau_0 \quad (5.3-32)$$

where  $\tau_0 = -\eta_0 \dot{\gamma}_0$  is the shear stress prior to recoil. According to the linear viscoelasticity theory, this quantity is given by

$$J_e^0 = \frac{\int_0^\infty s G(s) ds}{\left[ \int_0^\infty G(s) ds \right]^2} \quad (5.3-33)$$

This is obtained by combining the results in Eqs. 5.3-31 and 32.

### EXAMPLE 5.3-6 Creep after Imposition of Constant Shear Stress

The next experiment we consider is that shown in Fig. 3.4-1f. Prior to  $t = 0$  the fluid contained between two parallel plates is at rest. After  $t = 0$  the fluid sample is subjected to a constant applied shear stress, so that the strain has a response similar to that shown in Fig. 5.3-3. We want to find an expression for the intercept  $\gamma_0$ . Designate the applied shear stress by  $\tau_0$  and the ultimate velocity gradient by  $\dot{\gamma}_\infty$ .

**SOLUTION** During the creep process, the rate of strain (or velocity gradient) will be (see Eq. 5.1-8a)

$$\dot{\gamma}_{yx} = \frac{d}{dt} \gamma_{yx}(0, t) \quad (5.3-34)$$

and therefore at any time  $t$  the strain will be

$$\gamma_{yx}(0, t) = \int_0^t \dot{\gamma}_{yx}(t') dt' \quad (5.3-35)$$

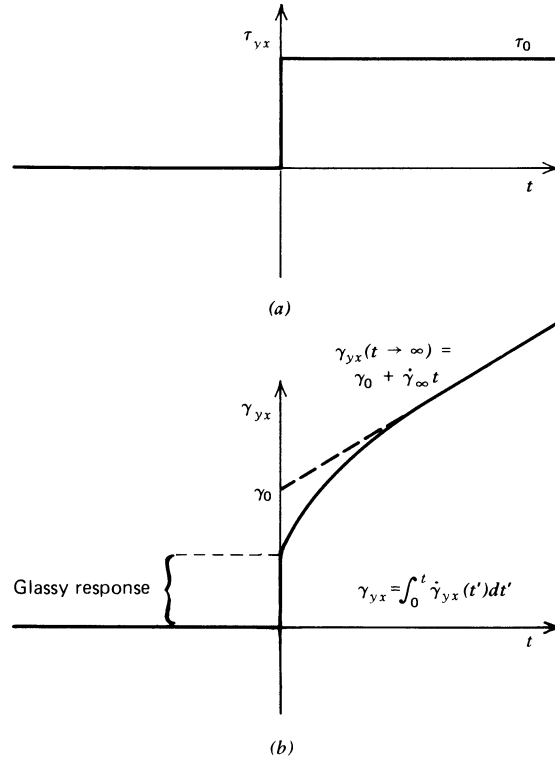


FIGURE 5.3-3. Creep experiment. (a) A constant shear stress  $\tau_0$  is applied at  $t = 0$  and maintained for all times greater than  $t = 0$ ; (b) the shear strain measured relative to  $t = 0$  in the creep experiment increases with time and approaches an asymptote with slope  $\dot{\gamma}_\infty$  for long times.

As in the preceding illustrative example we take  $t = 0$  to be the reference time. For very large time, the strain curve will approach the dashed-line asymptote in Fig. 5.3-3, which is given by the equation

$$\lim_{t \rightarrow \infty} \gamma_{yx}(0, t) = \gamma_0 + \dot{\gamma}_\infty t \quad (5.3-36)$$

If we write Eq. 5.3-35 for  $t \rightarrow \infty$  and equate the result to Eq. 5.3-36, then we get for the intercept  $\gamma_0$

$$\gamma_0 = \int_0^\infty (\dot{\gamma}_{yx}(t') - \dot{\gamma}_\infty) dt' \quad (5.3-37)$$

Now we get an expression for this quantity by using the constitutive equation for the linear viscoelastic fluid.

If we write Eq. 5.2-18 for the creep experiment, we have

$$\tau_0 = - \int_0^t G(t-t') \dot{\gamma}_{yx}(t') dt' \quad (5.3-38)$$

But we can also write Eq. 5.2-18 for the steady-state shear flow with  $\tau_{yx} = \tau_0$  and  $\dot{\gamma}_{yx} = \dot{\gamma}_\infty$

$$\tau_0 = - \int_{-\infty}^t G(t-t') \dot{\gamma}_\infty dt' \quad (5.3-39)$$

We now equate these two expressions for  $\tau_0$  to obtain

$$\dot{\gamma}_\infty \int_0^\infty G(s)ds = \int_0^t G(s)\dot{\gamma}_{yx}(t-s)ds \quad (5.3-40)$$

This may be rewritten as

$$\dot{\gamma}_\infty \int_t^\infty G(s)ds = \int_0^t G(s)[\dot{\gamma}_{yx}(t-s) - \dot{\gamma}_\infty]ds \quad (5.3-41)$$

Next we integrate both sides from  $t = 0$  to  $t = \infty$  and then interchange the order of integration of  $s$  and  $t$ ; this gives finally:

$$\frac{\gamma_0}{\dot{\gamma}_\infty} = \frac{\int_0^\infty sG(s)ds}{\int_0^\infty G(s)ds} \quad (5.3-42)$$

Here again we did not solve the integral equation for the velocity gradient, but extracted from the problem only the integral defined in Eq. 5.3-37.

From the above examples we find that certain quantities measured in different shearing experiments are given by the same ratio of integrals:  $\int_0^\infty sG(s)ds/\int_0^\infty G(s)ds$ . For future reference we list all of these results in Table 5.3-1. We also include one additional

**TABLE 5.3-1**  
**Shear Flow Experiments and "Analogous Quantities"**

Experiment	Meaning of Symbols	Measurable Quantity <sup>a</sup> Equal to $\int_0^\infty sG(s)ds/\int_0^\infty G(s)ds$
Small-amplitude oscillatory motion (Eq. 5.3-7)	$\omega$ = frequency of oscillation	$\lim_{\omega \rightarrow 0} \frac{\eta''/\omega}{\eta'}$
Stress relaxation after cessation of steady shear flow (Eq. 5.3-20)	$\dot{\gamma}_0$ = shear rate before stress relaxation	$\lim_{\dot{\gamma}_0 \rightarrow 0} \int_0^\infty \frac{\eta^-}{\eta_0} dt$
Stress growth after inception of steady shear flow (Eq. 5.3-24)	$\dot{\gamma}_0$ = shear rate during stress growth	$\lim_{\dot{\gamma}_0 \rightarrow 0} \int_0^\infty \left(1 - \frac{\eta^+}{\eta_0}\right) dt$
Constrained recoil after cessation of steady shear flow (Eq. 5.3-31)	$\dot{\gamma}_0$ = shear rate before recoil begins	$\lim_{\dot{\gamma}_0 \rightarrow 0} \frac{-\gamma_\infty}{\dot{\gamma}_0}$
Creep after application of steady shear stress (Eq. 5.3-42)	$\dot{\gamma}_\infty$ = shear rate when steady state is attained	$\lim_{\tau_0 \rightarrow 0} \frac{\gamma_0}{\dot{\gamma}_\infty}$
Steady-state shear flow (Problem 6B.3)	$\dot{\gamma}$ = shear rate at steady state	$\lim_{\dot{\gamma} \rightarrow 0} \frac{\Psi_1}{2\eta}$

<sup>a</sup>Note that this ratio of integrals has the dimensions of time and is often used as the "characteristic time of the fluid" to construct the Deborah number. For the generalized Maxwell model the ratio of integrals is approximately equal to the longest relaxation time  $\lambda_1$ .

entry—that for the normal stress coefficient in steady-state shear flow—for which nonlinear viscoelasticity theory is required; this result will be obtained in Problem 6B.3, but we include it in the table for completeness.<sup>4</sup>

These relations among various experiments have been the subject of considerable experimentation, and they are useful in providing cross-checks of experimental techniques. The establishment of these interrelations requires no assumptions regarding the relaxation modulus. It must be kept in mind that all of the quantities listed in the right column of Table 5.3-1 are limiting values, and for some fluids these may have to be obtained experimentally by tedious extrapolation processes.

#### EXAMPLE 5.3-7 Determination of the Relaxation Spectrum from Linear Viscoelastic Data

In the preceding six examples we have shown how the response of a viscoelastic fluid to small deformation gradient experiments is related to the relaxation modulus  $G(t)$ . Here we want to show how this information can be used to find  $G$  from linear data. Take the relaxation modulus to be given by the generalized Maxwell model expression in Eq. 5.2-14 and use the storage and loss moduli for low-density polyethylene presented in Fig. 3.4-3 to illustrate the procedure for fitting  $G$ . Because time-temperature superposition has been used in obtaining these data, an extremely wide range of frequencies has been covered.

**SOLUTION** We begin by selecting a set of relaxation times  $\lambda_j$  for the spectrum. The spacing of these is conveniently taken to be decade intervals in order to reduce the amount of computation, but smaller spacings can be taken if more accurate fitting is required. The longest relaxation time  $\lambda_j$  is chosen so that  $\lambda_1 \omega_{\min} > 1$ , where  $\omega_{\min}$  is the lowest frequency for which data are available, unless the zero-frequency region is reached in the experiments. In the latter case take  $\lambda_1 \omega_0 \doteq 0.1$  where  $\omega_0$  is the critical frequency that marks the end of the zero-frequency regime. Similarly the smallest relaxation time  $\lambda_{\min}$  is chosen so that  $\lambda_{\min} \omega_{\max} < 1$ , where  $\omega_{\max}$  is the highest frequency for which data are available. For the low-density polyethylene melt we choose the  $\lambda_j$  to be  $10^3, 10^2, \dots, 10^{-3}, 10^{-4}$  s.

It remains to fit the viscosities  $\eta_j$  for each relaxation time. This is done by minimizing the difference between the measured and predicted moduli at  $N$  frequencies  $\omega_j$ . If we denote the measured properties by  $G'_j$  and  $G''_j$  and the predicted properties by  $G'(\omega_j)$  and  $G''(\omega_j)$ , then the quantity to be minimized is

$$\sum_{j=1}^N \left\{ \left[ \frac{G'(\omega_j)}{G'_j} - 1 \right]^2 + \left[ \frac{G''(\omega_j)}{G''_j} - 1 \right]^2 \right\}$$

The calculated moduli are obtained from the following truncated forms of Eqs. 5.3-8 and 9:

$$G'(\omega_j) = \sum_{k=1}^N \frac{\eta_k \lambda_k \omega_j^2}{1 + (\lambda_k \omega_j)^2} \quad (5.3-43)$$

$$G''(\omega_j) = \sum_{k=1}^N \frac{\eta_k \omega_j}{1 + (\lambda_k \omega_j)^2} \quad (5.3-44)$$

For the low-density polyethylene this minimization<sup>5</sup> leads to the values of  $\eta_k$  shown in Table 5.3-2.

It is instructive to look at the spectral decomposition of the dynamic moduli that are predicted by the relaxation spectrum parameters in Table 5.3-2. Figure 5.3-4 shows the contribution of the

<sup>4</sup> The equality of the entries involving  $\eta''/\omega\eta'$  and  $\Psi_1/2\eta$  has been verified experimentally by T. Kotaka and K. Osaki, *J. Polym. Sci.*, **C15**, 453-479 (1966).

<sup>5</sup> A. C. Papanastasiou, L. E. Scriven, and C. W. Macosko, *J. Rheol.*, **27**, 387-410 (1983), discuss the use of nonlinear regression methods to determine simultaneously the best set of  $\lambda_k$  and  $\eta_k$  to fit  $G(t)$ .